*Physics – Uspekhi* **42** (10) 957 – 990 (1999) 

*REVIEWS OF TOPICAL PROBLEMS* PACS numbers: **75.10–b**, **75.30.–m**, **75.50.–y**

# On the relative contributions of precessional and longitudinal oscillations to the dynamics of magnets

V D Buchel'nikov, N K Dan'shin, L T Tsymbal, V G Shavrov

## Contents



**Abstract. Experimental studies of the high-frequency and acoustic properties of weak ferromagnets are reviewed and a theory that includes all possible mechanisms of the formation of magnet dynamics is presented. The dynamic properties of a magnet are shown to be generally determined by the precessional and longitudinal motions of magnetization and by their interaction with the elastic, paramagnetic, and dipole subsystems. It was found that the precessional and longitudinal contributions always coexist and are additive and that their relative magnitudes depend on both external factors and the relationship (which is characteristic of each specific magnet) between the temperatures of the spontaneous reorientation and ordering of the corresponding spin subsystem. Special attention is paid to the investigation of magnets near the reorientation phase transitions, where the effects due to changes in this relationship, as well as those caused by the interaction of various vibrational subsystems, are most pronounced.**

**V D Buchel'nikov** Chelyabinsk State University
ul. br. Kashirinykh 129, Chelyabinsk, 454021 Russia
Tel. (7-3512) 42-03 47. E-mail: buche@cgu.chel.su
**N K Dan'shin, L T Tsymbal** Donetsk Physicotechnical Institute, National Academy of Sciences of Ukraine
ul. R Lyuksemburg 72, Donetsk, 340114 Ukraine
Tel. (7-0622) 55-72 26. E-mail: tsymbal@host.dipt.donetsk.ua
**V G Shavrov** Institute of Radio Engineering and Electronics, Russian Academy of Sciences
ul. Mokhovaya 11, Moscow, 103907 Russia
Tel. (7-095) 203-24 26. E-mail: shavrov@mail.cplire.ru

Received November 18, 1998; revised May 20, 1999
*Uspekhi Fizicheskikh Nauk* **169** (10) 1049 – 1084 (1999)
Translated by S N Gorin; edited by S N Gorin

## 1. Introduction

We hope that the interested reader is acquainted with our review [1] devoted to the magnetoacoustics of rare-earth (RE) orthoferrites (OFs), which mainly concerned the theoretical and experimental investigations of the dynamics of REOFs in the field of various spontaneous reorientation phase transitions (RPTs) that occur in these compounds. Both the theory and the interpretation of experimental results in that review were based on the spin-wave approximation. This means that the magnetizations of the sublattices were postulated to be unaltered by the absolute value and only the precessional motion of the ferromagnetism and antiferromagnetism vectors was taken into account. This approach permitted us, nevertheless, to explain most experimental results that concerned the investigation of soft magnetoresonance modes, the anomalies of the sound velocity, and sound attenuation in the immediate vicinity of the RPTs. However, some effects have not received convincing explanation within this approach, especially, in the case of transitions induced by an external magnetic field rather than occurring spontaneously. One such effect that has not received satisfactory quantitative explanation is a very small (in comparison with the expected value) change in the sound velocity at the RPT points. According to the theory developed in Ref. [2], which ignores the longitudinal vibrations and the relaxation of magnetization, the velocity of the transverse sound should vanish at the points of those RPTs that occur as second-order

phase transitions (PT-2). However, no such effect has been observed experimentally to date. The maximum decrease in the sound velocity that was fixed in the vicinity of the $\Gamma_2 - \Gamma_4$ transition typical of REOFs is several percent instead of the predicted value of 100%. The same refers to the magnitude of the energy gap in the spectrum of spin waves. Upon the experimental restoration of spectra of soft magnetoresonance modes, significant energy gaps are revealed at the RPT points in all REOFs (and not only in them). In many cases, their frequency – field dependences could not be explained in terms of the spin-wave model. This suggested that even the full allowance for the contributions to the dynamic characteristics of REOFs from various vibrational subsystems that was used in the theory developed in Ref. [1] (which was modified as compared to [2]) cannot give adequate explanation for the entire body of experimental data within the framework of the above model.

To find the way from this situation, we turned to the idea, first stated by Yu M Gufan [3], that upon a thermodynamic description of the resonance properties of ordered magnets, one should take into account not only precessional, but also longitudinal vibrations of magnetization. This was also supported by later works of Gufan, Marchukov, Rudashevskiĭ, et al. (see, e.g., [4, 5]), who established that, indeed, under real experimental conditions (i.e., at $T > 0$), the longitudinal vibrations and the relaxation of magnetization could not be ignored if one wanted to obtain a correct description of experimental data. Moreover, the allowance for these factors leads to a quite different explanation of the effects that are observed in magnetoresonance measurements performed on REOFs. In particular, this refers to the understanding of the nature of energy gaps. Truly, the theory of Refs [4, 5] in the existent form is only applicable to transitions induced by an external magnetic field. However, as we recognized after a series of measurements carried out on various compounds, it can be successfully extended to spontaneous RPTs as well. This conclusion is supported by new experiments that were conducted on REOFs and on $Fe_3BO_6$, which is isomorphic to REOFs. The results of these experiments permit us to obtain a more comprehensive idea of the mechanisms of formation of the dynamics of magnets near RPTs than could be done within the framework of the classical spin-wave approach. Already the first theoretical works in this direction [6, 7] showed the availability of this approach. It turned out that even the allowance for only the magnetoelastic interaction in the thermodynamic theory [4] makes it possible to explain more fully and in a different way the magnetoacoustic anomalies experimentally observed at RPT points.

Before proceeding with the presentation of experimental and theoretical results on the questions that will be touched upon in this review, we turn to the problem of the method of description of the dynamics of magnets that has frequently appeared in recent years in science discussions and in the literature. Usually, the well-known Landau – Lifshitz equations are used in the investigations of the dynamics of magnets. In many works devoted to the calculation of the frequencies of magnetic resonance in antiferromagnets, the changes in the magnitudes of the magnetizations of the sublattices, as well as the longitudinal relaxation, are usually neglected both in statics and dynamics. This corresponds to the case where only a precessional motion of the vectors of ferromagnetism and antiferromagnetism is possible. This approximation, strictly speaking, holds in the range of relatively low temperatures — far from the Néel temperature. The method of the calculation of magnetic resonance frequencies based on the above approximations is called the spin-wave method. Gufan [3] suggested the use, instead of the Landau – Lifshitz equations, a more general phenomenological method — the Onsager theory of thermodynamic fluctuations. Later, Dzyaloshinskiĭ and Kukharenko [8] developed another phenomenological method of calculating magnetic resonance frequencies — the generalized Lagrange method of the theory of small oscillations. In both methods, the magnetizations of the antiferromagnet sublattices were assumed to change their magnitudes both in statics and dynamics. The calculation of the frequencies of magnetic resonance and of spin waves using the Onsager and Lagrange methods was performed in Refs [8 – 10]. The frequencies calculated by these methods turned out to differ from one another for some vibration modes, namely, for those modes that are excited by the longitudinal (directed along the antiferromagnetism vector) high-frequency field and do not retain the lengths of the sublattice magnetizations. In 1992, Mukhin and Prokhorov [11] showed that the difficulties that arise upon comparison of the results obtained by the Lagrange and Onsager methods are related to the neglect of longitudinal relaxation. They also noted that in the description of the dynamics of antiferromagnets whose sublattice magnetizations change their length in both statics and dynamics, one can use the Landau – Lifshitz equations with allowance for longitudinal relaxation. Such equations were suggested by Bar'yakhtar in Ref. [12]. The Landau – Lifshitz equations with allowance for the longitudinal relaxation and the changes in the magnitudes of the sublattice magnetizations in statics and dynamics were used in calculations of magnetic resonance frequencies and coupled magnetoelastic waves in Refs [6, 7]. Note that the results of our work [6, 7] coincide with those obtained by other methods mentioned above. Therefore, in this review we will use the classical approach based on the Landau – Lifshitz equations with allowance for the longitudinal relaxation and changes in the magnitudes of the sublattice magnetizations in statics and dynamics.

Our review [1] contains a detailed introduction to the magnetoacoustics of REOFs, a description of the objects of investigation, and the experimental techniques. Since this paper is a logical continuation of review [1], we thought it would be excessive to repeat in detail the relevant data, the more so that we will here consider virtually the same REOFs that were discussed in [1]. During the presentation, we will give in more detail only those new features of the experimental technique that are absent in Ref. [1]. The designations are the same as in [1].

Below the Néel temperature ($T_N = 620 - 740$ K), two magnetic subsystems typically exist in most REOFs, namely, a weakly ferromagnetic ordered structure of Fe ions (d subsystem) and a system of paramagnetic RE ions (f subsystem).

Most experiments can be explained in terms of a four-sublattice model, in which the magnetic structure of Fe ions corresponds to the irreducible representation $\Gamma_4(G_x, F_z)$, where $G_x$ and $F_z$ are the components of the vectors of antiferromagnetism ($\mathbf{G} = \mathbf{M}_1 - \mathbf{M}_2$) and ferromagnetism ($\mathbf{F} = \mathbf{M}_1 + \mathbf{M}_2$), respectively; and $\mathbf{M}_1$ and $\mathbf{M}_2$ are the magnetizations of the sublattices. In this model, two branches of vibrations of iron spins exist, namely, the quasiferromagnetic ($\gamma$ mode) and the quasiantiferromag-

netic ($\sigma$ mode). At $T > 10$ K, the RE ions are in the paramagnetic state, but magnetized due to the exchange interaction with the spin subsystem of iron ions. Two analogous vibration branches and the vectors of ferromagnetism and antiferromagnetism can also be put in correspondence to these ions. Thus, on the whole, the dynamics will be described in the approximation of two d and two f sublattices, i.e., by a four-sublattice model. In terms of this model, the resonance modes corresponding to RE ions can be considered as cooperative vibrations within the paramagnetic subsystem.

A characteristic feature of REOFs is the occurrence of various RPTs in them, caused by the temperature-dependent anisotropic f–d interaction [13]. In most cases, we will be interested in the dynamics of orthoferrites with the most common RPT of the $\Gamma_4(G_x, F_z) - \Gamma_{24}(G_{xz}, F_{xz}) - \Gamma_2(G_z, F_x)$ type, in which case a smooth rotation of the vectors **G** and **F** in the *ac* plane of the crystal occurs. At the boundaries of the spontaneous reorientation, at temperatures $T = T_1$ and $T = T_2$, PT-2 transitions of the $\Gamma_4 - \Gamma_{24}$ and $\Gamma_2 - \Gamma_{24}$ types occur, respectively. These RPTs can be induced on the whole by varying the temperature in the range of $T < T_N$. Individually, the $\Gamma_4 - \Gamma_{24}$ and $\Gamma_2 - \Gamma_{24}$ transitions can be induced by the fields $\mathbf{H}||\mathbf{c}(z)$ and $\mathbf{H}||\mathbf{a}(x)$, respectively.

One of the problems that arises upon the investigation of soft magnetoresonance modes is related to the clarifying of the nature of the observed energy gaps at the RPT points. The corresponding measurements have been performed to date on virtually all REOFs. In no one case could a frequency gap less than 15–20 GHz be revealed at the PT-2 points, whereas it follows from the solution to the set of Landau–Lifshitz type dynamic equations specific for the REOFs [14] that at these points the frequency of one of the branches of spin waves ($\sigma$ mode) should vanish. Upon an attempt to explain experimental results that do not agree with this conclusion, several questions arise immediately. Are the experimentally detected magnetoresonance branches soft in their origin? If yes, then which is the nature of the observed gaps? If no, then what is the soft mode? For this reason, two viewpoints on the nature of the above high-frequency effects, which a few years ago seemed to be alternative came into existence. One is based on the fact that in high-frequency experiments in the vicinities of different RPTs it is just the soft magnetoresonance mode that is detected, while the gaps observed are the result of a dynamic interaction of various vibrational subsystems of the magnet, such as the ordered spin subsystem, paramagnetic, elastic, and dipole [1] (electromagnetic) subsystems.

The corresponding theoretical calculations [15, 16] were laid down as the basis for the description of a series magnetoresonance and magnetoacoustic experiments presented in review [1]. In that review, we postulated the fulfillment of the condition that the magnetizations in the corresponding pair of sublattices remain constant in magnitude and are equal to one another [17], which corresponds to the spin-wave model. For example, for a two-sublattice antiferromagnet this condition has the form

$$\mathbf{M}_1^2 = \mathbf{M}_2^2 = M_0^2 = \text{const}\,, \tag{1.1}$$

which is equivalent to the conditions $\mathbf{FG} = 0$, $\mathbf{F}^2 + \mathbf{G}^2 = 4M_0^2$, where $M_0$ is the saturation magnetization of the sublattices.

[1] By dipole interaction, we understand the interaction of the magnetic moment of the crystal with the magnetic component of the electromagnetic wave that propagates in it.

Another approach, on the contrary, takes into account the longitudinal vibrations of $\mathbf{M}_1$ and $\mathbf{M}_2$, which are related to the finite longitudinal susceptibility at temperatures $T > 0$. In this case, naturally, condition (1.1) is not fulfilled. The allowance for longitudinal vibrations of the magnetizations and for dissipation gives an additional relaxational branch of spin waves with a complex frequency. It is this branch that is soft, whereas the experimentally observed magnetoresonance branches are not soft in reality. To the beginning of the experimental works that are considered in this review, each of the two above mechanisms of gap formation was tested, but on different REOFs and under different experimental conditions. Thus, the experiments on $YbFeO_3$ [18], $ErFeO_3$ [19], $TmFeO_3$ [20], $HoFeO_3$ [21], and some other REOFs could satisfactorily be explained by the theory [15, 16] that was mainly developed for the case of spontaneous RPTs. At the same time, the mechanism suggested in [4, 5] was tested on $YFeO_3$ and $DyFeO_3$ under conditions where the RPT was induced by an applied magnetic field.

The experimental investigations that are considered below were initially directed to searching for the manifestation of the effects of relaxational modes predicted in [3–5] (longitudinal vibrations of the sublattice magnetizations) in both RPTs induced by the field and in spontaneous transitions. It is important to emphasize that these experiments were performed on the same compounds for which the previous experiments were successfully explained on the basis of the spin-wave model without resort to relaxational and longitudinal vibrations.

## 2. Experimental studies

Going to the description of the results of specific experiments, we note that the sequence of presentation follows a logic that will be explained later. Here, we only indicate that the sequence of presentation corresponds to the increase in the parameter $\tau_{SR} = T_{SR}/T_N$, which we called the relative temperature of spontaneous transition ($T_{SR}$ is the averaged temperature of spontaneous transition $(T_1 + T_2)/2$). It is obvious that this parameter is specific to each particular REOF. Its increase, as will be seen below, leads to the change in the ratio of the contributions to the dynamics from one characteristic of the spin-wave to that specific of the thermodynamic mechanism.

### 2.1 Spectra of soft magnetoresonance modes under conditions that satisfy the spin-wave approximation

We begin the presentation from $YFeO_3$, which has the smallest $\tau_{SR}$ parameter among the orthoferrites that were studied in our work. In this compound, spontaneous spin reorientation occurs in a temperature range from $T_1 = 7.95$ K to $T_2 = 6.85$ K; its Néel temperature is $T_N = 627$ K, i.e., $\tau_{SR} \approx 0.01$. Therefore, this REOF corresponds best to the condition of applicability of the spin-wave approximation $\tau_{SR} \ll 1$ when the sublattice magnetizations reach the greatest saturation.

**2.1.1 Dynamic properties of the induced transition $\Gamma_2 - \Gamma_4$ in $YbFeO_3$.** The choice of the technique of measurement for $YbFeO_3$ was determined by the necessity of obtaining experimental results in a form suitable for comparison with the theory that existed at that time and with experiments that were performed to check that theory with previously performed experiments on $YFeO_3$ and $DyFeO_3$ [4, 5]. The

requirement of closeness of experimental conditions means, first, the coincidence of the character and type of the phase transitions; second, of the orientation of the magnetic field that induces the transition; and, third, of the nature of the soft modes. In order to clarify the importance of the fulfillment of the last condition and the limits of the applicability of the theory developed in [4, 5], experiments were performed on a number of orthoferrites with substantially differing relationships between the natural frequencies of the subsystems of iron ($\nu_\sigma$) and rare earth ($\nu_r$) ions. It has been reliably established to date [1, 17] that both the $\sigma$ and the RE modes can be soft near the RPT because of the intersection and strong interaction of different resonance branches. In $YbFeO_3$, as is known [18], the soft mode is the RE mode, and the relation $\nu_r \ll \nu_\sigma$ holds.

How does the transition induced by an applied magnetic field occur? We will demonstrate this using an RPT in a field $\mathbf{H}||\mathbf{a}$ as an example.

The switching on of an arbitrarily small field of this orientation at once transforms the symmetric phase $\Gamma_4(G_x, F_z)$ into a canted phase $\Gamma_{24}(G_{xz}, F_{xz})$. The further reorientation in an increasing field goes by the rotation of **F** and **G** to its completeness at the $\Gamma_{24}-\Gamma_2$ (PT-2) point.

The fact that this transition in $YbFeO_3$ (as, though, in all the other orthoferrites that were studied in our work) can be induced by both the temperature and the field gives certain methodical advantages. They are as follows. In the experiments on $YFeO_3$ and $DyFeO_3$ in the working temperature range (78 – 400 K), the transition can only be induced by a sufficiently strong magnetic field (50 – 100 kOe). As follows from the $H-T$ phase diagrams of these compounds, measurements in lower fields would require increasing the temperature to above 600 K, where no resonance could be detected in either $YFeO_3$ [23] or $DyFeO_3$ [24]. In the other REOFs, owing to the existence of second-order spontaneous transitions, the $\Gamma_2-\Gamma_{24}$ transitions similar to those observed in $YFeO_3$ and $DyFeO_3$ can be detected even in very weak magnetic fields. The methodical trick in experiments with $YbFeO_3$ consisted in that the 'starting position' was chosen by fixing one of the parameters, $H$ or $T$, whereas the scanning of the second parameter was used to initiate the transition. As follows from the experimental $H-T$ phase diagram (Fig. 1), the $\Gamma_2-\Gamma_{24}$ transition can be induced by an arbitrarily small magnetic field $H = H_{IR}$. The restrictions on $H$ from below are only due to the field width of the resonance line. In experiments, this width was 0.5 – 1.0 kOe, but the position of its peak can reliably be fixed at already as low a field as $H \approx 0.1$ kOe. Thus, the first condition for the compatibility of the techniques was fulfilled to the full extent: we have just the PT-2 of the $\Gamma_2-\Gamma_{24}$ type induced by the field $\mathbf{H}||\mathbf{a}$, as in $YFeO_3$ and $DyFeO_3$.

It is obvious from the above that the fulfillment of the second condition was actually predetermined. But in the experiments with $YbFeO_3$, apart from the $\Gamma_2-\Gamma_{24}$ RPT induced by the field $\mathbf{H}||\mathbf{a}$, a $\Gamma_4-\Gamma_{24}$ RPT was also induced by the field $\mathbf{H}||\mathbf{c}$. In the final account, this gave the opportunity to restore the total magnetoresonance spectrum in the vicinity of the RPT and obtain comprehensive information on the field dependence of both energy gaps — located at both $T_1$ and $T_2$.

As for the third conditions, we should note the following. Yttrium is a nonmagnetic ion; i.e., in $YFeO_3$ the entire statics and dynamics of the reorientation are controlled only by the sublattices of iron. Therefore, this compound may be considered as a model one for the theory developed in [4], whereas in $DyFeO_3$ the $\sigma$ mode is determined to a large extent by the f – d interaction [24]. This was noted in [5], but it was also concluded there that this factor exerts only an insignificant effect on the magnitude of the energy gap. We say here in advance that, in order to check this conclusion, orthoferrites with markedly different ratios $\nu_r$ and $\nu_\sigma$ were selected. And we remember that these ratios are directly related to the strength of the f – d interaction.

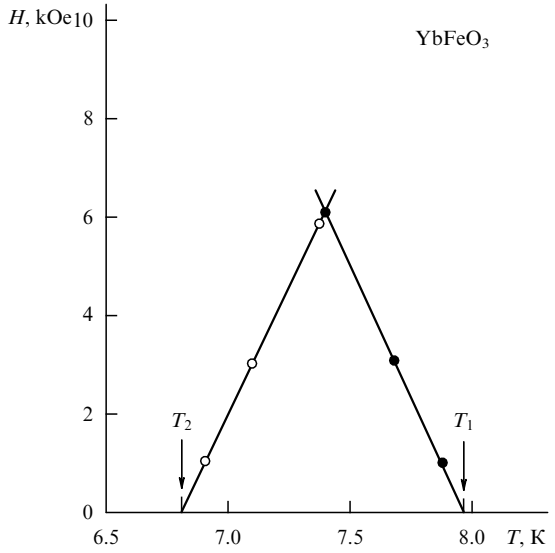


**Figure 1.** $H-T$ phase diagram of $YbFeO_3$ at various orientations of magnetic field: (○) $\mathbf{H}||\mathbf{a}$; and (●) $\mathbf{H}||\mathbf{c}$.

The measurements were carried out on a direct-gain spectrometer, in which the reflected absorption signals from spherical samples (0.8 – 0.9 mm in diameter, placed in the center of the cavity piston that short-circuited the waveguide) were detected (see, e.g., [25]). The orientation of the field **H** along the crystal axes was attained by trial experimental recordings and was fixed by the maximum separation of two resonance lines located on both sides of the transition point, similar to the way it was performed in [4]. The attained (and sufficient) accuracy of orientation was $\sim 10'$. The absorption was recorded in the process of scanning both in the temperature at a constant field and in the field at a constant temperature. The relative accuracy of measurements of the field and temperature was $10^{-3}$. The direction of the magnetic component of the linearly polarized high-frequency field **h** with respect to the crystal axes was chosen from the condition of the excitation of the soft mode at the $\Gamma_2-\Gamma_{24}$ RPT . This condition corresponds to $\mathbf{h} \perp \mathbf{a}$ in the $\Gamma_2$ phase ($T < T_2$) and $\mathbf{h} \perp \mathbf{c}$ in the $\Gamma_4$ phase ($T > T_1$). The accuracy of the orientation of the field **h** that was sufficient for this was 5°. The same technique was used in experiments with other REOFs. The only difference was in the accuracy of orienting **H** along the crystal axes, which was specific in each particular case. Thus, e.g., it was 30″ for the analogous measurements on $TmFeO_3$.

Figure 2 displays a fragment of a temperature dependence (characteristic of the REOFs) of the soft mode frequency, obtained in experiments with $YbFeO_3$ upon a spontaneous RPT. In a fuller form, these results were presented in review [1]. Here, they serve as a starting point, since in the context of this work we are interested in the temperature (field)

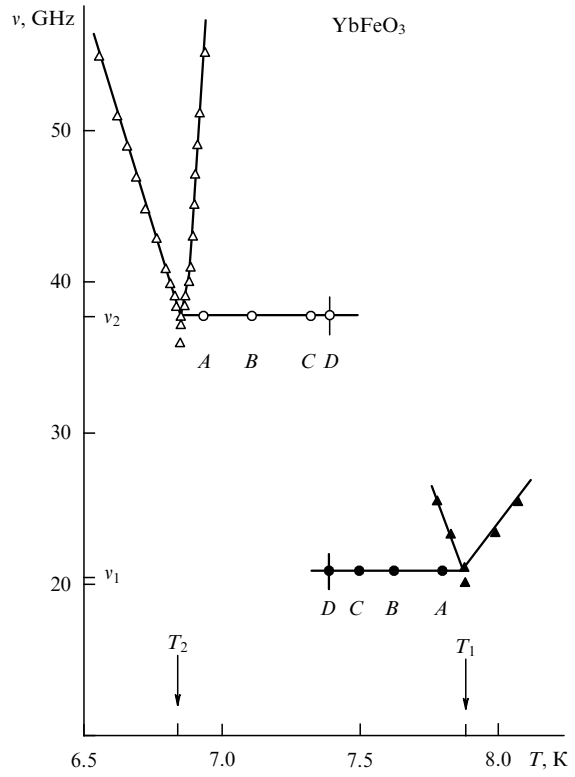


**Figure 2.** Temperature dependence of the frequency of the soft magnetoresonance mode in $YbFeO_3$ in the vicinity of spontaneous transitions $\Gamma_2-\Gamma_{24}$ (△) and $\Gamma_4-\Gamma_{24}$ (▲) and of the energy gaps for transitions induced by magnetic field **H**||**a** (○) and **H**||**c** (●) of the following magnitude: *A*, 1; *B*, 3; *C*, 5; and *D*, 6 kOe.

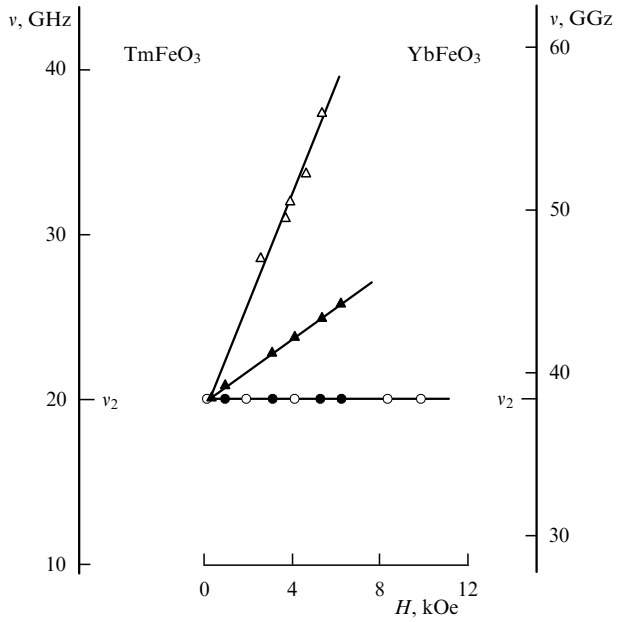


**Figure 3.** Field dependences of the energy gaps in $YbFeO_3$ (●) and $TmFeO_3$ (○) at the point of the $\Gamma_2-\Gamma_{24}$ transition and of the minimum resonance frequencies for a field departing from the *a* axis by 1° in the *ac* plane for $YbFeO_3$ (▲) and $TmFeO_3$ (△).

dependences of the energy gaps at the points of completion of the spin reorientation $T_1$ and $T_2$ rather than in the resonance spectra themselves. The magnetoresonance spectrum was obtained in a zero field by recording absorption lines at fixed frequencies upon scanning in temperature. Usually, in the restoration of the spectra of soft modes, the absorption from the slopes of the resonance lines at frequencies below those corresponding to the gap is also observed (see, e.g. [4]). This absorption decreases rapidly in amplitude and vanishes as the frequency decreases by a value equal to the width of the resonance line. From the position of the unsplit line of this absorption, we determined the values of $T_1$ and $T_2$ upon spontaneous transitions and of $H = H_{IR}$ upon the transitions induced by the field. The measured values of the gaps in the spontaneous RPTs at points $T_1$ and $T_2$ were $\nu_1 = 20.2$ GHz and $\nu_2 = 37.5$ GHz, respectively. The temperature dependences of the magnetic resonance frequencies upon field-induced transitions are similar to those shown in Fig. 2 for the spontaneous reorientation, but are displaced along the temperature axis in accordance with the phase diagram (see Fig. 1). This diagram was constructed by processing a series of temperature dependences of resonance frequencies at various values of the fixed field **H**||**a** and **H**||**c**. The effect of the angle of misorientation between the field **H** and the crystal axes **a** and **c** is seen from Fig. 3. The accuracy of the orientation of the field *H* with respect to the crystal axes in such experiments plays a decisive role, since the effect of the longitudinal vibrations of magnetization on the dynamic characteristics is determined (according to [3–5]) just by the changes in the inducing magnetic field. And this dependence may be substantially distorted by the inaccurate geometry of the experiment (see Fig. 3). Indeed, the deviation of **H** from the **a** and **c** axes necessarily transforms the sample into a canted phase $\Gamma_{24}(G_{xz}, F_{xz})$ at any temperature, even in the temperature ranges where the collinear phases $\Gamma_2$ and $\Gamma_4$ exist. In this case the second-order transitions under study disappear. At the $T_1$ and $T_2$ points, the energy gaps cease to be minimum, since now they include 'additions' due to the noncollinear-field-induced anisotropy.

Since the theory of [4, 5] only concerns the two-sublattice subsystem of iron ions, it does not take into account the f–d interaction, at least when deriving the expression for the gap. However, when $\nu_r \ll \nu_\sigma$, which takes place in $YbFeO_3$, the theory apparently can be extended to this compound without any restrictions, since in this case as well, the thing is the description of the dynamics of an ordered two-sublattice subsystem. A test to confirm the theory [4] must be a linear-in-field growth of the energy gap and the resulting temperature dependence of the ratio between the longitudinal and transverse susceptibilities ($\chi_\parallel/\chi_\perp$). The main information that should be obtained from the experiment at hand is shown in Fig. 2. This is the gap dependence on the temperature and field. The results shown indicate that in the limits of the accuracy attained, the energy gaps are independent of the external factor that induces the transition. As for the theory of [4], the gap at the point of the $\Gamma_2-\Gamma_4$ transition is (to the first approximation)

$$\nu_2|_{H=H_{IR}} = \frac{\gamma_2}{2\pi}\left(\frac{\chi_\parallel}{\chi_\perp}\right)^{1/2} H_{IR}\,, \qquad (2.1)$$

where $\gamma_2$ is an unknown kinetic coefficient, which at room temperature differs from the gyromagnetic ratio $\gamma_0 = ge/(2mc)$ by only 1–2%. Thus, according to [4], the gap should grow with increasing field and temperature. The independence of the gap of the temperature, found in our

experiment, equivalent to the condition $\partial\nu_2/\partial H = 0$, indicates that the longitudinal vibrations of magnetization yield only an insignificant contribution to the gaps measured. However, the equality $\chi_{||} = 0$ implies a transition to the conventional Landau – Lifshitz equations, which satisfy condition (1.1), and the vanishing of the gaps at the PT-2 point.

How could it be possible to correlate this, at first glance, negative result with the existent (at that time) theory [4, 5]? A comparative analysis performed in [20] reduced to the following. The experiments on $YFeO_3$ and $DyFeO_3$ were carried out in strong magnetic fields and at relatively high temperatures. The 'rigidity' of the magnetic sublattices decreases as $T \to T_N$, and the increasing magnetization fluctuations favor the growth of the longitudinal susceptibility. At the upper temperature boundary attained in [4] (400 K), the $\chi_{||}/\chi_{\perp}$ ratio is $\sim 0.5$, i.e., is half its limiting value that follows from the molecular-field theory. Therefore, the manifestations of the exchange relaxation mode should here be pronounced most vividly. Correspondingly, a decrease in the transition temperature and the induction of the transition by a relatively small field can significantly decrease the above effect. This would mean, in reality, a smooth transition from the requirement of the conservation of the absolute magnitude of **G** [4] to the condition of the conservation of the magnitudes of $\mathbf{M}_1$ and $\mathbf{M}_2$ (1.1). At temperatures $T < 100$ K, the contribution of longitudinal vibrations to the magnitude of the observed gap can be masked by more substantial contributions from precession-related mechanisms [15, 16]. It is this that most likely is observed in the above experiment. In this connection, we should first of all recall the magnetoelastic interaction, which is most frequently used to explain the formation of a gap. In the theory of Refs [4, 5], this interaction plays an insignificant role; the gaps observed in $YFeO_3$ and $DyFeO_3$ (107 and 136 GHz at room temperature, respectively) are greater by almost an order of magnitude than the estimated magnetoelastic contribution (no more than 20 GHz). A different picture takes place in those REOFs in which the reorientation occurs spontaneously and at lower temperatures. The values of $\nu_1$ and $\nu_2$ given above for $YbFeO_3$ coincide on the order of magnitude with the above estimate of the magnetoelastic contribution. But this contribution is not the only one here. As was shown in [1], each transition, depending on the specific RE ion, correlates with a quite definite set of exchange-enhanced dynamic interactions that affect the gap. Therefore, the independence of the gaps of temperature (field) obtained in this work does not contradict the results of [4, 5]. The mechanisms suggested in [4, 5] and in [15, 16] are most likely coexistent rather than alternative. At low temperatures, the longitudinal susceptibility is small, and the soft mode is usually represented by the usual magnetoresistance mode, whereas with increasing temperature, the contribution from the longitudinal susceptibility increases and now controls the magnitude of the gap. Each specific REOF should be associated with a certain transition range of fields where neither the mechanisms developed in [4, 5] nor those suggested in [15, 16] separately can adequately describe experimental results. In such a transition region, these mechanisms are competing and contribute additively to the observed energy gap values. Evidence for the existence of such a transition region can be found in measurements [5]: in the range of $T \sim 78 - 100$ K, the experimental values of $\chi_{||}/\chi_{\perp}$ ratios and gaps in $YFeO_3$ are virtually independent of temperature, whereas at $T > 100$ K, the results are excellently described by the model suggested. To summarize, we may say that the $\chi_{||}/\chi_{\perp}(T)$ dependence obtained in [5] cannot be regarded from the quantitative viewpoint as a universal characteristic of all compounds of this symmetry; the theory suggested in [15, 16] also cannot be considered all-embracing, since it ignores the contributions of the relaxation and the longitudinal vibrations of magnetization.

**2.1.2 Magnetoresonance and acoustic properties of $TmFeO_3$ near the $\Gamma_2 - \Gamma_4$ induced transition.** In Refs [25, 26], the following experimental values of characteristic quantities at the points of completion of the $\Gamma_2 - \Gamma_4$ spontaneous reorientation transition in $TmFeO_3$ were obtained: $T_1 = 93.0$ K, $T_2 = 84.0$ K, $\nu_1 = 23$ GHz, and $\nu_2 = 20$ GHz. With allowance for the value of the Néel temperature $T_N = 632$ K, we have for the $\tau_{SR}$ parameter of this orthoferrite $\sim 0.14$. $TmFeO_3$ is an antipode of $YbFeO_3$ in the sense that an opposite relationship between the characteristic frequencies takes place in it, i.e., $\nu_\sigma \ll \nu_r$. This means that the entire dynamics at frequencies close to the magnitude of the gap, i.e., at minimum magnetoresonance frequencies, is mainly determined by the ordered subsystem of iron spins, whereas the soft mode is the $\sigma$ mode. This property of $TmFeO_3$ gave all grounds to correlate its dynamic characteristics with the theory of Ref. [4], which also was developed on the basis of the iron sublattices.

Figure 4 displays the phase diagram of $TmFeO_3$ in a field $\mathbf{H}||\mathbf{a}$, which was constructed by the same method as in the case of $YbFeO_3$. This diagram differs from that of $YbFeO_3$ only in a quantitative respect, namely, in the larger values of the temperature and field of the transition.

Figure 5 displays the temperature dependence of the soft-mode frequency upon spontaneous RPT and the temperature (field) dependences of the energy gaps in inducing fields of various orientations. The latter dependences were restored by

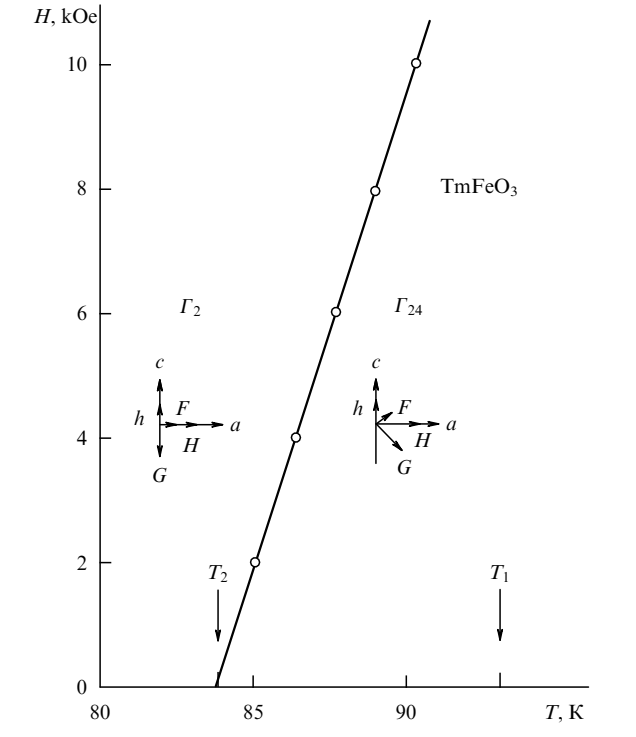


**Figure 4.** $H-T$ phase diagram of $TmFeO_3$ for a field $\mathbf{H}||\mathbf{a}$. Structures of the $\Gamma_2$ and $\Gamma_{24}$ phases are shown.

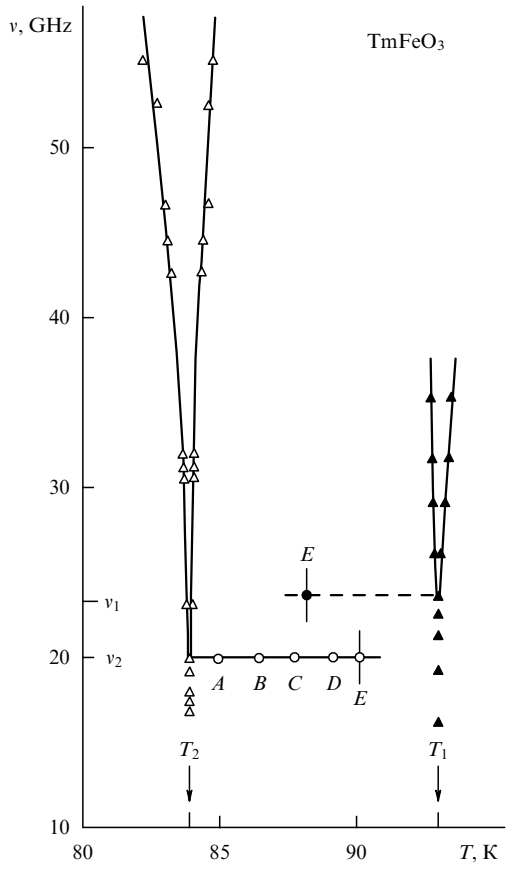


**Figure 5.** Temperature dependence of the soft-mode frequency in $TmFeO_3$ in the vicinity of the spontaneous reorientation transitions $\Gamma_2-\Gamma_{24}$ (△) and $\Gamma_4-\Gamma_{24}$ (▲), and of the energy gaps for the cases where these transitions are induced by fields **H**||**a** (○) and **H**||**c** (●) of the following strength: *A*, 2; *B*, 4; *C*, 6; *D*, 8; and *E*, 10 kOe.

scanning in temperature at fixed values of $H$. At the line of the $\Gamma_2-\Gamma_{24}$ transition, this was carried out in more detail: the gap was measured at the values of the field **H**||**a** equal to 2, 4, 6, 8, and 10 kOe. It can be seen from Fig. 5 that within the attained accuracy, the gap at the line of the induced $\Gamma_2-\Gamma_{24}$ transition is independent of the field (temperature). Since the process of measuring the gap is rather laborious, the authors of Refs [25, 26], having been convinced of its independence of $T$ and $H$ at the $\Gamma_2-\Gamma_{24}$ line, restricted themselves, when investigating the dynamics in the region of the $\Gamma_4-\Gamma_{24}$ transition, to measuring the gap only in the field **H**||**c** equal to 10 kOe, which is most easily experimentally accessible. The gap here also is independent of field (temperature). Thus, a picture is obtained which is qualitatively absolutely the same as in the case of $YbFeO_3$. Its main result is the independence of the energy gaps of the *field* at both points of the completion of spin reorientation induced by the fields **H**||**a** and **H**||**c**.

Therefore, all the conclusions of the previous section concerning $YbFeO_3$ can completely be referred to $TmFeO_3$ as well. Note only that no signs of the contribution of longitudinal vibrations of magnetization to the magnitudes of the energy gaps were found upon an increase in the parameter $\tau_{SR}$ by more than an order of magnitude in comparison with that for $YbFeO_3$. This means that the values $T_1$ and $T_2$ involved here are also 'insufficiently high' for the sought effect to be found, and that the initial (at $H=0$) gaps are formed through mechanisms that were investigated in detail in [1]. On the other hand, if the mechanisms developed in [4, 5] worked here, then the increase in the gap that should be expected in a field of 10 kOe would be, according to (2.1), ~8.4 GHz [25]. This significantly exceeds the error in the determination of the absolute magnitudes of the gaps.

**2.1.3 Temperature–field dependence of the energy gap at the point of the induced $\Gamma_2-\Gamma_{24}$ transition in $ErFeO_3$.** While $YbFeO_3$ and $TmFeO_3$ are characterized by the relations $\nu_r \ll \nu_\sigma$ and $\nu_\sigma \ll \nu_r$, respectively, for most REOFs a situation where $\nu_r \sim \nu_\sigma$ is characteristic. In this case, because of the strong dynamic f–d interaction, the experimentally observed soft mode cannot be considered as being caused by only one spin subsystem (iron or RE ions). This situation is characteristic of $ErFeO_3$, in particular. For this reason, further experiments were carried out on this crystal [27]. Note that the static characteristics of the orthoferrites of erbium and thulium are virtually coincident both qualitatively and quantitatively. Indeed, the boundaries of the spontaneous reorientation region in $ErFeO_3$ given in [27] ($T_1 = 100$ K and $T_2 = 90$ K) are virtually coincident with those of $TmFeO_3$. The same can be said about the temperature of ordering in the iron sublattice and, consequently, about the parameter $\tau_{SR}$. In $ErFeO_3$, we have $T_N \equiv T_{N1} = 636$ K, and $\tau_{SR} = 0.15$ (in $ErFeO_3$, as is known, apart from the temperature $T = T_{N1}$ for the iron ions, there is also a temperature of ordering of erbium ions, $T = T_{N2}$). The energy gap $\nu_2$ measured at the point $T = T_2$ for the spontaneous $\Gamma_2-\Gamma_{24}$ transition is equal to $26.2 \pm 0.2$ GHz. Note that in the conventional form the soft mode is detected only in the vicinity of $T_2$ and, as was shown in [15, 22], it is mainly formed by the vibrations of the spins of iron. Thus, we are dealing here with the σ mode at the point of the $\Gamma_2-\Gamma_{24}$ transition, i.e., precisely with that situation that is realized in $YFeO_3$ [4]. What is going on with the gap $\nu_2$ in a magnetic field **H**||**a**? The answer to this question will give an idea of which of the mechanisms is prevailing in the process of formation of the gap, i.e., whether this is the one developed in [4] or in [15]. The gap was measured in [27] at the field values of 1, 5, an 10 kOe. The results of these measurements are given in Fig. 6. In order to avoid giving the phase diagram of $ErFeO_3$, which in its main features coincides absolutely with that for $TmFeO_3$ (see Fig. 4) and only differs insignificantly in the values of the temperature and the field at the transition point, we give in Fig. 6 the field scale as well, apart from the temperature scale. The answer to the above question is obvious: within the accuracy of measurements (2 GHz), no increase in the magnitude of the gap was found. Therefore, in $ErFeO_3$ as well, at temperatures of $T < 100$ K, the longitudinal susceptibility and, correspondingly the contribution of longitudinal vibrations to the magnitude of the gap are negligibly small (as follows from measurements performed in [5], we have $\chi_{||}/\chi_\perp \ll 1$ at $T = 90$ K). In this compound, the gap is formed, both in the spontaneous and induced RPTs, by mainly precessional mechanisms. As was shown in [15], the gap at the point of the $\Gamma_2-\Gamma_{24}$ transitions is caused by the magnetoelastic and dipole contributions. Thus, based on the experiments with $YFeO_3$, $TmFeO_3$, and $ErFeO_3$, we may conclude that the independence of the gap magnitude on the field (temperature) is likely to be a common property of all REOFs in which the reorientation occurs at temperatures $T_1$, $T_2$ that are significantly less than the temperatures $T_N$ of ordering in the iron sublattice and, correspondingly, in relatively low fields. This fact is independent of the ratio of

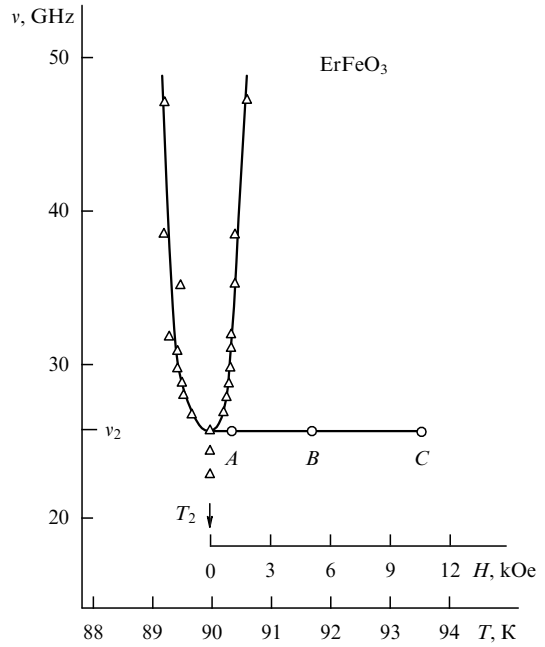


**Figure 6.** Temperature dependence of the soft magnetoresonance mode frequency (△) in $ErFeO_3$ in the vicinity of the spontaneous reorientation transition $\Gamma_2-\Gamma_{24}$ and of the energy gap (○) for the case when this transition is induced by fields $\mathbf{H}\|\mathbf{a}$ of the following strength: *A*, 1; *B*, 5; and *C*, 10 kOe.

the characteristic resonance frequencies $\nu_r$ and $\nu_\sigma$ and, consequently, of the degree of dynamic interaction of vibrational subsystems of iron and RE ions. This has not yet been explained in the existent thermodynamic theory [4, 5]. On the other hand, we may predict with a large degree of certainty that the analogous, in the technology and geometry of experiment, measurements on the same REOFs but in stronger fields ($H \sim 50-60$ kOe) should reveal noticeable effects of the manifestation of longitudinal vibrations in the dynamics of the considered magnets near an RPT. In view of the arguments that were stated in section 2.1.2, the most suitable compound for the comparison of the results of high-field measurements with the existent theory is $TmFeO_3$.

## 2.2 Dynamics of magnets near reorientation transitions at comparable contributions of the precessional and longitudinal vibrations of magnetization

Based on the above arguments, we should expect comparable contributions from the precessional and longitudinal vibrations to the dynamics of magnets in the RPT region either in compounds with relatively high temperatures of spontaneous reorientation $\tau_{SR}$ or in sufficiently strong magnetic fields. From the viewpoint of $\tau_{SR}$, the only REOF that falls into this group is $SmFeO_3$ ($T_1 = 478$ K, $T_2 = 450$ K, $T_N = 674$ K, $\tau_{SR} \approx 0.7$). However, attempts to carry out corresponding magnetoresonance measurements on this orthoferrite were unsuccessful. The reason is the small intensity and large width of the absorption lines [28], which appear to be due to the strong attenuation introduced at these high temperatures by the RE subsystem. Therefore, the necessity arose to search for a suitable compound outside the known set of REOFs. The compound most suitable for the attainment of this purpose turned out to be the weak ferromagnet $Fe_3BO_6$; the next section is therefore devoted to this compound.

### 2.2.1 High-frequency and acoustic properties of $Fe_3BO_6$ upon spontaneous RPT.

As all orthoferrites, $Fe_3BO_6$ has an orthorhombic structure. At $T < T_N = 508$ K, it is a weak ferromagnet. At $T = T_{SR} = 415$ K, a $\Gamma_2-\Gamma_4$ reorientation occurs in it, which is conventional for the REOFs. However, in contrast to the orthoferrites of rare earth metals, in $Fe_3BO_6$ this reorientation occurs as a first-order phase transition (PT-1), i.e., jumpwise, rather than through the canted phase $\Gamma_{24}$. The latter can be induced in this compound only by an applied field; we consider this question in the next sections. Here, we only consider the dynamic characteristics that are observed upon a spontaneous RPT. Since the corresponding results were not mentioned in review [1], we dwell on them in more detail. Upon the spontaneous reorientation, the magnetic resonance spectrum in $Fe_3BO_6$ was restored in most detail in Ref. [30], where an antiferromagnetic $\gamma$ mode with a frequency jump at the RPT point characteristic of the PT-1s was revealed for the first time. At the same time, it followed from the theory developed in Ref. [30] that the frequency of the ferromagnetic $\sigma$ mode at this point becomes zero without any frequency jump. The first experiments on the investigation of the soft $\sigma$ mode in the millimeter wave range [31] showed that in reality the spectrum of this mode contains a significant energy gap, equal to 17.5 GHz. Note that the temperature dependence of the resonance frequencies in this case has the conventional form characteristic of the soft mode (see, e.g., Fig. 6).

Thus, the concept of the full softening of the $\sigma$ mode stated in Ref. [30] has not been confirmed. Note that, proceeding from general considerations, it did not have to be confirmed, since at the PT-1 point (in contrast to the PT-2) the anisotropy energy and, consequently, the magnetic resonance frequency do not vanish. The residual anisotropy in this case causes the presence in the PT-1 point of a finite frequency gap. Consequently, the energy gap that was revealed in [31] may be of a quite different origin than in the case of a PT-2. If the residual anisotropy is large, it can completely mask the fine mechanisms of gap formation originating from both the dynamic interaction of various vibrational systems [15, 16] and the relaxational mode [4, 5]. Therefore, the experimental result obtained at this stage could be explained in at least three ways. One of these ignores the mechanisms developed in Refs [4, 5, 15, 16], since usually in a PT-1 the gap is determined by the residual anisotropy, and the transition vicinity itself is characterized by a certain range of phase lability. The extrapolation of the temperature dependences (on both sides of the RPT) to zero frequency yields lability temperatures of 419 and 410 K for the $\Gamma_2$ and $\Gamma_4$ phases, respectively. Another possibility consists in that the gap is completely determined by the mechanisms considered in Refs [4, 5, 15, 16] with a zero range of lability. This situation would mean that here the PT-1 is close to PT-2. The third possibility is a combination of the first two, when contributions come from both the mechanisms indicated and the residual anisotropy.

Because of the insufficient resolution of the technique used in [31], no unambiguous conclusion could be made on the presence or absence of a frequency jump at the RPT point. Therefore, later new experiments were conducted [32] with the use of a modified technique, aimed specially at this work. We consider these experiments in next sections.

Here, we also touch some magnetoacoustic measurements in the vicinity of the spontaneous $\Gamma_2-\Gamma_4$ transition in $Fe_3BO_6$. In Ref. [33], the experiments were mainly carried

out with the aim of establishing the character of the phase transition. As a result, various effects were revealed; some of them speak in favor of the PT-1, while others indicated PT-2. On this basis, a conclusion was drawn that the spontaneous RPT in $Fe_3BO_6$ in essence is of a boundary nature, intermediate between PT-1 and PT-2. One unusual effect that was revealed in this experiment consists in that, unlike all known ultrasonic measurements on REOFs, a decrease in the attenuation of sound passing through the sample is here observed at the RPT point. The velocity of the active sound wave in this case decreases, as could be expected, although insignificantly — by only 0.2%.

**2.2.2 Temperature (field) dependences of the energy gaps in $Fe_3BO_6$ upon induced $\Gamma_2-\Gamma_{24}$ and $\Gamma_4-\Gamma_{24}$ transitions.** As can be seen from the above, the conclusion that in real experiments the contributions of precessional and longitudinal vibrations of magnetization to the dynamics of reorientation should always be considered as coexistent and competing was not drawn until the spin-wave [15, 16] and thermodynamic [4, 5] models were checked in experiments that were conducted under essentially different conditions. These conditions were dictated by the properties of particular magnets that were used in experiments. And although in almost all cases these were REOFs with virtually the same ordering temperatures of iron ions ($T_N = 620-640$ K), the decisive factor turned out to be the difference in their static characteristics in the reorientation region.

It turned out upon comparison of the results of the corresponding experiments that the experiments that, taken separately, each confirmed one or another model were carried out in different ranges of temperature and field. As a result, the spin-wave model sufficiently well described the experimentally observed dynamics of magnets only near spontaneous transitions or induced transitions caused by relatively small fields ($H < 10$ kOe) at temperatures of the induced reorientation $T_{IR} \ll T_N$, whereas the thermodynamic model was first confirmed at $T_{IR}/T_N > 0.3-0.6$ in magnetic fields $H > 60$ kOe [4]. The latter circumstance permits one to interpret the significant role of the longitudinal susceptibility as the effect of a strong field. However, our analysis of the whole body of experiments devoted to the investigation of the dynamics upon induced reorientation shows that the very fact of the manifestation of longitudinal vibrations in resonance properties is independent of the magnitude of $H$, although the absolute magnitude of the gap increment in a field, predicted by the theory of Refs [4, 5], undoubtedly increases with the field. The ratio of the contributions to the dynamics from precessional and longitudinal vibrations correlates rather with the relative temperature of the induced reorientation $\tau_{IR} = T_{IR}/T_N$, which at $H = 0$ is identical to $\tau_{SR}$. We will show, using $Fe_3BO_6$ as an example, that the longitudinal vibrations at the relatively large value of $\tau_{SR}$ characteristic of this compound give a noticeable contribution to the dynamics even at $H = 0$. First of all, we note some specific technical and methodical features of these measurements.

A sample of $Fe_3BO_6$ of volume about 2.5 mm$^3$ had a form close to that shown in the inset in Fig. 7. It was glued by its *ac* plane in the center of the piston that short-circuited the rectangular $H_{10}$ microwave type waveguide. The mutual orientation of the vectors of ferromagnetism **F** and the magnetic component of the microwave field **h** which is optimum for the detection of the soft ferromagnetic mode is $\mathbf{F} \perp \mathbf{h}$. However, in order to have the opportunity to carry out

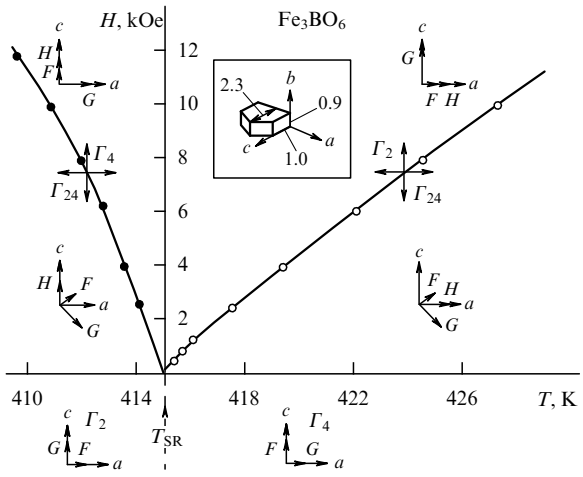


**Figure 7.** $H-T$ phase diagram and the structure of the field-induced phase transitions in $Fe_3BO_6$: $\Gamma_4-\Gamma_{24}$ in a field $\mathbf{H}\|\mathbf{c}$ (•) and $\Gamma_2-\Gamma_{24}$ in a field $\mathbf{H}\|\mathbf{a}$ (○). In the bottom portion of the figure, the structure of the spontaneous transition $\Gamma_2-\Gamma_4$ (at $H = 0$) is shown; $T_{SR}$ is the spontaneous transition temperature; in the inset, the shape and the characteristic dimensions of the sample are shown (in mm).

measurements in both the $\Gamma_2-\Gamma_{24}$ and $\Gamma_4-\Gamma_{24}$ transitions without changing the geometry of the experiment and without remounting the sample, the vector **h** was oriented at an angle of 45° to the crystal axes **a** and **c**.

The measurements were carried out on a direct-gain spectrometer in the regime of reflected power. The facility permitted us to record the resonance absorption by scanning both in the temperature at $H = \text{const}$ and in the field at $T = \text{const}$.

The main results were obtained in the regime of changing temperature at fixed values of the magnetic field modulated with a frequency of 39 Hz. In this case, using a number of frequencies in the range 12–26 GHz, we recorded the derivative of the signal with respect to temperature. From these records, we restored the temperature dependences of magnetoresonance frequencies for each specified value of $H$. The application of the modulation technique permitted us to increase the sensitivity and the resolution of the spectrometer by more than an order of magnitude in comparison with that attained in Ref. [1].

Figure 7 displays a low-field fragment of the $H-T$ phase diagram of $Fe_3BO_6$ corresponding to the points of termination of the $\Gamma_4-\Gamma_{24}-\Gamma_2$ reorientation in a field $\mathbf{H}\|\mathbf{c}$ (at $T < T_{SR}$) and $\Gamma_2-\Gamma_{24}-\Gamma_4$ in a field $\mathbf{H}\|\mathbf{a}$ (at $T > T_{SR}$). The figure also shows the structures of these transitions. The diagram was obtained from the results of high-frequency measurements shown in Fig. 8. Each point in Fig. 7 corresponds to the position of the minimum frequency of the soft magnetoresonance mode in the temperature and in the field. The vertical and horizontal arrows arbitrarily indicate two ways of intersecting phase boundaries in the $H-T$ phase diagram when recording absorption signals by scanning in $H$ and $T$. The diagram shown was obtained by scanning in temperature. In this case, each point in the diagram corresponds to a specified transition field, and the temperature of the transition is determined by the position of the absorption peaks obtained from the slopes of the resonance lines. This position, as is seen from Fig. 8, is independent of the frequency within the measurement error, but behaves individually depending on $H$.

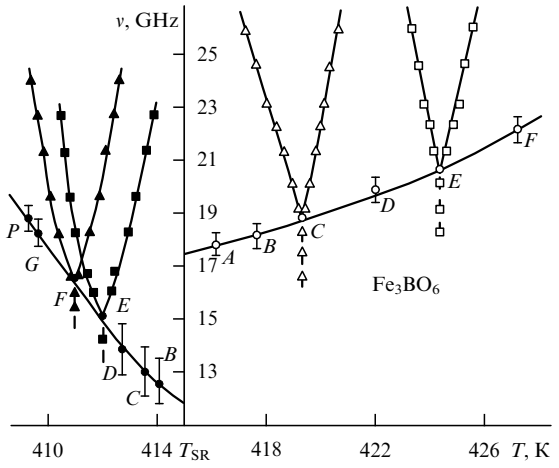


**Figure 8.** Temperature dependences of the soft-mode frequencies and energy gaps at the point of completion of the reorientation in $Fe_3BO_6$. Characteristic dependences of the soft-mode frequency in fields **H**||**c** of strengths 8 kOe (■) and 10 kOe (▲) and in fields **H**||**a** of strengths 4 kOe (△) and 8 kOe (□). Dependences of the gap magnitudes at the point of completion of the spin reorientation in fields **H**||**c** (•) and **H**||**a** (○). The points in the temperature dependences of the gaps correspond to the following values of the field : *A*, 1.25; *B*, 2.5; *C*, 4; *D*, 6; *E*, 8; *F*, 10; *G*, 12; and *P*, 12.5 kOe. Vertical dashed lines connect the points that correspond to the absorption peaks obtained from the slopes of the resonance lines.

The phase diagram of $Fe_3BO_6$ given in Fig. 7 differs from those typical of REOFs in the vicinity of the $\Gamma_2-\Gamma_4$ transitions in that here the phase boundaries do not intersect one another (cf., e.g., with Fig. 1). The fact that the lines of the second-order phase transitions concur at the point $H=0$, $T=T_{SR}$, where the $\Gamma_2-\Gamma_4$ first-order phase transition occurs, is unique. This means that the spontaneous PT-1 (its structure is shown in the lower part of Fig. 7) can simultaneously be regarded as a $\Gamma_2-\Gamma_{24}-\Gamma_4$ type PT-2 in which the boundaries $T_1$ and $T_2$ (the temperatures of the start and finish of reorientation) coincide. Note that in REOFs the width of the region of existence of the canted phase $\Gamma_{24}$ upon spontaneous transitions, $\Delta T=T_1-T_2$, usually varies from a few to tens of Kelvins. Since the spontaneous transitions $\Gamma_2-\Gamma_{24}$ and $\Gamma_4-\Gamma_{24}$ in REOFs are second-order phase transitions, in all cases we have $\Delta T>0$. Here, however, we have a situation corresponding to $\Delta T=0$, which, in turn, permits one to assume that the spontaneous $\Gamma_2-\Gamma_4$ type PT-1 that is realized in $Fe_3BO_6$ is close to PT-2. This viewpoint, based on the results of high-frequency [31] and ultrasonic [33] measurements, has already been stated above. In this connection, we should note the calculation of magnetoresonance frequencies in $Fe_3BO_6$ [30], from which it follows that at the point of the spontaneous $\Gamma_2-\Gamma_4$ transition both the energy gap and the frequency jump in the soft-mode spectrum characteristic of PT-1s are absent. As was noted above, Arutunyan et al. [31] did find a significant energy gap, although no frequency jump was, indeed, detected. The latter circumstance, as we now understand, is connected with the insufficient resolution of the technique that was used in Ref. [31], and the frequency jump, as was shown in later measurements [32], does exist. However, this does not affect the conclusion that here we are dealing with a PT-1 close to PT-2.

Figure 8 gives examples of temperature dependences of the soft-mode frequency in magnetic fields of various amplitudes and orientations. The minimum frequency of each such dependence is the energy gap $\nu_{IR}$ at the point of completion of the reorientation induced by the field **H**||**a** or **H**||**c**. From the whole body of the results of such measurements, we restored the temperature dependences of the gap $\nu_{IR}$, which are also given in Fig. 8. Their extrapolation to the point of the spontaneous transition $\Gamma_2-\Gamma_4$ yields a value of the gap $\nu_{SR}=11.8\pm1.5$ GHz from the low-temperature side and a value of $17.5\pm0.5$ GHz from the high-temperature side. Note that the absolute value of the frequency jump at the phase boundary significantly exceeds the measurement error of determining the gaps.

It is obvious that the results of measurements given above may also be represented in the frequency-field coordinates. This is of interest because it is that form in which the results of the high-field measurements of $Fe_3BO_6$ in the submillimeter wave range were published [34], which we will use below for a comparison with the results of Ref. [32]. The field dependences of the gaps obtained experimentally in [32] are shown in Fig. 9. We distinguish the following most important results of these measurements.

1. In contrast to all previous cases cited above, it was revealed here for the first time that the curves of the temperature and field dependences of the energy gaps at the line of phase transitions approach the point $T=T_{SR}$, $H_{IR}=0$ with nonzero derivatives $\partial\nu_{IR}/\partial T$ and $\partial\nu_{IR}/\partial H$.

2. The field derivative is positive at any temperatures ($\partial\nu_{IR}/\partial H>0$), whereas $\partial\nu_{IR}/\partial T<0$ in the range $T<T_{SR}$ and $\partial\nu_{IR}/\partial T>0$ in the range $T>T_{SR}$.

3. The temperature (field) dependences of the energy gaps at temperatures above and below $T_{SR}$ are substantially different. Their extrapolation to $H=0$, $T=T_{SR}$ yields different values of the gaps $\nu_{SR}$, i.e., there is a frequency jump at the point of the spontaneous $\Gamma_2-\Gamma_4$ transition, and both gaps $\nu_{SR}$ have significant absolute values.

Let us compare these data with other experiments and with the theory that existed at the time when the experiments described were performed. First of all, we consider the latter

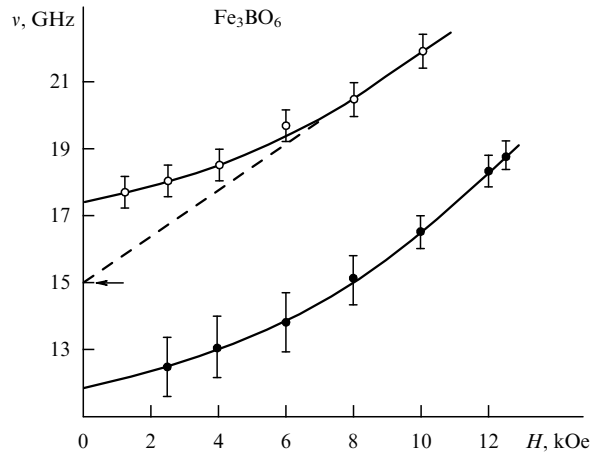


**Figure 9.** Field dependences of the energy gaps in $Fe_3BO_6$ at the points of completion of the spin reorientation transitions $\Gamma_4-\Gamma_{24}$ (•) and $\Gamma_2-\Gamma_{24}$ (○) in fields **H**||**c** and **H**||**a**, respectively. The arrow shows the magnitude of the gap ($15\pm1.5$ GHz) at the point of the spontaneous transition $\Gamma_2-\Gamma_4$; this magnitude was obtained by extrapolation of the field dependence of the gap measured in [29] from the region $H=40-80$ kOe. The dashed line corresponds to a linear extrapolation of the field dependence (given in this work) of the gap at the line of the $\Gamma_2-\Gamma_{24}$ transition from the region of fields $H>8$ kOe to the point $H=0$.

result. The frequency jump revealed at the point of the spontaneous transition has no direct relation to the purpose of the present investigation, but it should be taken into account in the interpretation of experimental data. This effect is unexpected, since it not only does not follow from the calculations of the magnetoresonance spectra of $Fe_3BO_6$, but in the theory of Ref. [30] its absence has been specially substantiated, although, as is known, such a jump is a characteristic sign of a PT-1.

Since a magnetic field transforms the PT-1 into a PT-2, the above frequency jump should vanish in an applied field, according to the existent concept. But, then, what does its retention upon such a transformation of the character of the transition in $Fe_3BO_6$ mean? We may assume that in relatively small fields, i.e., under the conditions of an already induced PT-2, but near the spontaneous PT-1, this is a kind of a memory of the last transition. This resembles the situation when in an inclined magnetic field the energy gaps $\nu_1$ and $\nu_2$ transform into merely the minimum frequencies as a kind of a memory of the vanished PT-2, when at any values $H$, $T$, only the canted phase $\Gamma_{24}$ is realized (see, e.g., Fig. 2). Thus, the anisotropy of the energy gap in a magnetic field is induced by the proximity to the PT-1. This influence may be explained by the fact that in $Fe_3BO_6$ the spontaneous PT-1 is close to PT-2 in its nature. As a result, the PT-2 induced by a relatively small field becomes unstable and the more so, the closer (both in $T$ and $H$) it is located to the point of the spontaneous PT-1.

Such an explanation of the results is confirmed by the extrapolation of the temperature (field) dependences of the gaps to the point of the spontaneous transition from the regions of $T$ and $H$ that are maximally distant from this point. For the $\Gamma_{24}-\Gamma_2$ transition, we will use the results of measurements [34] at $H > 8$ kOe and $T > 425$ K, whose extrapolation to the zero field yields $\nu_{SR} \cong 15$ GHz (Fig. 9). For the $\Gamma_{24}-\Gamma_4$, it is preferable to use the data of Ref. [29], in which the field dependences of the gap were restored in the ranges of $H = 40-80$ kOe and $T = 290-380$ K. Their extrapolation to the zero field yields the same value of the gap at the point of the spontaneous transition. Although this approach is rough, we should note that the tendency to the coincidence of the thus-obtained values of the gaps is logical, since this extrapolation is carried out from the regions where the PT-2 is sufficiently stable, and we remember that for the PT-2 the absence of a frequency jump is a fundamental property. It is this value of $\nu_{SR}$ that should be considered as the 'starting' gap, i.e., inherent in the spontaneous RPT. But in $Fe_3BO_6$, this is the common starting gap upon the induction of the RPT by both the field $\mathbf{H}||\mathbf{a}$ and $\mathbf{H}||\mathbf{c}$. For an REOF, this would mean that $\nu_1 = \nu_2$. The field gradient of this gap is 0.7 GHz kOe$^{-1}$ (dashed line in Fig. 9), whereas the extrapolation of the field dependences to the zero field from the range of 1–3 kOe for both transitions yields $\partial\nu_{IR}/\partial H \cong 0.2$ GHz kOe$^{-1}$ (solid lines in the same figure). Somehow or other, we in any case have $\partial\nu_{IR}/\partial H > 0$ even at $H = 0$. Note that in fields of 10–12 kOe the increments of the starting gaps are several times the maximum error of measurements. To what extent do the results presented here agree with the thermodynamic theory? To answer this question, we turn to expression (2.1). Its modification to suit $Fe_3BO_6$ [34] does not violate the main conclusion: as $H \to 0$, the gap at the point of the termination of induced reorientation also tends to zero. Thus, neither the initial nor the modified theoretical models correspond to the experimentally observed dynamics of $Fe_3BO_6$ near the RPT, when $H \to 0$. However, their fundamental property, i.e., the fact that $\partial\nu_{IR}/\partial H > 0$ at $H_{IR} > 0$, as the evidence of the contribution of longitudinal vibrations of magnetization and relaxation to the dynamics, is indubitable and gives an easy test for the identification of this contribution in experiments.

With such a relatively high temperature of spontaneous reorientation ($\tau_{SR} \cong 0.8$), $Fe_3BO_6$ seems to be better than other similar compounds for comparison with the thermodynamic theory. The field dependence of the energy gaps obtained in Ref. [34] for a range of fields $H = 40-80$ kOe at appropriate temperatures $\tau_{IR} = 0.5-0.7$ is indeed explained by this theory very well. This dependence, as was noted above, is almost linear, which permits one to easily extrapolate it to zero field. The first of the above-mentioned results, in our opinion, is indeed related to the large value of $\tau_{SR}$, which, in turn, causes the large value of the factor $\chi_{||}/\chi_{\perp}$ in the expression for the gap. From the temperature dependence of $\chi_{||}/\chi_{\perp}$ for the $\Gamma_2-\Gamma_{24}$ transition in $YFeO_3$, we may estimate the value of this factor for $Fe_3BO_6$ as well. As a result, for the point $T = T_{SR}$ we obtain $\chi_{||}/\chi_{\perp} \approx 0.7$. The correctness of resorting to the results of Ref. [4] is well warranted by the fact that the entire dynamics in both $YFeO_3$ and $Fe_3BO_6$ is caused by only the subsystem of iron ions.

The large value of the ratio $\chi_{||}/\chi_{\perp}$ in $Fe_3BO_6$ even in a zero field permits us to look at the nature of the energy gap observed here upon the spontaneous transition in a different way. In the above-presented experiments with the orthoferrites of ytterbium, thulium, and erbium, we dealt with relatively low temperatures of spontaneous transitions $\tau_{SR}$ and, consequently, with small $\chi_{||}/\chi_{\perp}$. Therefore, the corresponding results were described well within the framework of the spin-wave approximation taking into account only precession. If we follow the logic of the redistribution of partial contributions of the precessional and longitudinal vibrations depending on $\tau_{SR}$, then we should assume that in $Fe_3BO_6$ even the starting gap is formed to a significant extent at the expense of the latter. As an outward sign of this, the nonzero derivative $\partial\nu_{IR}/\partial H$ at $H = 0$ may serve. An increase in the field $\mathbf{H}||\mathbf{c}$ or $\mathbf{H}||\mathbf{a}$ increases the amplitude of this contribution. But the presence of an applied magnetic field by no means is a necessary condition for the participation of longitudinal vibrations of magnetization in the formation of the spin dynamics of reorientation. And it is only in this sense that the related partial contribution to the magnitude of the gap is not the effect of a strong field. Naturally, this does not follow from the existent thermodynamic theory, in which not only $\nu_{IR} \to 0$, but also $\partial\nu_{IR}/\partial H \to 0$ as $H \to 0$. The question of the exact relationship between the contributions of precessional and longitudinal vibrations at $H \to 0$ requires, of course, special calculations, especially when the expected contributions are comparable in magnitude. At present, the theory yields a satisfactory answer only in the limiting cases: at $T_{IR}/T_N \ll 1$ (spin-wave model) and at $T \to T_N$ (thermodynamic model).

Now, we turn to the field dependences of the gaps shown in Fig. 9. From the fact that at $H = 0$ not only $\nu_{IR}$, but also $\partial\nu_{IR}/\partial H$ do not vanish, there follows one more aspect that should be taken into account when describing the actually observed dynamics in most compounds of this type. This aspect consists in the following. The initial theory [4] was developed for $YFeO_3$, in which no spontaneous RPTs occur and the resonance mode in the zero field softens only at the point $T = T_N$. As applied to $YFeO_3$, this theory is valid without any restrictions. Its extension to $DyFeO_3$ [4] proved

to be possible only in a range of temperatures that are much higher than $T_{SR}$. Thus, both in $YFeO_3$ and in $DyFeO_3$ the transition field is nonzero over the whole working temperature range where the role of longitudinal vibrations becomes noticeable. A question arises: How can the situation be described when $H_{IR}$ vanishes not only at $T = T_N$, but also at an intermediate point from a temperature range $0 - T_N$? In compounds with small $\tau_{SR}$, the contribution of longitudinal vibrations to the magnitude of the gap can manifest itself in the corresponding increase in $T_{IR}$. This took place, e.g., in $DyFeO_3$ [4] in fields $H > 40$ kOe at $T = 100 - 400$ K. In this situation, the contribution of longitudinal vibrations to the dynamics of the magnet near an RPT can indeed be regarded as a strong-field effect. A new aspect in experiments with $Fe_3BO_6$, which has already been noted previously, consists in that here the spontaneous transition occurs at large $\tau_{SR}$, so that the increment $\Delta\nu_{SR} \neq 0$ even in fields $H = H_{IR} \to 0$.

### 2.3 Dynamics of magnets near the reorientation transition under conditions where the longitudinal susceptibility predominates over the transverse susceptibility

In the simplest case of two-sublattice antiferromagnets (e.g., $MnF_2$, $CuCl_2{\cdot}2H_2O$) or weak ferromagnets (e.g., $YFeO_3$, $Fe_3BO_6$), the field-induced transitions occur under conditions where the exchange energy substantially exceeds the energy of magnetic anisotropy. Therefore, in such compounds a classical situation is realized where the $\chi_{||}/\chi_{\perp}$ ratio cannot be greater than unity. The value $\chi_{||}/\chi_{\perp} = 1$ is attained only at $T = T_N$, i.e., when the compound passes into the paramagnetic state. We have already mentioned this above when considering experiments on $YFeO_3$ and $DyFeO_3$. The same situation undoubtedly takes place in all the other REOFs if we mean only the subsystem of iron ions.

It turns out that in $ErFeO_3$ the opposite relationship between the exchange and anisotropy energies can be realized. This, in turn, gives the opportunity to induce a kind of a metamagnetic transition in it, whose distinctive property is the unusually high longitudinal susceptibility. Let us consider the magnetoresonance and acoustic properties of the erbium orthoferrite near this RPT.

**2.3.1 Frequency (field) dependences of the energy gap upon the metamagnetic transition in $ErFeO_3$.** The d–d, d–f, and f–f exchange interactions in $ErFeO_3$ play different roles in the formation of its static and dynamic properties in different temperature ranges. The evolution of the magnetic structure of this orthoferrite is well known. A whole number of spontaneous RPTs are realized in it. Apart from the above-mentioned $\Gamma_2 - \Gamma_{24} - \Gamma_4$ transition, there occurs one more spontaneous reorientation at helium temperatures, namely, $\Gamma_2(F_xG_z) - \Gamma_{12}(F_xG_{zy})$. In its structure, this transition is combined: 'order–order' in the subsystem of iron ions and 'disorder – order' in the subsystem of erbium ions. At $T < T_{N2} \approx 4$ K, a rotation of the antiferromagnetism vector **G** of the iron subsystem in the *bc* plane starts and simultaneously an antiferromagnetic ordering of erbium spins along the *c* axis commences. Because of the large single-ion anisotropy of erbium, which substantially exceeds the energy of the exchange f–f interaction, the rare-earth subsystem can be regarded as a metamagnet. The field **H**||**c** (i.e., directed along the axis of antiferromagnetism of the subsystem of erbium ions) can cause a metamagnetic transition consisting in the collapse of the magnetic moments of erbium ions [35]. The dynamics of the erbium orthoferrite near this transition is precisely what will interest us in what follows. Figure 10 displays a fragment of the $H-T$ phase diagram of $ErFeO_3$ obtained by the dielectric resonance method [36] on a spherical sample of diameter $d = 1.8$ mm, which was diminished later to a diameter $d = 0.9$ mm and used in magnetoresonance experiments. The main parameters of the diagram are as follows: the ordering temperature of the erbium subsystem $T_{N2} = 3.9 \pm 0.1$ K; the tricritical-point temperature $T_t = 2.7 \pm 0.1$ K; and the tricritical-point field $H_t = 4.1 \pm 0.1$ kOe. Since the region of the PT-2 of interest, as is known [35], can only be in the range of $T_t - T_{N2}$, it is sufficient to conduct the investigations in the ranges of temperatures $T = 2.7 - 4$ K and fields $H = 0 - 4.1$ kOe.

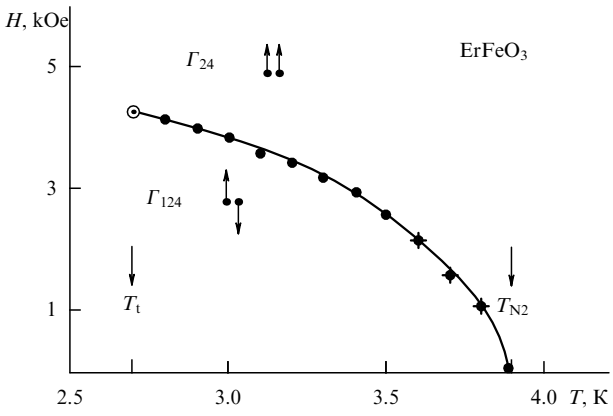


**Figure 10.** $H-T$ phase diagram of $ErFeO_3$ upon the metamagnetic $\Gamma_{24} - \Gamma_{124}$ transition in the erbium subsystem at **H**||**c**. The solid arrows indicate the directions of the erbium sublattice magnetizations on both sides of the transition line. $T_{N2} = 3.9$ K is the temperature of the spontaneous $\Gamma_2 - \Gamma_{12}$ transition; $\odot$ is the tricritical point $T_t = 2.7$ K.

The temperature dependence of the soft-mode frequency was established for the first time in Ref. [19]. To date, the qualitative and quantitative characteristics of this dependence and the nature of this mode have already been determined. It was reliably established that it is caused by the spin vibrations of erbium ions. Since in the context of this paper we will only be interested in the temperature (field) dependence of the gap, rather than the magnetoresonance spectrum itself, we will not give it here once more. We will only use the value of the energy gap in this spectrum, $\nu_{N2} = 26.1 \pm 0.2$ GHz, measured at the point of the spontaneous transition $\Gamma_2 - \Gamma_{12}$ at $T_{N2} = 3.9$ K and trace what will happen with this gap at the line of the metamagnetic transition $\Gamma_{24} - \Gamma_{124}$.

As can be seen from Fig. 11, $\nu_{N2}$ starts to increase rapidly with the decrease in the temperature and the corresponding increase in the field **H**||**c** [37]. At the line of the PT-2 transition, the gap increases from 26.1 GHz at $T = T_{N2}$ to 38 GHz at the point $T = T_t$, passing through an insignificant maximum. How can we explain the increase in the gap in this induced transition? Note that the conditions of the realization of this transition from the viewpoint of the relationship between the temperatures of reorientation and ordering differ substantially from those characteristic of all the above-considered RPTs in REOFs. If for the subsystem of iron ions in $ErFeO_3$ we have $T_2/T_{N1} \ll 1$, for erbium this ratio changes from $T_t/T_{N2} \cong 0.7$ at the tricritical point to 1 at $T = T_{N2}$. In the subsystem of iron ions, this would corre-

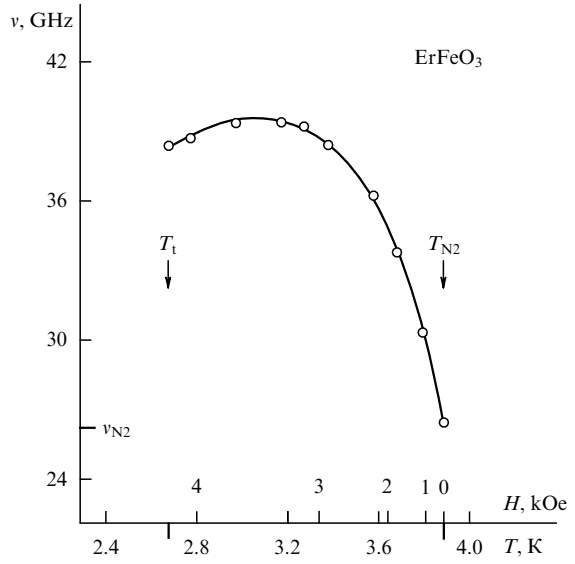


**Figure 11.** Temperature (field) dependence of the energy gap upon the metamagnetic $\Gamma_{24}-\Gamma_{124}$ transition in the erbium subsystem of $ErFeO_3$ at **H**||**c**.

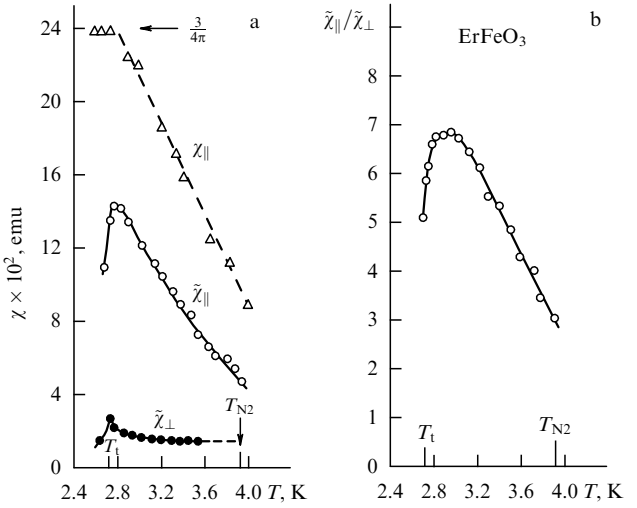


**Figure 12.** (a) Temperature dependences of the susceptibility at the line of the second-order metamagnetic transition in the erbium subsystem of $ErFeO_3$: (△) longitudinal static susceptibility $\chi_{||}$; (○) longitudinal high-frequency susceptibility $\tilde{\chi}_{||}$; and (•) transverse high-frequency susceptibility $\tilde{\chi}_{\perp}$. (b) Temperature dependence of the susceptibility ratio $\tilde{\chi}_{||}/\tilde{\chi}_{\perp}$.

spond to the change in $\chi_{||}/\chi_{\perp}$ from 0.7 to 1 [5] and to a noticeable increase in the magnitude of the gap. The fact that at the line of the metamagnetic transition $\chi_{||}/\chi_{\perp}$ in reality increases stimulated the conduction of corresponding measurements of susceptibility.

A characteristic property of metamagnets is an extremely high longitudinal susceptibility and a vanishing transverse susceptibility. The purely formal resort to the model of Ref. [4] gives grounds to expect a corresponding increase in the gap value in this case. Although the metamagnetic transition in the subsystem of erbium ions occurs against the background of the spin reorientation of the iron sublattices, the longitudinal susceptibility here is mainly determined by the erbium subsystem, since at helium temperatures the contribution of the iron subsystem to the magnetization of $ErFeO_3$ is insignificant [38, 39]. Therefore, all the results of measurements that will be given below just characterize the sublattice of erbium, whose longitudinal susceptibility can be measured directly. The introduction of a field **H**||**c** transforms the ferromagnetic structure of erbium into a ferrimagnetic one and, in the final account, causes the collapse of its sublattices when a field $H = H_{IR}$ is reached. Measurements of static susceptibility in this transition were carried out in Ref. [34]. It was established that the external susceptibility at the transition line increases with decreasing temperature and increasing field, attaining its maximum value close to $3/4\pi$ (the inverse value of the demagnetizing factor of the spherical sample) at the point $T = T_t$ (Fig. 12a). This fact by itself indicates the existence of a relation (following from [4]) between the longitudinal susceptibility and the gap width. But since in this work we are investigating dynamic effects, it was more logical to turn to the high-frequency susceptibility. The measurements of the longitudinal ($\tilde{\chi}_{||}$) and transverse ($\tilde{\chi}_{\perp}$) high-frequency susceptibilities were carried out in magnetic fields **H**||**c**, **h**||**c** and **H**||**c**, **h**||**a**, respectively, using the dielectric-resonance method [36] at frequencies of the millimeter wave range, i.e., substantially lower in comparison with those characteristic of the corresponding experiments performed by the magnetoresonance methods. The latter circumstance permits us to identify the high-frequency susceptibility measured in this way with the static susceptibility $\chi$ when performing a qualitative comparison of the theory and experiment. It was found that at the transition line $\tilde{\chi}_{||}$ increases monotonically, reaching a maximum at $T = T_t$ as well. However, in the temperature dependence of the $\tilde{\chi}_{||}/\tilde{\chi}_{\perp}$ ratio, a maximum appears at $T = 3$ K (Fig. 12a, 12b).

It can be seen from a comparison of Fig. 11 and 12b that there is a clearly pronounced correlation between the temperature dependences of $\tilde{\chi}_{||}/\tilde{\chi}_{\perp}$ and the magnitude of the gap $\nu_{N2}$. Qualitatively, this corresponds to the model of Ref. [4]. Note that here $\tilde{\chi}_{||}/\tilde{\chi}_{\perp}$ reaches a value $\sim 7$ (Fig. 12b), whereas upon the conventional reorientation of iron sublattices in the $\Gamma_2-\Gamma_{24}$ transition the limiting value of $\tilde{\chi}_{||}/\tilde{\chi}_{\perp}$ by definition cannot be greater than unity. This difference is related to the specific difference between the induced transitions $\Gamma_2-\Gamma_{24}$ and $\Gamma_{24}-\Gamma_{124}$. When the temperature increases, at the point $T_{N1}$ there proceeds an 'order–disorder' transition in the pure form, i.e., iron subsystem goes from a weakly ferromagnetic state into a paramagnetic state. A similar transition in the erbium subsystem is actually a transition of the 'antiferromagnet–ferromagnet' type. This causes the difference in the behavior of their susceptibilities: the maximum value $\tilde{\chi}_{||}/\tilde{\chi}_{\perp} = 1$ in the iron subsystem is attained at the ordering point $T_{N1}$, whereas the $\tilde{\chi}_{||}/\tilde{\chi}_{\perp}$ value at the ordering point of the erbium subsystem $T_{N2}$, on the contrary, is minimum ($\sim 3$). If we assume that the magnetic field, represented by the linear factor in the expression for the gap (2.1), plays an equal role in the formation of both $\nu_2$ and $\nu_{N2}$, then we may note the following. Whereas at the $\Gamma_2-\Gamma_{24}$ transition point the effect of the increase in the gap $\nu_2$ has not been found even at $H = 10$ kOe, upon the metamagnetic transition this effect is clearly pronounced; already at as low a field as $H \approx 4$ kOe, the gap increases by a factor of 1.5. Therefore, upon the comparison of the dynamics of the erbium orthoferrite near the above transitions the increase in the energy gap in a magnetic field should be related to precisely the magnitude of the longitudinal susceptibility. The results obtained in this part of the work can be explained

quantitatively by none of the above models. Apart from already mentioned disadvantages, these models, naturally, do not take into account the specificity of the $\Gamma_{24}-\Gamma_{124}$ transition, which is mainly based on its complex (combined) character. The maximum in the temperature dependence $v_{N2}(T)$ can be a result of both this specificity and the additive summation of the partial contributions to the formation of the gap from the mechanisms developed in Refs [5] and [15]. No correct explanation of this feature can now be made quantitatively in terms of the existent theories. However, its presence does not affect the main result of this experiment: the conclusion that the magnitude of $v_{N2}(T)$ correlates with $\tilde{\chi}_{||}/\tilde{\chi}_{\perp}(T)$. This is the most convincing evidence of the fact that the increment in the gap upon the metamagnetic transition in $ErFeO_3$ is mainly related to the longitudinal vibrations of the magnetization of the erbium sublattices. Comparing these experimental results with those presented in Section 2.1.3, we may, using $ErFeO_3$ as an example, draw an important conclusion that the spin-wave and thermodynamic approaches are not contradictory. Indeed, using the same compound, a good agreement with experiment was demonstrated for both the first and second approaches. At temperatures $T = T_2 \ll T_{N1}$, the $\Gamma_2-\Gamma_{24}$ transition in a field $\mathbf{H}||\mathbf{a}$, typical of REOFs, agrees with the model of Ref. [15], according to which the gap $v_2$ is caused by the magnetoelastic and dipole contributions. On the other hand, at the point of the metamagnetic $\Gamma_{24}-\Gamma_{124}$ transition, the gap is formed as a result of both transverse and longitudinal vibrations of magnetization and is a result of the additive summation of these partial contributions. The starting value of the gap $v_{N2}$ can well be explained by the spin-wave theory [15], whereas the increment in $v_{N2}$ in a field $\mathbf{H}||\mathbf{c}$ is, rather, caused by the longitudinal vibrations of magnetization [5, 40].

**2.3.2 Correlation between the high-frequency and acoustic characteristics of $ErFeO_3$ near the metamagnetic transition.** As was shown in review [1], in terms of the spin-wave approximation the dominating interaction upon the formation of energy gaps can be magnetoelastic coupling. However, in the thermodynamic (exchange) approximation, when the main role is played by the longitudinal vibrations, the energy gap at the transition point can exceed the magnetoelastic contribution by almost an order of magnitude [4]. This was established in experiments [5] with $YFeO_3$ and $DyFeO_3$. However, in contrast to these orthoferrites, in $ErFeO_3$ the magnetoelastic contribution to the formation of the gap $v_{N2}$ proved to be comparable with the contribution from the longitudinal vibrations. In this connection, we may expect a corresponding response of the elastic subsystem to the redistribution of the roles of the transverse and longitudinal susceptibilities in the formation of the spin dynamics of magnets near the metamagnetic transition. As a result, because of the dynamic interaction of the spin and elastic subsystems, their initial vibrational spectra should suffer corresponding deformations due to not only transverse, but also longitudinal vibrations of magnetization. Before we turn to the results of acoustic experiments, we note the following. It is known that the numerical values of $T_t$ and $T_{N2}$ are very sensitive to impurities and to the technology of growing single crystals. The samples that were used in high-frequency and ultrasonic experiments were prepared from different batches of the starting materials and differed somewhat in their parameters: in the first case, they have $T_{N2} = 3.9 \pm 0.1$ K, $T_t = 2.7 \pm 0.1$ K; in the second case, $T_{N2} = 4.1 \pm 0.1$ K and $T_t = 2.6 \pm 0.1$ K. The magnetic field $H_t$ corresponding to the tricritical point was $4.1 \pm 0.1$ kOe for the spherical sample 0.9 mm in diameter, on which magnetoresonance measurements were conducted. For the samples that were used for ultrasonic measurements (disks 4 mm in diameter, 1.9 mm thick), this field was of the same order of magnitude: $6 \pm 0.5$ kOe. Therefore, we represent the set of the quantities measured at the line of the metamagnetic transition as a function of the dimensionless temperature

$$\tau = \frac{T - T_t}{T_{N2} - T_t} . \tag{2.2}$$

The resort to the dimensionless temperature permits one to compare results obtained on samples prepared of different raw materials. For convenience, the results of ultrasonic measurements are given in Fig. 13 together with the high-frequency characteristics shown in Figs 11, 12 [41]. For this transition, the active mode, i.e., one that interacts with magnons, is the transverse acoustic mode with a wave vector $\mathbf{q}||\mathbf{c}$ and polarization of the vector of shear deformation $\boldsymbol{\varepsilon}||\mathbf{b}$ (either $\mathbf{q}||\mathbf{b}$, $\boldsymbol{\varepsilon}||\mathbf{c}$). The anomalies of its velocity and absorption were first revealed experimentally in [42] and later studied in detail both experimentally [43, 44] and theoretically [15]. Their specific features are the giant decrease in the velocity ($\Delta s/s \approx 25\%$), asymmetric with respect to $T$ and having a resonance form, and increase in the sound absorption $\Delta\Gamma \approx 100$ dB cm$^{-1}$), which have not been registered either previously or later in any one REOF. In Fig. 13, $s = 3.98 \times 10^5$ cm s$^{-1}$ is the speed of the active transverse sound far from the transition, which is virtually the same at temperatures both greater and less than $T_{N2}$. The figure displays the temperature dependences of the decrease in the velocity of the active sound wave and of the increase in the attenuation of the longitudinal (inactive) sound mode at the line of the PT-2. As is seen, the point of the spontaneous transition ($\tau = 1$) corresponds to the maximum changes of acoustic characteristics of both sound modes ($\Delta s/s \approx 20\%$, $\Delta\Gamma \approx 1.2$ dB cm$^{-1}$). The quantities $\Delta s/s$ and $\Delta\Gamma$ were qualitatively explained in [1], and on the whole the dynamics of this spontaneous transition is satisfactorily described in

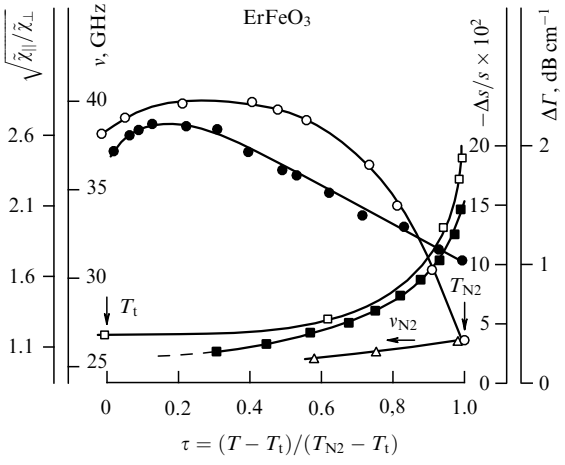


**Figure 13.** Temperature (field) dependences of various dynamic parameters at the line of the second-order metamagnetic phase transition in $ErFeO_3$: (•) square root of the high-frequency susceptibility ratio $\sqrt{\tilde{\chi}_{||}/\tilde{\chi}_{\perp}}$; (○) energy gap at $\mathbf{H}||\mathbf{c}$; (□) relative change in the velocity of the active transverse sound mode $\Delta s/s$ (at $\mathbf{q}||\mathbf{c}$, $\boldsymbol{\varepsilon}||\mathbf{b}$); (■) change in the attenuation of longitudinal sound $\Delta\Gamma$; and energy gap at $\mathbf{H}||\mathbf{a}$ (△).

terms of the spin-wave approach. We emphasize that in the chosen geometry of the experiment the sound waves selected are, respectively, transverse and longitudinal relative to not only **q**, but also to the vector of antiferromagnetism of the subsystem of erbium ions. This permits us to suggest that the transverse and longitudinal vibrations of magnetization of the erbium ions are related to the corresponding acoustic excitations.

As previously, when turning to the induced RPT, we will consider quantities measured at the point of the spontaneous transition as the starting values. Then, the possible effects of the manifestation of longitudinal vibrations of magnetization should be sought among the temperature (field) gradients of the parameters measured. Both models can be used in this case. Indeed, although in the existent form the theory [10] was developed for spontaneous transitions, it does not contain any specific effects related to the magnetic field or restrictions concerning induced transitions. In many cases, it successfully describes the dynamics of both transitions, whereas in the model of Ref. [5] the spontaneous transitions are not considered at all, and the predicted effects are caused by the presence of a magnetic field.

In what follows, we will not be interested in the numerical values of the fields at each point in the dependences in Fig. 13. It is only important to understand the general situation: that the field at the line of the phase transition increases monotonically with decreasing temperature (see Fig. 10).

Note a number of important circumstances that follow from the dependences shown in Fig. 13. In addition to the conclusions of Section 2.3.1 on the existence of a correlation between the temperature dependences of $\nu_{N2}$ and $\tilde{\chi}_{||}/\tilde{\chi}_{\perp}$ at $\mathbf{H}||\mathbf{c}$, we add that in the field $\mathbf{H}||\mathbf{a}$, when the induced transition has the same structure as the spontaneous one (i.e., $\Gamma_2-\Gamma_{12}$), the initial gap $\nu_{N2}$ virtually does not alter (to be exact, it even has a small tendency to decrease with decreasing temperature). Let us perform a comparative analysis of high-frequency and acoustic characteristics.

First of all, note that at the point of the spontaneous transition all of the above characteristics and their gradients with respect to temperature (field) are extremal. With decreasing temperature and corresponding increasing field, the gradients decrease monotonically (by the absolute values) and all become softly sloped in the region of $\tau \sim 0.3-0.5$. If we ignore the insignificant decrease in $\nu_{N2}$ and $\tilde{\chi}_{||}/\tilde{\chi}_{\perp}$ upon the decrease in temperature in the region of $\tau \sim 0-0.3$, then we can speak of the existence of a correlation between the dynamic characteristics of the spin and elastic subsystems at the line of the metamagnetic PT-2. This already suggests the necessity of taking into account the magnetoelastic interaction in the description of the dynamics of orthoferrites in the region of RPTs induced by the field. Until a more perfect and full theory arises, the experimental results given above could only be explained qualitatively [41]. On the whole, they are consistent with the concept of the redistribution of the roles of the transverse and longitudinal magnetization vibrations in the formation of the dynamics of orthoferrites in the reorientation region.

We begin from a well-known fact. The anomaly of the sound velocity upon the spontaneous transition is caused by the coupling of the transverse sound wave with the transverse magnetization vibrations at the natural frequency of the soft magnetoresonance mode. The extent of this coupling is shown in Ref. [15]. In the field $\mathbf{H}||\mathbf{c}$, the susceptibility of the f subsystem substantially exceeds the transverse susceptibility and increases with increasing $H$ and decreasing $T$ in the range from $T_{N2}$ to $T_t$. But the sound wave, which has a transverse polarization, does not interact with longitudinal vibrations of magnetization. Therefore, with decreasing temperature, the anomaly of the velocity of this wave decreases in accordance with the extent of the redistribution of the roles of transverse and longitudinal vibrations in the formation of the spin dynamics and, consequently, with decreasing the effect of the spin subsystem on the acoustic subsystem through the magnetoelastic coupling. For the iron subsystem, this temperature range, undoubtedly, satisfies the spin-wave approximation, since $T_{N2} \ll T_{N1}$. Virtually no changes in the longitudinal components of the vectors **F**, **G** are observed here. At the same time their transverse components can take part in the formation of the dynamics. The residual anomaly of the sound velocity in the range $\tau = 0-0.3$, which is $\sim 4\%$ of the value of $s$, is most likely to be due to just transverse vibration of iron spins. Indeed, on the order of magnitude it is comparable with the change in the velocity of active sound in the range of the 'high-temperature' reorientation of the iron subsystem at $T = 90-100$ K, where $\Delta s/s$ reaches $\sim 1.5\%$ [44]. The reasons for which the anomaly in the velocity in the last case may be less than for the 'low-temperature' reorientation of iron $\Gamma_2-\Gamma_{12}$ have been analyzed in detail in [15]. But, on the contrary, in $TmFeO_3$, where the dynamics of the $\Gamma_2-\Gamma_4$ transition is determined almost completely by the iron sublattices, $\Delta s/s$ reaches $\sim 3\%$ [45], which is even closer to the value obtained here. To date, it has been established in many experiments that acoustic waves suffer attenuation (the longitudinal waves to a lesser degree and the transverse ones to a greater) upon various spin-reorientation transitions in REOFs. We in this case are interested in the longitudinal wave with $\mathbf{q}||\mathbf{H}||\mathbf{c}$. How can its attenuation be related to the longitudinal susceptibility? At the point of the spontaneous transition the attenuation of this wave is maximum. With decreasing temperature and increasing field, $\Gamma$ decreases. With an appropriate choice of scales on the $\Delta\Gamma$ and $\Delta s/s$ axes, we can see that the dependences of $\Delta\Gamma$ and $\Delta s/s$ on $T$ and $H$ virtually coincide in general. The most evident reason for the decrease in sound attenuation on approaching the tricritical point is the increase in the rigidity of the magnetic sublattices of erbium (as a result of both the spontaneous saturation of magnetization as $T \to 0$ and the effect of the applied magnetic field $\mathbf{H}||\mathbf{c}$). Although the total longitudinal susceptibility increases in this case, the attenuation of the longitudinal sound is rather related to its fluctuating part. The component of the longitudinal susceptibility can be represented as a sum of two terms: $\chi_{zz}^{L} + \chi_{zz}^{F}$, where $\chi_{zz}^{L}$ is the susceptibility jump at the point of the PT-2, predicted by the Landau – Lifshitz theory, and $\chi_{zz}^{F}$ is the fluctuational increase in the susceptibility. For $ErFeO_3$, this is also justified by that the RPT at hand is a combination of transitions of two types: reorientation in the subsystem of iron ions and ordering in the erbium subsystem. In this case, the first summand reflects the 'rigid' portion of the erbium susceptibility whose ordering through the f–d coupling causes the reorientation of the vector **G**, and the second term is due to fluctuations of the components of the vectors of ferromagnetism and antiferromagnetism of erbium. It was shown in Ref. [46] that on approaching the tricritical point the relative contribution of fluctuations to the magnitude of the longitudinal susceptibility at the PT-2 line decreases: theoretically, we have $\Delta\chi_{zz}^{F}/\Delta\chi_{zz}^{L} \to 0$ as $T \to T_t$, $H \to H_t$. The absolute value of $\Delta\chi_{zz}^{L}$ grows faster than $\Delta\chi_{zz}^{F}$, which, in the final account, just

causes the increase in the role of the longitudinal susceptibility in the formation of the energy gap, as follows from the theory of Refs. [4, 5]. Finally, it is expedient to note the following. The field **H**||**c**, in contrast to **H**||**a**, not only induces the transition, but also changes the structure of the initial phase. If in the second case the transition has, as was noted, the same structure as the spontaneous transition has, then at **H**||**c** it transforms into the $\Gamma_{24}-\Gamma_{124}$ type. In the structure of the initial phases of both Fe and the RE sublattices, components of the ferromagnetism vectors of iron and erbium that are longitudinal with respect to **H** arise, which are characteristic of the representation $\Gamma_4$. Upon the introduction of a magnetic field **H**||**c**, erbium, which is spontaneously ordered to form an antiferromagnetic structure, actually becomes a ferrimagnet with a difference between the magnetizations of the sublattices in the form of the $z$ component of the ferromagnetism vector of erbium. It is possible that it is the change in the structure of the initial phases that causes the maximum gradients of the characteristics shown in Fig. 13 just at the point of such a transformation.

### 2.4 Summary of the results of experimental investigations

To close the presentation of the results of the experimental investigation of the dynamics of REOFs near various RPTs, we draw some general conclusions. They were obtained based on a comparative analysis of the whole body of experimental data both presented here and described in previous studies of the low-energy dynamics of these compounds in the region of reorientation transitions.

1. The dynamics of REOFs in the RPT region under real experimental conditions is formed under the action of both precessional and longitudinal vibrations of magnetization. The relationship between these two contributions to the magnitudes of the energy gaps depends on the properties (mainly, static) of the particular compound.

2. The ratio of the temperature of the spontaneous transition $T_{SR}$ to the temperature of ordering $T_N$ of a corresponding spin subsystem can serve as a parameter that characterizes the ratio of these contributions near the points of spontaneous transitions; this ratio is individual for each particular magnet. It was established that if this ratio $\tau_{SR}$ is less than 0.15, the longitudinal vibrations introduce no noticeable contribution to the experimentally observed dynamics.

3. At $\tau_{SR} > 0.7$, the contribution of longitudinal vibrations of magnetization can even be revealed in weak fields. In this case, the energy gap at the transition point can be a result of additive and comparable in magnitude contributions from both spin-wave and thermodynamic mechanisms.

4. In the presence of two spin subsystems in a magnet (which is characteristic of the REOFs), the nature of the soft mode at the transition point has no effect on the redistribution of the contributions of the precessional and longitudinal motions of magnetization to the magnitude of the energy gap.

5. The starting gap (the value of the gap at $T = T_{SR}$ and $H = 0$) at a sufficiently large magnitude of $\tau_{SR}$ (when the effect of longitudinal vibrations is no longer masked by other mechanisms of gap formation) always grows with increasing field, but the corresponding temperature may in this case both increase and decrease. This means that the thermodynamic theory [3–5] in the existent form can adequately describe the results of only high-field experiments, when the gap is mainly determined by the magnetic field and longitudinal susceptibility.

6. The observed correlation of various dynamic characteristics at the line of the metamagnetic transition in erbium orthoferrite, i.e., of the high-frequency susceptibility, energy gap, and the velocity and attenuation of sound, indicates the necessity of taking into account the magnetoelastic coupling in the thermodynamic description as well. The allowance for this effect is also of great importance for the reason that the reorientation in most REOFs occurs in the temperature range where neither spin-wave nor thermodynamic approximations work rigorously.

7. The last conclusion suggests an actual necessity for the creation of a new, more complete and universal, theory of the dynamic properties of magnets near RPTs, which would be suitable for arbitrary values of the temperature and field. Then the existent spin-wave and thermodynamic models could be its limiting cases at $T \to 0$ and $T \to T_N$, respectively. In this case, one should be forced to accept the unusual statement that most experimentally observed soft modes can be classified neither as purely relaxational, nor as being caused by only precessional motion, or modes of solely spin origin. Moreover, the soft magnetoresonance modes (in the classical understanding) not only are never observed in real experiments, but even in principle cannot be observed in view of restrictions of a fundamental character (e.g., because of the spontaneously broken symmetry [17]). The entire previous review [1] is actually devoted to presenting experimental and theoretical evidence that in reality (even without the allowance for the longitudinal vibrations) a system of coupled vibrations always persists. The role of longitudinal vibrations of magnetization in the formation of the dynamics of magnets in the spin-reorientation region was established in experiments that are given here.

## 3. Theory

The experimental part of this review is devoted to the investigation of the dynamic properties of magnets with a complex many-sublattice structure. At the present time, the theory that takes into account the effect of longitudinal vibrations of sublattice magnetizations and their relaxation on the spectrum of spin and coupled magnetoelastic waves has only been developed for the simplest magnetically ordered substances, i.e., a ferromagnet and a two-sublattice antiferromagnet [6, 7]. However, as we will see below, this theory is of a more general character and proves to be sufficient for a qualitative description of all the above-considered experimental results for complex magnets such as REOFs and other similar compounds.

### 3.1 Effect of magnetization relaxation on the spectrum of spin and elastic vibrations of a ferromagnet in the region of a reorientation phase transition

In ferromagnets in a ferromagnetically ordered state in the dissipationless approximation, the vibrations of transverse components of magnetization represent spin waves [47]. Spin waves can be considered as the precession of magnetization about the direction of the effective magnetic field. With allowance for the dissipation in the magnetic subsystem, the spin waves are damped. In this case, there also exist longitudinal vibrations of magnetization. They are relaxational. Usually, the dissipation in magnets is small and, therefore, the spin waves are regarded to be weakly damped. This takes place if the ferromagnet is in states far from RPT points, when the real parts of $\omega_{pr}$ of spin wave frequency are much greater

than the imaginary parts $|\omega_r|$: $\omega_{pr} \gg |\omega_r|$. However, as is shown below, near an RPT (the RPT point is usually determined by the condition $\omega_{pr} \to 0$) the real part of the frequency of spin waves may become less than the imaginary part, which, of course, will affect the frequency spectrum of vibrations of the ferromagnet.

Following Refs [6, 48], we clarify how the relaxation of the magnetization of a ferromagnet affects its magnetic and elastic vibrations in the regions of an RPT and a magnetic phase transition of the order–disorder type (Curie point).

**3.1.1 The ground state, equations of motion, and dispersion relation of a ferromagnet.** As an example, we consider a biaxial ferromagnet with isotropic elastic and magnetoelastic properties, whose free-energy density is

$$F = \frac{1}{2}\alpha\left(\frac{\partial \mathbf{M}}{\partial x_i}\right)^2 + \frac{1}{2}A\mathbf{M}^2 + \frac{1}{4}B\mathbf{M}^4 + \frac{1}{6}C\mathbf{M}^6 + \frac{1}{2}\beta_1 M_x^2 + \frac{1}{2}\beta_2 M_y^2 + \frac{1}{2}\beta_3 M_z^2 - \mathbf{MH} + \frac{1}{2}b_0\mathbf{M}^2 u_{ll} + \frac{1}{2}b_1 M_i M_k u_{ik} + \frac{1}{2}\lambda u_{ll}^2 + \mu u_{ik}^2 , \tag{3.1}$$

where $\alpha$, $A$, $B$, $C$, $\beta$, and $b$ are the exchange, anisotropy, and magnetostriction constants, respectively; $\mathbf{M}$ is the magnetization of the ferromagnet; $\mathbf{H}$ is the strength of the applied magnetic field; $\hat{u}$, the deformation tensor; and $\lambda$ and $\mu$, the Lamé constants.

Without restricting the generality, we now consider the case of $\mathbf{H}||\mathbf{x}$ and the ground state of the ferromagnet, in which $\mathbf{M}||\mathbf{H}$. This phase is stable at

$$\beta_2 - \beta_1 + \frac{H}{M} \geqslant 0 ,$$
$$\beta_3 - \beta_1 + \frac{H}{M} \geqslant 0 ,$$
$$2\widetilde{B}M^2 + 4CM^4 + \frac{H}{M} \geqslant 0 , \tag{3.2}$$

where the magnitude of $M$ is determined from the equation

$$(A + \beta + \widetilde{B}M^2 + CM^4)M = H , \tag{3.3}$$

and $\widetilde{B}$ is the exchange constant renormalized by the magnetoelastic interaction:

$$\widetilde{B} = B - \frac{b_0 b_1 + 3b_0^2/2 + b_1^2(\lambda+\mu)/(2\mu)}{3\lambda + 2\mu} . \tag{3.4}$$

The tensor of equilibrium deformations $u_{ik}^{(0)}$ in the phase $\mathbf{M}||\mathbf{H}||\mathbf{x}$ has the form

$$u_{ik}^{(0)} = -\frac{2b_0\mu - \lambda b_1}{4\mu(3\lambda+2\mu)}M^2\delta_{ik} - \frac{b_1}{4\mu}M_i M_k . \tag{3.5}$$

When studying the dynamics of the magnetic and elastic subsystems, we proceed from the Landau – Lifshitz equations and the elasticity equation [47, 49, 50]

$$\dot{\mathbf{M}} = g(\mathbf{M} \times \mathbf{H}_{ef}) + \mathbf{R} ,$$
$$\rho u_i = \frac{\partial \sigma_{ik}}{\partial x_k} , \tag{3.6}$$

where $\rho$ is the density of the material; $\mathbf{u}$ is the displacement vector; $\mathbf{H}_{ef} = -\delta F/\delta\mathbf{M}$ is the effective magnetic field; and $\sigma_{ik} = \partial F/\partial u_{ik}$ is the stress tensor. Following Landau and Khalatnikov and Hilbert, we write the relaxation term $\mathbf{R}$ in the form

$$\mathbf{R} = r_1\frac{\mathbf{M}\times\dot{\mathbf{M}}}{M} + r_2 gM\mathbf{H}_{ef} . \tag{3.7}$$

Here, $r_{1,2}$ are the dimensionless attenuation constants. The linearized set of equations of motion that determine the dynamics of magnetization and the displacement vector of the ferromagnet in the phase with $\mathbf{M}||\mathbf{H}||\mathbf{x}$ for magnetoelastic waves propagating along the $x$ axis is

$$(\omega + ir_2\omega_{1k})m_x - gM^2 r_2(b_0+b_1)ku_x = 0 ,$$
$$\frac{1}{\rho}ik(b_0+b_1)Mm_x + (\omega^2 - \omega_l^2)u_x = 0 ,$$
$$\omega m_{y,z} \mp (i\omega_{3,2k} + r_1\omega)m_{z,y} \pm \frac{1}{2}gM^2 b_1 k u_{z,y} = 0 ,$$
$$\frac{1}{2\rho}ikb_1 Mm_{y,z} + (\omega^2 - \omega_t^2)u_{y,z} = 0 . \tag{3.8}$$

Here, $\mathbf{m}$ and $\mathbf{u}$ are the Fourier components of the oscillatory part of the magnetization and displacement vector of the ferromagnet, respectively; $\mathbf{k}$ is the wave vector; $\omega_{l,t} = s_{l,t}k$; and $s_l^2 = (\lambda+2\mu)/\rho$ and $s_t^2 = \mu/\rho$ are the squared velocities of the longitudinal and transverse sound, respectively. The characteristic frequencies of the magnetic subsystem are expressed as

$$\omega_{1k} = gM(\alpha k^2 + A + \beta_1 + 3\widetilde{B}M^2 + 5CM^4 + h_{l1}) ,$$
$$\omega_{2,3k} = gM\left(\alpha k^2 + \beta_{2,3} - \beta_1 + \frac{H}{M} + h_t\right) , \tag{3.9}$$

where

$$h_{l1} = M^2\frac{\mu(b_0+b_1)^2 + 2\mu b_0^2 + \lambda b_1^2}{\mu(3\lambda+2\mu)} ,$$
$$h_t = \frac{b^2M^2}{4\mu} \tag{3.10}$$

are the dimensionless magnetoelastic fields.

Note that at the points of loss of the stability of the phase with $\mathbf{M}||\mathbf{H}||\mathbf{x}$, which are determined by the equality signs in (3.2) and coincide with the points of anhysteretic first-order RPTs and with the Curie point (at $H = 0$), the $\omega_{2k}$, $\omega_{3k}$, and $\omega_{1k}$ frequencies, respectively, soften (at $h_{l1,t} = 0$) or, otherwise, the precession mode $\omega_{pr} = (\omega_{2k}\omega_{3k})^{1/2}$ and one of the relaxation modes: (a) $\omega_{r2} = -ir_1\omega_{2k}$ or $\omega_{r3} = -ir_1\omega_{3k}$; (b) $\omega_{r1} = -ir_2\omega_{1k}$. The dispersion relation for coupled vibrations has the form

$$\{(1+r_1^2)\omega^6 + ir_1\omega^5(\omega_{2k}+\omega_{3k}) - \omega^4[2\omega_t^2(1+r_1^2) + \omega_{2k}\omega_{3k}] - 2ir_1\omega^3\omega_t^2(\omega_{2k}+\omega_{3k}-\omega_{me\,t}) + \omega^2\omega_t^2[\omega_t^2(1+r_1^2) + \omega_{2sk}\omega_{3k} + \omega_{3sk}\omega_{2k}] + ir_1\omega\omega_t^4(\omega_{2sk}+\omega_{3sk}) - \omega_t^4\omega_{2sk}\omega_{3sk}\} \times [(\omega^2-\omega_l^2)(\omega + ir_2\omega_{1k}) + r_2\omega_l^2\omega_{me\,l}] = 0 , \tag{3.11}$$

where

$$\omega_{2,3sk} = \omega_{2,3k} - \omega_{me\,t} , \quad \omega_{me\,t} = gMh_t ,$$
$$\omega_{me\,l} = gMh_{l2} = gM^3\frac{(b_0+b_1)^2}{\lambda+2\mu} . \tag{3.12}$$

The first factor on the left-hand side of this equation describes the vibrations of the interacting transverse components of the magnetization and of the displacement vector, and the second factor describes the vibrations of the longitudinal components of the magnetization and of the displacement vector. We consider these vibrations separately.

**3.1.2 Effect of the transverse relaxation of the magnetization on the spectrum of spin waves.** We first investigate in more detail the vibration spectrum of transverse components of the magnetization of the ferromagnet in the absence of magnetoelastic coupling ($h_t = 0$). In this case, the dispersion equation takes on the form

$$(1 + r_1^2)\omega^2 + \mathrm{i}r_1\omega(\omega_{2sk} + \omega_{3sk}) - \omega_{2sk}\omega_{3sk} = 0\,. \qquad (3.13)$$

Its solution (at $r_1 \ll 1$) has the form

$$\omega_{1,2} = -\frac{1}{2}\mathrm{i}r_1(\omega_{2sk} + \omega_{3sk}) \pm \left[\omega_{2sk}\omega_{3sk} - \frac{1}{4}r_1^2(\omega_{2sk} - \omega_{3sk})^2\right]^{1/2}. \qquad (3.14)$$

It can be seen that far from the RPT points, in which, according to (3.2), (3.9), and (3.12) we have $\omega_{2s0} = 0$ (transition $M_x \to M_x, M_y$) or $\omega_{3s0} = 0$ (transition $M_x \to M_x, M_z$), when $\omega_{2sk}\omega_{3sk} \gg r^2(\omega_{2sk} - \omega_{3sk})^2$, the entire effect of the relaxation of magnetization on the precessional vibrations of its transverse components reduces to that the spin waves become weakly damped. As to the points near an RPT, e.g., those at which $\omega_{2s0} \to 0$ (in this case $\omega_{2sk} \ll \omega_{3sk}$ if $k \to 0$), the situation can change dramatically. Thus, in the case where $\omega_{2sk}\omega_{3sk} \ll r^2(\omega_{2sk} - \omega_{3sk})^2$, the solution to (3.14) represents purely relaxational vibrations:

$$\omega_1 = -\mathrm{i}\frac{\omega_{2sk}\omega_{3sk}}{r_1(\omega_{3sk} - \omega_{2sk})}\,, \qquad \omega_2 = -\mathrm{i}r_1\omega_{3sk}\,. \qquad (3.15)$$

These frequencies determine the inverse relaxation times of the transverse components of the magnetization of the ferromagnet. The relaxation mode $\omega_1$ is soft; its frequency tends to zero at the boundary of stability of the phase as $k \to 0$. In the RPT region where $\omega_{3s0} \to 0$, the solution is expressed by the formulas (3.15) in the right-hand sides of which the indices 3 should be replaced by 2 and *vice versa*.

Thus, in the absence of magnetoelastic coupling, far from an RPT, the vibrations of the transverse components of magnetization represent weakly decaying spin waves, whereas near the RPT, the precessional character of motion of these components can change to become purely relaxational. In this last case, the soft mode is the relaxational transverse mode (its frequency is zero at the transition point itself at $k = 0$), and the RPT itself in this case occurs just through this mode.

**3.1.3 Effect of the transverse relaxation of magnetization on the spectrum of magnetoelastic waves.** Now, we introduce a magnetoelastic interaction. For definiteness, we investigate the spectrum of coupled vibrations near the RPT where $\omega_{2s0} \to 0$. By equating the first braces in (3.11) to zero, we obtain the dispersion relation for the transverse components of the magnetization and of the displacement vector. First, we write its solution at $k = 0$:

$$\omega_{1,2} = \pm\left[\omega_{20}\omega_{30} - \frac{1}{4}r_1^2(\omega_{20} - \omega_{30})^2\right]^{1/2} - \frac{1}{2}\mathrm{i}r_1(\omega_{20} + \omega_{30})\,, \qquad (3.16)$$

$$\omega_{3,4,5,6} = 0\,.$$

At the RPT point ($\omega_{2s0} = 0$), it follows from (3.2), (3.9), and (3.12) that $\omega_{20} = \omega_{me\,t}$. So, it can be seen that with allowance for the magnetoelastic coupling the solution $\omega_{1,2}$ describes the damped precessional motion of magnetization both far from the RPT and near it, since the condition $\omega_{me\,t}\,\omega_{30} > r_1^2(\omega_{me\,t} - \omega_{30})^2$ is fulfilled virtually always if $r_1 \ll 1$. The other four frequencies can describe both relaxational and elastic vibrations. In order to clarify their origin, we find the solution to the dispersion equation (3.11) at $k \neq 0$ (but $k \to 0$). This solution is as follows:

$$\omega_{1,2} = \pm\left[\omega_{2k}\omega_{3k} - \frac{1}{4}r_1^2(\omega_{2k} - \omega_{3k})^2\right]^{1/2} - \frac{1}{2}\mathrm{i}r_1(\omega_{2k} + \omega_{3k})\,,$$

$$\omega_{3,4} = \pm\omega_t\left(1 - \frac{\omega_{me\,t}}{\omega_{3k}}\right)^{1/2} - \frac{1}{2}\mathrm{i}r_1\omega_t^2\frac{2\omega_{3k} + \omega_{me\,t}}{\omega_{3k}^2}\,,$$

$$\omega_{5,6} = \omega_t \pm \frac{(4\omega_{2k}\omega_{2sk} - r_1^2\omega_t^2)^{1/2} - \mathrm{i}r_1\omega_t}{2\omega_{2k}}\,. \qquad (3.17)$$

Formulas (3.17) were obtained at $\omega_t \ll \omega_{2k}, \omega_{3k}$ and $r_1 \ll 1$. It follows from these formulas that the spectrum of coupled vibrations of the ferromagnet near the RPT at $k \neq 0$ consists of a weakly damped quasispin branch $\omega_{1,2}$, a weakly damped transverse quasielastic branch $\omega_{3,4}$, and an $\omega_{5,6}$ branch whose character is determined by the relationship between the quantities $\omega_{2k}\omega_{2sk}$ and $r_1^2\omega_t^2$. At $\omega_{2k}\omega_{2sk} \gg r_1^2\omega_t^2$, the $\omega_{5,6}$ branch represents a weakly damped transverse quasielastic branch of vibration with a quadratic dispersion law (because it follows from (3.2), (3.9), (3.12) that $\omega_{2sk} = gM\alpha k^2$ at the RPT point):

$$\omega_{5,6} = \pm\omega_t\left(\frac{\omega_{2sk}}{\omega_{2k}}\right)^{1/2} - \frac{1}{2}\mathrm{i}r_1\frac{\omega_t^2}{\omega_{2k}}\,. \qquad (3.18)$$

For $\omega_{2k}\omega_{2sk} \ll r_1^2\omega_t^2$, the $\omega_{5,6}$ branches represent relaxation vibrations (quasimagnetic and quasielastic) with a quadratic dependence on the absolute value of the wave vector:

$$\omega_5 = -\mathrm{i}\frac{\omega_{2sk}}{r_1}\,, \qquad \omega_6 = -\mathrm{i}r_1\frac{\omega_t^2}{\omega_{2k}}\,. \qquad (3.19)$$

The $\omega_{1,2}$ branch at $k \to 0$ is activational, with a gap that is determined according to (3.17) by the magnetoelastic coupling and magnetization relaxation. The other branches are activationless. One of the quasielastic branches of vibrations ($\omega_{3,4}$) near the RPT has a linear dispersion law at $k \to 0$ with a small dispersion of the propagation velocity [the factor $(1 - \omega_{me\,t}/\omega_{3k})^{1/2}$ in Eqn (3.17)]. The allowance for the magnetization relaxation leads to a decay of this elastic branch. The interaction between the magnetic and elastic vibrations exerts the strongest effect on the dispersion law of the second activationless branch of coupled vibrations $\omega_{5,6}$. This branch can be both quasielastic and quasimagnetic. In both cases, the dispersion law of this branch is quadratic. At $\omega_{2k}\omega_{2sk} \gg r_1^2\omega_t^2$, the $\omega_{5,6}$ is quasielastic. At $\omega_{2k}\omega_{2sk} \ll r_1^2\omega_t^2$, the $\omega_{5,6}$ branches describe purely relaxational vibrations (quasispin and quasielastic, respectively). It is these two modes that become softened on approaching an RPT.

Note that near the RPT the condition $\omega_{2k}\omega_{2sk} \ll r_1^2\omega_t^2$ actually reduces to the condition imposed on the parameters of the problem. Since at $k \to 0$ and near the RPT we have $\omega_{2k} \approx \omega_{\mathrm{me}\,t}$ and $\omega_{2sk} \approx gM_0\alpha k^2$, this condition can be written as $gM_0\alpha\omega_{\mathrm{me}\,t} \ll r_1^2 s_t^2$, i.e., it reduces to the condition imposed on the attenuation parameter. At typical values of the ferromagnet parameters, e.g., $g \approx 10^7$ $\mathrm{Oe}^{-1}\,\mathrm{s}^{-1}$, $M_0 \approx 10^2$ G, $\alpha \approx 10^{-12}\,\mathrm{cm}^{-2}$, $s_t \approx 10^5\,\mathrm{cm\,s}^{-1}$, $b_1 \approx 10^2$, $\mu \approx 10^{12}\,\mathrm{erg\,cm}^{-3}$, the following restriction on the decay parameter is obtained: $r_1 \gg 10^{-4}$. This condition can well be fulfilled near the RPT, since it is known that the attenuation of spin waves increases strongly with approaching the RPT [51].

Near an RPT with $\omega_{3s0} \to 0$, the expressions for the spectrum can be obtained from (3.16)–(3.19) by replacing 2 by 3.

Thus, in the RPT region all types of transverse motions in a ferromagnet (of both magnetization and lattice) can be reduced to purely relaxational vibrations. In this case, the transition occurs precisely through relaxational soft modes. With allowance for magnetoelastic coupling, the spectrum of coupled vibrations of the ferromagnet always contains a weakly damped quasispin mode. The transformation of the softening quasielastic branch of vibrations near the RPT into a purely relaxational mode may serve as an explanation to why neither its 100% decrease at the RPT point predicted by the previous theory [2] nor its dispersion on approaching the RPT point were observed in experiments on sound velocity measurements in the RPT region [43, 52].

**3.1.4 Interaction of longitudinal vibrations of the magnetization and the elastic subsystem.** It is known that the allowance for the magnetoelastic interaction in magnets in the RPT region leads, along with the effect of the formation of a magnetoelastic gap in the spectrum of spin waves, to a quadratic dispersion law for at least one of transverse elastic waves [17]. The propagation velocity of such waves in the theoretical limit tends to zero at the RPT point as $k \to 0$. Under real experimental conditions, this shows up in the anomalous decrease of the velocity of the transverse sound (to 50% or even greater) on approaching the RPT [52]. Near the RPT, the minimum theoretical value of the transverse sound velocity is given as $\tilde{s}_l = s_l(1 - s_t^2/s_l^2)^{1/2}$, where $s_t$ and $s_l$ are the velocities of the noninteracting transverse and longitudinal elastic waves, respectively [17]. According to this formula, the maximum theoretical value of the change in the velocity of longitudinal sound $\Delta s_l/s_l$ cannot exceed 25% (at $s_t = s_l\sqrt{2}$ [50]). The experimentally observed decrease in the velocity of longitudinal sound near the RPT and Curie points [53–55] did not exceed this theoretical limit.

In Refs [48, 56], it was theoretically predicted that in the region of magnetic phase transitions the velocity of longitudinal sound can decrease anomalously (down to zero) due to the interaction of elastic longitudinal vibrations with longitudinal relaxational vibrations of magnetization. These coupled vibrations are described by a dispersion equation that is obtained by equating the second factor in Eqn (3.11) (in square brackets) to zero. The solution to this dispersion equation can approximately be written as follows. If the condition $\omega_l^2 \ll r_2^2\omega_{1k}(\omega_{1k} - \omega_{\mathrm{me}\,l})$ (or $s_l \ll v_{\min}$, where $v_{\min}$ is the minimum phase velocity of relaxational modes) is fulfilled, we have

$$\omega_{1,2} = \pm\frac{\omega_l(\omega_{1k} - \omega_{\mathrm{me}\,l})}{\omega_{1k}} - \frac{\mathrm{i}\omega_l^2}{2r_2\omega_{1k}}\,,\quad \omega_3 = -\mathrm{i}r_2\omega_{1k}\,. \tag{3.20}$$

At $r_2^2\omega_{1k}^2 \gg \omega_l^2 \gg r_2^2\omega_{1k}(\omega_{1k} - \omega_{\mathrm{me}\,l})$, we obtain

$$\omega_1 = -\mathrm{i}r_2(\omega_{1k} - \omega_{\mathrm{me}\,l})\,,\quad \omega_2 = -\frac{\mathrm{i}\omega_l^2}{r_2\omega_{1k}}\,,\quad \omega_3 = -\mathrm{i}r_2\omega_{1k}\,. \tag{3.21}$$

And, finally, when $\omega_l \gg r_2\omega_{1k}$, then

$$\omega_{1,2} = \pm\left[\omega_l^2 - \frac{1}{4}\,r_2^2\omega_{1k}^2\right]^{1/2} - \frac{1}{2}\mathrm{i}r_2\omega_{1k}\,,$$

$$\omega_3 = \mathrm{i}r_2(\omega_{1k} - \omega_{\mathrm{me}\,l})\,. \tag{3.22}$$

We see, thus, that the $\omega_{1,2}$ branches in (3.20) and (3.22) describe progressive (weakly damped) quasielastic longitudinal waves. The solutions (3.21) are purely relaxational. No progressive waves exist in this region of wave numbers.

Now, we consider the behavior of weakly damped branches $\omega_{1,2}$ near the magnetic phase transition (Curie point), which is determined by the equality sign in the third condition for the stability of the phase with $\mathbf{M}||\mathbf{H}||\mathbf{x}$ in (3.2). Depending on the sign of the constant $\widetilde{B}$, at $H = 0$ this transition is either a second-order transition ($\widetilde{B} > 0$) or a first-order transition ($\widetilde{B} < 0$) [57]. At the Curie point, we have $M \to 0$ in the first case, whereas $M$ remains finite in the second case. Because of the different behavior of the magnetization at the Curie point upon the phase transitions of the first and second order, we consider the vibrational spectrum of the ferromagnet in these cases separately.

Let first $\widetilde{B} < 0$ be negative. At the Curie point itself, at $H = 0$ and in the long-wavelength limit $\alpha k^2 \ll h_{l1}$, the $\omega_{1,2}$ branches are written as

$$\omega_{1,2} = \pm\frac{\omega_l(\alpha k^2 + h_{l1} - h_{l2})}{h_{l1}}\,. \tag{3.23}$$

This implies that the anomalous decrease in the velocity of longitudinal quasielastic waves $\tilde{s}_l = |\omega_{1,2}|/k$ will take place only when $h_{l1} = h_{l2}$, i.e., the relation

$$2\mu b_0 = \lambda b_1\,, \tag{3.24}$$

is fulfilled between the magnetostriction and elasticity constants.

If (3.24) is fulfilled, the dispersion law for the quasielastic longitudinal vibrations becomes cubic:

$$\omega_{1,2} = \pm s_l\alpha\frac{k^3}{h_{l1}} \tag{3.25}$$

(for transverse elastic waves at the RPT points, we have $\omega_t \propto \alpha k^2$ [17]). The velocity $\tilde{s}_l$ in this case depends on $k$ quadratically:

$$\tilde{s}_l = s_l\alpha\frac{k^2}{h_{l1}} \tag{3.26}$$

and tends to zero as $k \to 0$.

Note that, under the restriction that relation (3.24) is fulfilled, the condition $\omega_l^2 \ll r_2^2\omega_{1k}(\omega_{1k} - \omega_{\mathrm{me}\,l})$ at the point of the transition becomes the condition imposed on the parameters of the ferromagnet:

$$s_l^2 \ll r_2^2 gM\alpha\omega_{\mathrm{me}\,l} = v_{\min}^2\,. \tag{3.27}$$

This condition, in principle, can be fulfilled either at the expense of an increase in the damping parameter $r_2$ near the Curie point or at the expense of the magnetostriction constant $b_0$, which enters into the frequency $\omega_{\mathrm{me}\,l}$ and usually is very large near the transition.

When the condition opposite to (3.27) is fulfilled, the vibrational spectrum of the ferromagnet will be determined by formulas (3.21) and (3.22). In this case, as $k \to 0$, all the vibrations are purely relaxational, with a quadratic dependence of the frequency on $k$. In the range of wave numbers $k \gg r_2\omega_{\mathrm{me}\,l}/s_l$, the $\omega_{1,2}$ branch (3.22) describes weakly damped longitudinal quasielastic vibrations with a linear dispersion law.

Note also the fact that one of the relaxational $\omega_3$ branches, namely, that that corresponds to the noninteracting relaxational mode of longitudinal vibrations of magnetization at the transition point, becomes, as $k \to 0$ and with allowance for the magnetoelastic interaction, activational with an activation proportional to $r_2\omega_{\mathrm{me}}$. This suggests that at the Curie point the relaxation time of the longitudinal vibrations of magnetization $\tau \propto |\omega_3|^{-1}$ remains finite.

With allowance for the magnetic field, the first-order phase transition is retained at small $H$ and is absent at large $H$ [59]. Thus, we should expect that the anomalous decrease in the sound velocity (down to zero) would occur only at small fields.

Let now consider the case of $\widetilde{B} > 0$. At $H = 0$, the phase transition is a second-order phase transition; on approaching the transition point, we have $M \to 0$. Consequently, according to (3.20)–(3.22), only either purely relaxational vibrations (3.21) or longitudinal elastic waves (3.22) can exist near this point, since the condition $\omega_l^2 < r_2^2\omega_{1k}(\omega_{1k} - \omega_{\mathrm{me}\,l})$ (which, if (3.24) is fulfilled, goes into (3.27) at the transition point itself) may not be fulfilled as $M \to 0$. If $H \neq 0$, the phase transition is absent [60]. Nevertheless, here we may expect a significant decrease in the velocity of longitudinal sound at small fields, when the susceptibility of the ferromagnet is small. Indeed, if the magnetic field is such that conditions (3.24) and (3.27) are fulfilled, then the dispersion law for the $\omega_{1,2}$ branches in the long-wavelength limit $\alpha k^2 \ll h_{l1}$ can be written in the following form:

$$\omega_{1,2} = \pm\frac{\omega_l(1 + \chi\alpha k^2)}{1 + \chi h_{l1}}\,, \tag{3.28}$$

where $\chi = (A + \beta_1 + 4\widetilde{B}M^2 + 5CM^4)^{-1}$ is the differential susceptibility of the ferromagnet. At $H \to 0$, we have $\chi \to \infty$ at the Curie point. The velocity of the quasielastic longitudinal waves as $k \to 0$ is expressed as

$$\tilde{s}_l = \frac{s_l}{1 + \chi h_{l1}}\,. \tag{3.29}$$

From this, it follows that at $\chi h_{l1} \gg 1$ we can observe a significant decrease in the velocity of longitudinal sound also near the second-order phase transition. However, no theoretical limit $\tilde{s}_l \to 0$ (similar to that observed in first-order phase transitions at $\widetilde{B} < 0$) exists in this case.

Thus, the allowance for longitudinal vibrations of the ferromagnet magnetization leads to the following results. First, far from the Curie point, in a certain range of wave numbers, all vibrations can become nonpropagating. Second, at the point of a phase transition of the first order (at the Curie point at $\widetilde{B} < 0$), the velocity of the longitudinal quasielastic waves under a certain condition imposed on the elastic and magnetoelastic constants (3.24) can drop to zero as $k \to 0$. Third, the magnetoelastic interaction leads to the appearance of activation in the spectrum of the relaxational branch at the Curie point.

Note that here we did not consider the role of fluctuations in the immediate vicinity of the Curie point. Therefore, all the results obtained above are valid for that region near the Curie point in which the fluctuations can be ignored. However, in analogy with relaxation in liquid helium, the effect of the anomalous decrease in the velocity of longitudinal sound had to occur in the fluctuational region as well (see, e.g., [60]).

### 3.2 Effect of longitudinal susceptibility and relaxation on the spectrum of spin and elastic waves in an antiferromagnet upon spin reorientation

When describing static and dynamic properties of antiferromagnets, the conditions of the constancy and equality to one another of the absolute values of sublattice magnetizations are frequently used [17]. For an antiferromagnet consisting of two sublattices, these conditions are written as (1.1), or in an equivalent form

$$\mathbf{ML} = 0\,,$$

$$\mathbf{M}^2 + \mathbf{L}^2 = 4M_0^2\,, \tag{3.30}$$

where $\mathbf{M} = \mathbf{M}_1 + \mathbf{M}_2$, $\mathbf{L} = \mathbf{M}_1 - \mathbf{M}_2$ are the vectors of ferromagnetism and antiferromagnetism, respectively; $\mathbf{M}_i$ is the magnetization of the $i$th sublattice; and $M_0$ is the saturation magnetization of the sublattices. The first condition in (3.30) is fulfilled in all the phases of the antiferromagnet in the absence of an applied magnetic field $H$. In antiferromagnets placed in a magnetic field, the first condition of (3.30) can be fulfilled only for those phases in which $\mathbf{H} \perp \mathbf{L}$ [61]. At the same time, this condition is not satisfied in those phases in which the antiferromagnetism vector $\mathbf{L}$ is not perpendicular to the magnetic field. In most antiferromagnets placed in an arbitrary magnetic field, there exists at least one phase in which $\mathbf{ML} \neq 0$. In this case, the fulfillment of the condition $\mathbf{ML} = 0$ can be attained by letting the coefficient at the invariant $(\mathbf{ML})^2$ tend to infinity in the expansion of the free-energy density of the antiferromagnet in powers of $\mathbf{M}$ and $\mathbf{L}$. In this case, in the ground state of the antiferromagnet, those phases in which $\mathbf{ML} \neq 0$ either vanish or become distorted so that the first of the conditions (3.30) becomes valid in them. This approximation is equivalent to the vanishing of the longitudinal magnetic susceptibility $\chi_{||}$. Strictly speaking, the longitudinal susceptibility of the antiferromagnet is equal to zero only at absolute zero ($T = 0$), but there are magnets in which $\chi_{||}(T = 0) \neq 0$ [8]. Thus, in the general case, when describing the statics and dynamics of an antiferromagnet, we should discard condition (3.30).

Now, let us investigate the ground state and the spectrum of spin and coupled magnetoelastic waves in an antiferromagnet without allowance for conditions (3.30).

**3.2.1 Choice of object for investigation, the ground state, and the equations of motion of an antiferromagnet.** Without restricting the generality, we consider a two-sublattice antiferromagnet with isotropic elastic and magnetoelastic properties. The density of free energy is written as

$$F = \frac{1}{2} A\mathbf{L}^2 + \frac{1}{4} B\mathbf{L}^4 + \frac{1}{2} a\mathbf{M}^2 + \frac{1}{2} D(\mathbf{ML})^2 + \frac{1}{2} D'\mathbf{M}^2\mathbf{L}^2 + \frac{1}{2}\alpha\left(\frac{\partial \mathbf{L}}{\partial x_i}\right)^2 + \frac{1}{2}\beta_1 L_z^2 + \frac{1}{2}\beta_2 L_y^2 + \frac{1}{2}\beta_3 L_x^2 - \mathbf{MH} + \frac{1}{2} bL_i L_k u_{ik} + \frac{1}{2}\lambda u_{ll}^2 + \mu u_{ik}^2 . \quad (3.31)$$

Here, the first six terms represent the energy of the exchange interaction. The next three terms are related to the anisotropy energy. The term that contains the magnetic field describes the energy of the antiferromagnet in an applied magnetic field (the Zeeman energy). Note that for simplicity we omitted the energy of the Dzyaloshinskii interaction in (3.31). The effect of this interaction on the static and dynamic properties of antiferromagnets will be discussed below.

At $\mathbf{H}||\mathbf{x}$, the following magnetic phases can exist in the ground state of the ferromagnet:

1. $\mathbf{L}||\mathbf{x}$, $\mathbf{M}||\mathbf{x}$, $M = \chi_{||} H \equiv \chi_\perp (1-\eta) H$,
$A + \beta_3 + (D + D')M^2 + BL^2 = 0$, $a + D'L^2 \geqslant 0$,
$a + (D + D')L^2 \geqslant 0$, $(\beta_3 - \beta_1)L^2 + \chi_\perp \eta H^2 \leqslant 0$,
$A + \beta_3 + (D + D')M^2\left[1 + 2(D + D')\chi_{||} L^2\right] \leqslant 0$;

2. $\mathbf{L}||\mathbf{y}$, $\mathbf{M}||\mathbf{x}$, $M = \chi_\perp H$, $A + \beta_2 + D'M^2 + BL^2 = 0$,
$a + D'L^2 \geqslant 0$, $a + (D + D')L^2 \geqslant 0$,
$(\beta_3 - \beta_2)L^2 + \eta\chi_\perp H^2 \geqslant 0$, $\beta_1 - \beta_2 \geqslant 0$,
$A + \beta_2 + D'M^2(1 + 2D'\chi_\perp L^2) \leqslant 0$;

3. $\mathbf{L}||\mathbf{z}$, $\mathbf{M}||\mathbf{x}$, $M = \chi_\perp H$, $A + \beta_1 + D'M^2 + BL^2 = 0$,
$a + D'L^2 \geqslant 0$, $a + (D + D')L^2 \geqslant 0$,
$(\beta_3 - \beta_1)L^2 + \eta\chi_\perp H^2 \geqslant 0$, $\beta_1 - \beta_2 \leqslant 0$,
$A + \beta_1 + D'M^2(1 + 2D'\chi_\perp L^2) \leqslant 0$;

4. $\mathbf{L} = 0$, $\mathbf{M}||\mathbf{x}$, $M = \chi H$, $a \geqslant 0$,
$A + \beta_3 + (D + D')M^2 \geqslant 0$, $A + \beta_2 + D'M^2 \geqslant 0$,
$A + \beta_1 + D'M^2 \geqslant 0$. (3.32)

Here, $\chi_\perp^{-1} = a + D'L^2$, $\chi_{||}^{-1} = \chi_\perp^{-1} + DL^2$, $\eta = 1 - \chi_{||}/\chi_\perp$, and $\chi = 1/a$. The equilibrium deformations in phases 1–4 are as follows:

$$u_{ik}^{(0)} = -\frac{b}{4\mu} L_i L_k + \frac{\lambda b L^2}{4\mu(3\lambda + 2\mu)}\delta_{ik} .$$

The imposition of the condition $\mathbf{ML} = 0$, as was already noted above, is equivalent to the zero longitudinal susceptibility of the antiferromagnet: $\chi_{||} = 0$ (as $D \to \infty$). In this case, we have $\eta = 1$. Thus, the parameter $\eta$ is as if a measure of the departure from the condition $\mathbf{ML} = 0$. Note also that the parameter $\eta$ enters into the phase equilibrium in the product with the magnitude of the magnetic field $H$. Therefore, at $H = 0$ the condition $\mathbf{ML} = 0$ is fulfilled for all phases (3.32). It also follows from (3.32) that in the general case we have $\mathbf{ML} \neq 0$ in the first phase and $\mathbf{ML} = 0$ in the other phases.

At the lines that are determined from the condition of equality of phase energies, phase transitions can occur between the phases. Since we are interested in the dynamics of the antiferromagnet, for simplicity we will not give expressions for the phase energies and lines of phase transitions here. When considering the dynamics of magnets, it is only important to know the lines of phase stability, since it is at these lines that softening of the magnetic vibration frequency occurs [17]. Note only that in their character the $1 \leftrightarrow 2$ and $1 \leftrightarrow 3$ transitions are hysteretic first-order phase transitions; the $2 \leftrightarrow 3$ transition also is a first-order phase transition, but is anhysteretic; the transformations $2 \leftrightarrow 4$ and $3 \leftrightarrow 4$, which occur in strong fields (of the order of the exchange one), are second-order phase transitions; and the $1 \leftrightarrow 4$ transition also refers to second-order phase transitions.

When describing the dynamics of the antiferromagnet, we proceed from the coupled set of equations of elasticity and Landau – Lifshitz equations:

$$\rho\ddot{u}_i = \frac{\partial(\partial F/\partial u_{ik})}{\partial x_k} ,$$
$$\dot{\mathbf{M}} = g(\mathbf{M} \times \mathbf{H}_M + \mathbf{L} \times \mathbf{H}_L + \tilde{r}_1 M_0 \mathbf{H}_M) ,$$
$$\dot{\mathbf{L}} = g(\mathbf{M} \times \mathbf{H}_L + \mathbf{L} \times \mathbf{H}_M + \tilde{r}_2 M_0 \mathbf{H}_L) , \quad (3.33)$$

where $g$ is the gyromagnetic ratio, $\mathbf{H}_x = \delta F/\delta \mathbf{x}$ ($\mathbf{x} = \mathbf{M}, \mathbf{L}$) are the effective magnetic fields, and $\tilde{r}_i$ are the dimensionless relaxation parameters. Note that the allowance for the relaxational terms in the Landau – Lifshitz equations is equivalent to the rejection of conditions (3.30) in the dynamics of the antiferromagnet [11].

**3.2.2 Spectrum of spin waves in a two-sublattice antiferromagnet.** Here, we investigate the vibrational spectrum of the antiferromagnet. To this end, we represent $\mathbf{M}$, $\mathbf{L}$, and $\mathbf{u}$ in the forms $\mathbf{M}^{(0)} + \mathbf{m}$, $\mathbf{L}^{(0)} + \mathbf{l}$, and $\mathbf{u}^{(0)} + \tilde{\mathbf{u}}$, where $\mathbf{m}$, $\mathbf{l}$, and $\tilde{\mathbf{u}}$ are small deviations from equilibrium values given by (3.32). Once again, for simplicity we only consider the propagation of waves along the $\mathbf{z}$ axis (wave vector $\mathbf{k}||\mathbf{z}$). The set of equations (3.33) linearized in this way is solved by the Fourier method.

First, we write down the spectrum of spin waves without allowance for the magnetoelastic coupling ($b \equiv 0$). Consider each of the phases of (3.32) separately. The set of equations (3.33) and the vibrational spectrum in them are as follows.

**1.** Phase $\mathbf{L}||\mathbf{M}||\mathbf{x}$. The linearized set of equations (3.33) in this phase is

$$\left(\frac{r_1\omega_E}{1-\eta} - i\omega\right)m_x + 2r_1\omega_H(D + D')\chi_{||}L^2 l_x = 0 ,$$
$$(r_2\omega_B - i\omega)l_x + 2r_2\omega_H(D + D')\chi_{||}L^2 m_x = 0 ,$$
$$(r_1\omega_E - i\omega)m_{z,y} \pm \omega_H m_{y,z} \pm \left(\omega_{2,13} + \frac{\eta\omega_H^2}{\omega_E}\right)l_{y,z} + r_1\eta\omega_H l_{z,y} = 0 ,$$
$$\left[r_2\left(\omega_{1,23} + \frac{\eta^2\omega_H^2}{\omega_E}\right) - i\omega\right]l_{z,y} \pm \omega_H\left[\eta + (1-\eta)\frac{\omega_{2,13}}{\omega_E} + \eta^2(1-\eta)\frac{\omega_H^2}{\omega_E^2}\right]l_{y,z} \pm \left[\omega_E + \eta(1-\eta)\frac{\omega_H^2}{\omega_E}\right]m_{y,z} + r_2\eta\omega_H m_{z,y} = 0 , \quad (3.34)$$

where

$$\omega_{\rm E} = gL\chi_{\perp}^{-1}\,, \quad \omega_B = 2gL^3B\,,$$
$$\omega_{ij} = gL(\alpha k^2 + \beta_i - \beta_j) - \eta\frac{\omega_H^2}{\omega_{\rm E}}\,,$$
$$\omega_H = gH\,, \quad r_i = \tilde{r}_i\frac{M_0}{L}\,. \tag{3.34a}$$

The dispersion equations for the waves that propagate in this phase can be written as

$$(1-\eta)\omega^2 + {\rm i}\omega\left[r_1\omega_{\rm E} + r_2\omega_B(1-\eta)\right] - r_1r_2\omega_{\rm E}\tilde{\omega}_B = 0\,,$$
$$\omega^4 + 2{\rm i}r_1\omega_{\rm E}\omega^3 - \omega^2\left[\omega_{\rm E}(\omega_{13}+\omega_{23}) + \omega_H^2(1+\eta)^2\right]$$
$$- {\rm i}r_1\omega\omega_{\rm E}^2(\omega_{13}+\omega_{23}) + \omega_{\rm E}^2\omega_{13}\omega_{23} = 0\,, \tag{3.35}$$

where $\tilde{\omega}_B = 2gL^3[B - 2(D+D')^2\chi_{\parallel}^3H^2]$. The last equation here has been written in the following approximation: $\omega_{\rm E} \gg \omega_H$, $\omega_{ij}$, and $r_i \ll 1$. This equation is given in the full form in the Appendix (formula A.1). The solutions to equations (3.35) have the form

$$\omega_{1,2} = \frac{1}{2(1-\eta)}\Big(-{\rm i}\left[r_1\omega_{\rm E} + r_2\omega_B(1-\eta)\right]$$
$$\pm\left\{4r_1r_2\omega_{\rm E}\tilde{\omega}_B(1-\eta) - \left[r_1\omega_{\rm E} + r_2\omega_B(1-\eta)\right]^2\right\}^{1/2}\Big)\,. \tag{3.36a}$$

At $\omega_{\rm E}r_1^2 \ll \omega_{13}\omega_{23}/(\omega_{13}+\omega_{23})$, we obtain

$$\omega_{3,4}^2 = \omega_+^2 - {\rm i}r_1\omega_{\rm E}\Delta\omega_+\,,$$
$$\omega_{5,6}^2 = \omega_-^2 - {\rm i}r_1\omega_{\rm E}\Delta\omega_-\,, \tag{3.36b}$$

where

$$\omega_{\pm}^2 = \frac{1}{2}\Big(\omega_{\rm E}(\omega_{13}+\omega_{23}) + \omega_H^2(1+\eta)^2 \pm$$
$$\pm\left\{\left[\omega_{\rm E}(\omega_{13}+\omega_{23}) + \omega_H^2(1+\eta)^2\right]^2 - 4\omega_{\rm E}^2\omega_{13}\omega_{23}\right\}^{1/2}\Big)\,,$$

$$\Delta\omega_{\pm} = 1 \pm \frac{\omega_H^2(1+\eta)^2}{\left\{\left[\omega_{\rm E}(\omega_{13}+\omega_{23}) + \omega_H^2(1+\eta)^2\right]^2 - 4\omega_{\rm E}^2\omega_{13}\omega_{23}\right\}^{1/2}}\,.$$

At $\omega_{\rm E}r_1^2 \gg \omega_{13}\omega_{23}/(\omega_{13}+\omega_{23})$, we have

$$\omega_3 = \frac{-{\rm i}\omega_{13}\omega_{23}}{r_1(\omega_{13}+\omega_{23})}\,,$$
$$\omega_4 = \frac{-{\rm i}r_1\omega_{\rm E}^2(\omega_{13}+\omega_{23})}{\omega_{\rm E}(\omega_{13}+\omega_{23}) + \omega_H^2(1+\eta)^2}\,. \tag{3.36c}$$

Note that the $\omega_2$ and $\omega_1$ branches describe the longitudinal relaxational vibrations of the vectors **L** and **M**, respectively, and the $\omega_3$ and $\omega_4$ branches correspond at $\omega_{\rm E}r_1^2 \gg \omega_{13}\omega_{23}/(\omega_{13}+\omega_{23})$ to the transverse relaxation of these vectors.

It follows from the two first equations of the set (3.34) that at low temperatures, when we can neglect the longitudinal susceptibility ($\eta \to 1$), the $x$ components of the vectors of ferromagnetism and antiferromagnetism vanish ($\mathbf{m} = 0$, $\mathbf{l} = 0$). This situation corresponds to the absence of longitudinal vibrations of these vectors and the fulfillment of the second of the conditions (3.30) in the dynamics of the antiferromagnet. From the set of equations (3.34), it also follows that the longitudinal and transverse vibrations of the vectors of ferromagnetism and antiferromagnetism in the phase at hand can be separated. As is seen from (3.32) and (3.34)–(3.36), the effect of the longitudinal susceptibility on the ground state and the spectrum of the transverse components of the **M** and **L** vectors reduces not only to the displacement of the point of phase transition (point of phase stability in the first-order phase transition) in the statics. In the dynamics, the longitudinal susceptibility gives an additive contribution to the activation of precessional branches of vibrations in the product with the magnetic field (3.36b), (3.36c). It is seen from (3.36) that in the dynamics also, relaxation should be taken into account upon the consideration of the vibrations of transverse components of the above vectors. The allowance for the relaxation has an especially strong effect near the phase transitions $1 \to 2$ ($\omega_{23}(0) \to 0$) and $1 \to 3$ ($\omega_{13}(0) \to 0$), where a single precessional branch (with activation $\omega_{5,6}$) exists, and the soft branch at the point of phase transition is the relaxational branch $\omega_3$ (3.36c).

**2.** Phase **L**||**y**, **M**||**x**. The linearized set of equations (3.33) in this phase has the form

$$\left[r_1\omega_{\rm E} - {\rm i}(1-\eta)\omega\right]m_y - (1-\eta)\omega_H m_z + r_1\eta\omega_H l_x = 0\,,$$
$$(r_1\omega_{\rm E} - {\rm i}\omega)m_z - \left(\omega_{32} - \frac{\eta\omega_H^2}{\omega_{\rm E}}\right)l_x + \omega_H m_y = 0\,,$$
$$\left\{r_2\left[\omega_{32}(1-\eta) + \frac{\eta^2\omega_H^2}{\omega_{\rm E}}\right] - {\rm i}(1-\eta)\omega\right\}l_x$$
$$+ (1-\eta)\omega_{\rm E}m_z + r_2\eta\omega_H m_y = 0\,,$$
$$(r_1\omega_{\rm E} - {\rm i}\omega)m_x + \omega_{12}l_z + 2r_1\omega_H\chi_{\perp}D'L^2l_y = 0\,,$$
$$(r_2\omega_B - {\rm i}\omega)l_y - \omega_{12}\omega_H\frac{l_z}{\omega_{\rm E}} + 2r_2\omega_H\chi_{\perp}D'L^2m_x = 0\,,$$
$$(r_2\omega_{12} - {\rm i}\omega)l_z + \omega_H(\omega_B - 2\omega_{\rm E}\chi_{\perp}D'L^2)\frac{l_y}{\omega_{\rm E}}$$
$$- \left(\omega_{\rm E} - \frac{2\omega_H^2\chi_{\perp}D'L^2}{\omega_{\rm E}}\right)m_x = 0\,, \tag{3.37}$$

where

$$\omega_{32} = gL(\alpha k^2 + \beta_3 - \beta_2) + \frac{\eta\omega_H^2}{\omega_{\rm E}}\,,$$
$$\omega_{12} = gL(\alpha k^2 + \beta_1 - \beta_2)\,. \tag{3.37a}$$

The set of equations (3.37) in the approximation $\omega_{\rm E} \gg \omega_H$, $g\alpha k^2/L$, and $\omega_{ij}$ and $r_i \ll 1$ corresponds to the following dispersion equations:

$$(1-\eta)\omega^3 - r_1(2-\eta)\omega_{\rm E}\omega^2$$
$$- {\rm i}\omega\left\{r_1^2\omega_{\rm E}^2 + (1-\eta)\left[\omega_{\rm E}\omega_{32} + \omega_H^2(1-\eta)\right]\right\} + r_1\omega_{32}\omega_{\rm E}^2 = 0,$$

$$-{\rm i}\omega^3 - \omega^2\left[r_1\omega_{\rm E} + r_2(\omega_B + \omega_{12})\right] - {\rm i}\omega\left[r_1r_2\omega_{\rm E}(\omega_{12} + \omega'_B)\right.$$
$$\left. + r_2^2\omega_B\omega_{12} + \omega_{12}\omega'_{\rm E}\right] + \omega_{12}\omega_{\rm E}\omega'_B = 0\,, \tag{3.38}$$

where

$$\omega'_B = 2gL^3[B - 2D'^2\chi_{\perp}^3H^2]\,,$$
$$\omega'_{\rm E} = \omega_{\rm E}\left[1 + 2\chi_{\perp}^3H^2(B - 2D')\right]. \tag{3.38a}$$

The complete dispersion equations for this phase are given in the Appendix (formulas (A.2 and A.3, respectively).

Note that the formal equating of the quantity $\eta$ to unity (i.e., the vanishing of the longitudinal susceptibility) in equations (3.37) leads to the fulfillment of the condition $\mathbf{ML} = 0$ in the dynamics of the antiferromagnet.

Let us first investigate the first dispersion equation in (3.38). At low temperatures and small fields, far from the $2 \to 1$ RPT point, this equation only contains three small parameters: $1-\eta$, $r_1$, and $\omega_H(1-\eta)$. Near the transition point, the frequency $\omega_{32}$ is also small. The presence of several small parameters makes the analysis of the dispersion equation more complex. Therefore, we only consider those cases that can be realized under the conditions of the above indicated experiments.

At the point of the $\omega_{32}(0) = 0$ RPT, this dispersion equation has the following solutions:

$$\omega_1 = 0\,, \quad \omega_{2,3} = \frac{1}{2(1-\eta)}\Big\{ -\mathrm{i}r_1(2-\eta)\omega_{\mathrm{E}} \pm \big[ -r_1^2\eta^2\omega_{\mathrm{E}}^2 + 4(1-\eta)^3\omega_H^2\big]^{1/2}\Big\}. \quad (3.39)$$

It is seen that in small fields, when $(1-\eta)^3\omega_H^2 < r_1^2\eta^2\omega_{\mathrm{E}}^2$, the $\omega_{2,3}$ branches are purely relaxational; in the opposite case, they are precessional, with an activation that is determined by the magnetic field and longitudinal magnetic susceptibility.

At $\omega_{32}(0) \neq 0$, the approximate solutions to the first dispersion equation of those given by (3.38) are as follows in some limiting cases:

(i) $r_1\omega_{\mathrm{E}} \gg (\omega_{32}\omega_{\mathrm{E}})^{1/2}$, $\tilde{\omega}_{32}(1-\eta)^{1/2}$. Under this condition, we obtain

$$\omega_1 = -\mathrm{i}\frac{\omega_{32}}{r_1}\,, \quad \omega_2 = -\mathrm{i}r_1\omega_{\mathrm{E}}\,, \quad \omega_3 = -\mathrm{i}r_1\frac{\omega_{\mathrm{E}}}{1-\eta}\,. \quad (3.40)$$

This approximation is fulfilled near the RPT ($\omega_{32}(0) \to 0$), at small magnetic fields, or low temperatures, when $\eta \to 1$. It can be seen that, as in the previous cases, all three branches here are relaxational. At the point of the $\omega_{32}(0) \to 0$ RPT, a softening of the relaxational mode $\omega_1$ occurs.

(ii) $(\omega_{32}\omega_{\mathrm{E}})^{1/2} \gg r_1\omega_{\mathrm{E}} \gg (1-\eta)^{1/2}\tilde{\omega}_{32}$. This condition corresponds to the representative points far from the RPT, to small magnetic fields, or low temperatures ($\eta \to 1$). One of the solutions in this approximation is a purely relaxational mode

$$\omega_1 = -\mathrm{i}\frac{\omega_{32}}{r_1}\,. \quad (3.41a)$$

The second solution may be represented in the form of an expansion in powers of the parameter $1-\eta$, which is small at low temperatures:

$$\omega_{2,3} = \pm\big[\omega_0 + (1-\eta)\omega_1 + (1-\eta)^2\omega_2 + \ldots\big] + \mathrm{i}\omega_0'\,, \quad (3.41b)$$

where

$$\omega_0 = \left(\frac{\omega_{32}\omega_{\mathrm{E}}}{2-\eta}\right)^{1/2}, \quad \omega_1 = (3\eta-1)\left(\frac{\omega_{32}\omega_{\mathrm{E}}}{(2-\eta)^5}\right)^{1/2},$$

$$\omega_0' = \frac{r_1\omega_{\mathrm{E}}}{2(2-\eta)}\,,$$

$$\omega_2 = (3\eta-1)(7-3\eta)\left[\frac{\omega_{32}\omega_{\mathrm{E}}}{16(2-\eta)^9}\right]^{1/2} - \frac{\omega_H^2}{[16(2-\eta)^3\omega_{32}\omega_{\mathrm{E}}]^{1/2}}\,.$$

It is seen that the dependence on the magnetic field here arises only in terms that are proportional to the second power of the small parameter $1-\eta$. Thus, at low temperatures, when the longitudinal magnetic susceptibility is small, far from the RPT the dependence of the frequency of precessional vibrations on the magnitude of the magnetic field is weak.

(iii) $(1-\eta)^{1/2}\tilde{\omega}_{32} \gg r_1\omega_{\mathrm{E}}$. This inequality is fulfilled far from the RPT, at large magnetic fields, or at high temperatures, when the parameter $1-\eta$ is not small. The frequencies of the vibrations are determined by the formulas

$$\omega_1 = -\mathrm{i}r_1\frac{\omega_{32}\omega_{\mathrm{E}}^2}{(1-\eta)[\omega_{32}\omega_{\mathrm{E}} + (1-\eta)\omega_H^2]}\,, \quad (3.42a)$$

$$\omega_{2,3}^2 = \omega_{32}\omega_{\mathrm{E}} + (1-\eta)\omega_H^2 + \frac{r_1^2\omega_{\mathrm{E}}^2\big\{(6-6\eta+\eta^2)[\omega_{32}\omega_{\mathrm{E}} + (1-\eta)\omega_H^2]^2 - \omega_{32}^2\omega_{\mathrm{E}}^2\big\}}{2(1-\eta)^2\big[\omega_{32}\omega_{\mathrm{E}} + (1-\eta)\omega_H^2\big]^2} - \frac{\mathrm{i}r_1\omega_{\mathrm{E}}\big[2\omega_{32}\omega_{\mathrm{E}} + (2-\eta)\omega_H^2\big]}{\big[\omega_{32}\omega_{\mathrm{E}} + (1-\eta)\omega_H^2\big]^{1/2}}\,. \quad (3.42б)$$

Note that the condition imposed on the parameter $\eta$ is related to expression (3.42b) on the whole, rather than referring to its first term. The precessional contribution to the magnitude of the gap of spin vibrations exists at any values of $\eta$. It follows from (3.42b) that at high temperatures far from the RPT [like at the RPT point, see (3.39)], the effect of the magnetic field (at sufficiently large magnitude) on the activation of the $\omega_2$ branch can be decisive. Here, we also give the relaxational contribution to the gap of the precessional spin branch $\omega_{2,3}$, which is caused by the interaction of spin and relaxation vibrations, in order to illustrate that this contribution always enters into the activation of the precessional branch along with the contributions from other interactions.

Now, we turn to the second dispersion equation in (3.38). Its solutions are the frequencies

$$\omega_4 = -\frac{\mathrm{i}\omega_{12}\omega_{\mathrm{E}}\omega_B' r_2}{r_1 r_2\omega_{\mathrm{E}}\omega_B' + \omega_{12}\big[r_1 r_2\omega_{\mathrm{E}} + r_2^2\omega_B + \omega_{\mathrm{E}}'\big]}\,, \quad (3.43a)$$

$$\omega_{5,6} = \frac{1}{2}\Big( -\mathrm{i}\big[r_1\omega_{\mathrm{E}} + r_2(\omega_B + \omega_{12})\big] \pm \big\{4\big[r_1 r_2\omega_{\mathrm{E}}(\omega_{12} + \omega_B') + r_2^2\omega_B\omega_{12} + \omega_{12}\omega_{\mathrm{E}}'\big] - \big[r_1\omega_{\mathrm{E}} + r_2(\omega_B + \omega_{12})\big]^2\big\}^{1/2}\Big)\,. \quad (3.43b)$$

In (3.39)–(3.43), the $\omega_1$ and $\omega_4$ branches correspond to the transverse relaxation of the components of the vector $\mathbf{L}$. The transverse relaxation of the vector $\mathbf{M}$ affects the branches $\omega_2$ and $\omega_3$, and the longitudinal relaxation of the vectors $\mathbf{M}$ and $\mathbf{L}$ exerts influence on the branches $\omega_5$ and $\omega_6$.

**3.** Phase $\mathbf{L}||\mathbf{z}$, $\mathbf{M}||\mathbf{x}$. Expressions for the frequencies of spin waves $\omega_i$ ($i = 1-6$) can be obtained by replacing the frequencies $\omega_{12}$ and $\omega_{32}$ by the frequencies $\omega_{21}$ and $\omega_{31}$ with the corresponding replacement of the indices at the constants $\beta$.

Thus, it follows from the above results that if condition (3.30) is abandoned both in statics and dynamics and if

relaxation is taken into account, the spectrum of spin waves of an antiferromagnet consists of six branches. All vibrational frequencies are complex. The imaginary parts of the frequencies damp the vibrations. The purely imaginary frequencies describe the relaxation vibrations of the vectors **M** and **L**; the frequencies that have a nonzero real part correspond to damped spin waves of the antiferromagnet (damped precessional vibrations of the vectors **M** and **L**). In the last case, the attenuation of spin waves is caused by their interaction with relaxational vibrations. The extent of damping of spin waves depends on the relationship between the imaginary part of the relaxational mode ($\operatorname{Im}\omega_{\mathrm{r}}$) and the real part of the precessional mode ($\operatorname{Re}\omega_{\mathrm{pr}}$). If $\operatorname{Re}\omega_{\mathrm{pr}} \gg \operatorname{Im}\omega_{\mathrm{r}}$, then the precessional mode represents a slightly damped spin wave. At $\operatorname{Re}\omega_{\mathrm{pr}} \ll \operatorname{Im}\omega_{\mathrm{r}}$, the precessional motion goes into relaxational motion. In ferromagnets, the first condition is usually fulfilled. However, if the magnet is in the region of the RPT where $\omega_{\mathrm{pr}} \to 0$, the second condition can also be fulfilled. A similar situation can take place in the case of vibrations of a paramagnetic subsystem which is under the field of a magnetized subsystem, when damping in the first of these is very large (e.g., vibrations of the RE subsystem at high temperatures in rare-earth orthoferrites).

In our case, the RPT points are determined by the equality signs in the stability conditions for the phases of the antiferromagnet (3.32). Based on the designations (3.34a) and (3.37a), the RPT points can also be determined from the condition of vanishing of the corresponding frequencies $\omega_{ij}$ at $k = 0$, i.e., $\omega_{ij}(k = 0) = 0$. We consider the behavior of the vibrational spectrum of the antiferromagnet separately for the states of far from and close to the RPT points.

Far from the RPT, when we can assume that $r_{1,2} \ll (\omega_{ij}/\omega_{\mathrm{E}})^{1/2}$ for all $i$ and $j$, the spectrum of vibrations of the antiferromagnet in each phase consists of two relaxational branches ($\omega_{1,2}$ in phase 1, $\omega_{1,4}$ in phases 2 and 3), two slightly damped precessional branches ($\omega_{3,4}$ in phase 1, $\omega_{2,3}$ in phases 2 and 3), and $\omega_{5,6}$ branches (only positive values of the frequencies are physically meaningful). In the RPT region, the spectrum of vibrations depends on the particular type of the RPT point. Near the RPTs of types $1 \to 2$ ($\omega_{23}(0) \to 0$), $1 \to 3$ ($\omega_{13}(0) \to 0$), and $2 \leftrightarrow 3$ ($\omega_{12,21}(0) \to 0$) in the case where $r_{1,2} \gg (\omega_{ij}/\omega_{\mathrm{E}})^{1/2}$ ($ij = 23; 13; 12, 21$ for RPTs of types $1 \to 2$, $1 \to 3$, and $2 \leftrightarrow 3$, respectively), the spectrum of vibrations in each phase of the antiferromagnet consists of four relaxational branches ($\omega_{1,2,3,4}$ for phase 1 and $\omega_{1,4}$, $\omega_{5,6}$ for phases 2 and 3; two of them correspond to the longitudinal relaxation, and the two others to the transverse relaxation of the vectors **M** and **L**) and one slightly damped precessional branch ($\omega_{5,6}$ in phase 1 and $\omega_{2,3}$ in phases 2 and 3). For the latter branch, the condition $r_{1,2} \ll (\omega_{ij}/\omega_{\mathrm{E}})^{1/2}$, where $ij = 13, 23$, and 31 for the $1 \to 2$, $1 \to 3$, and $2 \leftrightarrow 3$ RPTs, respectively, is expected to be fulfilled. With respect to these modes, the antiferromagnet is far from the RPT. One of the above relaxational branches near the RPT is soft, and its frequency becomes zero at the transition point itself as $k \to 0$. This is the frequency $\omega_3$ in phase 1 near the $1 \to 2$ and $1 \to 3$ RPTs and the frequency $\omega_4$ in phases 2 and 3 near the $2 \to 3$ and $3 \to 2$ transitions, respectively:

$$\omega_{3,4} = \mathrm{i}g\alpha k^2/(r_1 L) \to 0\,, \quad k \to 0\,. \tag{3.44}$$

The precessional branch at the above points of the RPTs at $k \to 0$ is activational. Its activation (in the zeroth approximation in powers of $r$ and $1 - \eta$) is determined by exchange, anisotropy, and the magnetic field [see, also, (3.37a)]:

$$\operatorname{Re}\omega_{5,6}^2 = \omega_{\mathrm{E}}\omega_{23,13}(0) + \omega_H^2(1+\eta)^2\,, \quad \text{phase 1, RPTs } 1 \to 2\,,\ 1 \to 3\,;$$

$$\operatorname{Re}\omega_{3,4}^2 = \omega_{\mathrm{E}}\omega_{32,31}(0)\,, \quad \text{phases 2, 3, RPTs } 2 \leftrightarrow 3. \tag{3.45}$$

Similar behavior is shown by the spectrum of vibrations of the antiferromagnet in the region of the RPT $2 \to 1$ ($\omega_{32}(0) \to 0$) and in the region of the RPT $3 \to 1$ ($\omega_{31}(0) \to 0$) at $r \gg \omega_H(1-\eta)^{3/2}/(\omega\eta) \gg (\omega_{ij}/\omega_{\mathrm{E}})^{1/2}$, where $ij = 32, 31$ for the $2 \to 1$ and $3 \to 1$ RPTs, respectively [see, e.g., formulas (3.40) and (3.43)], as well as at $r_1 \ll (\omega_{ij}/\omega_{\mathrm{E}})$ [see formulas (3.41a) and (3.41b)]. At $\omega_H\,(1-\eta)^{3/2}/(\omega_{\mathrm{E}}\eta) \gg r_1 \gg (\omega_{ij}/\omega_{\mathrm{E}})^{1/2}$, the spectrum of vibrations, just as for regions far from RPT, consists of two relaxational ($\omega_{1,4}$) and two slightly damped ($\omega_{2,3}$ and $\omega_{5,6}$) precessional branches (it is assumed, as above, that the modes that are not involved in the RPTs obey the condition $r_{1,2} \ll (\omega_{ij}/\omega_{\mathrm{E}})^{1/2}$, where $ij = 12, 21$ for phases 2 and 3, respectively). The relaxational branch $\omega_1$ is soft near the RPT at hand, and its frequency becomes zero at the transition points as $k \to 0$:

$$\omega_1 = \frac{\mathrm{i}g\alpha k^2 r_1 \omega_{\mathrm{E}}^2}{r_1^2\omega_{\mathrm{E}}^2 + (1-\eta)^2\omega_H^2} \to 0\,, \quad k \to 0\,. \tag{3.46}$$

The $\omega_{2,3}^2$ branch at $r_1 \gg \omega_H(1-\eta)^{3/2}/(\omega_{\mathrm{E}}\eta) \gg (\omega_{ij}/\omega_{\mathrm{E}})^{1/2}$ is relaxational; and at $(\omega_{ij}/\omega_{\mathrm{E}})^{1/2} \ll r_1 \ll \omega_H(1-\eta)^{3/2}/(\omega_{\mathrm{E}}\eta)$, it is precessional with an activation that is mainly determined by the magnitude of the magnetic field and by the longitudinal susceptibility [see formula (3.42b)]:

$$\operatorname{Re}\omega_{2,3}^2(0) = \omega_H^2(1-\eta)\,. \tag{3.47}$$

The activation of the precessional branch $\omega_{5,6}$ is determined by the anisotropy and exchange:

$$\operatorname{Re}\omega_{5,6}^2(0) = \omega_{12,21}(0)\omega_{\mathrm{E}}' \cong \omega_{12,21}(0)\omega_{\mathrm{E}}\,. \tag{3.48}$$

Note that at $H = 0$ none of the vibrational branch suffers significant softening in phase 1. This is explained by the fact that at the point $H = 0$ the mode that should become soft is the $\omega_2$ mode, corresponding to the longitudinal relaxation of the vector **L**. Its complete softening can proceed only at the Néel point, when $L \to 0$. At the same time, as $H \to 0$ a narrowing (in the attenuation parameter) of the region of existence of the slightly damped precessional vibrations of the $\omega_{2,3}$ mode occurs in phases 2 and 3.

Thus, on discarding condition (i) in the statics and dynamics, the spectrum of magnetic vibrations of the antiferromagnet near the RPT and in the range of small fields consists of one precessional and four relaxational branches. The precessional branch at the RPT point has an activation that is determined by the exchange, anisotropy, and the magnetic field. One of the relaxational branches is soft (its frequency becomes zero as $k \to 0$ at the RPT point itself). In large fields, two precessional branches arise in the spectrum of vibrations of the antiferromagnet in phases with $\mathbf{ML} = 0$ (phases 2 and 3) near the reorientation transition into a phase with $\mathbf{ML} \neq 0$ (phase 1). However, in this case again the soft mode in the RPT region is a relaxational mode. The last case with the discarded condition $\mathbf{ML} = 0$ (with allowance for the condition $\mathbf{L}^2 = \text{const}$) was investigated

theoretically and experimentally [4, 25] in rare-earth orthoferrites. The results that were obtained in these works correspond to the case $\omega_H(1-\eta)^{3/2}/(\omega\eta) \gg r_{1,2} \gg (\omega_{ij}/\omega_E)^{1/2}$.

**3.2.3 Spectrum of coupled magnetoelastic waves in a two-sublattice antiferromagnet.** Now, we introduce a magnetoelastic interaction ($b \neq 0$). An analysis of the coupled set of equations (3.33) shows that the main features of the spectrum of magnetoelastic vibrations are the same in all phases (3.32). Therefore, we restrict ourselves to consideration of the spectrum behavior in phase 3 in the region of the $3 \to 1$ RPT. In this case, the magnetic branches $\omega_1$ and $\omega_{2,3}$ only interact with another transverse elastic branch with a polarization along the $x$ axis. The other transverse branch (with the polarization along the $y$ axis) and the longitudinal sound interact with the magnetic branches $\omega_4$ and $\omega_{5,6}$. The interaction of the latter in the region of the $3 \to 1$ RPT can be neglected. The linearized set of equations (3.33) for the interacting magnetic and elastic vibrations has the form

$$\begin{aligned}
&\big[r_1\omega_E - i(1-\eta)\omega\big]m_z + (1-\eta)\omega_H m_y + r_1\eta\omega_H l_x = 0\,,\\
&(r_1\omega_E - i\omega)m_y + \left(\omega_{31} + \omega_{me} - \frac{\eta\omega_H^2}{\omega_E}\right)l_x\\
&\qquad - \omega_H m_z + \frac{i}{2}kgbL^2\tilde{u}_x = 0\,,\\
&\left\{r_2\left[(\omega_{32}+\omega_{me})(1-\eta) + \frac{\eta^2\omega_H^2}{\omega_E}\right] - i(1-\eta)\omega\right\}l_x\\
&\qquad - (1-\eta)\omega_E m_y + r_2\eta\omega_H m_z + \frac{i}{2}\,r_2 kgbL^2\tilde{u}_x = 0\,,\\
&(\omega^2 - \omega_{tk}^2)\tilde{u}_x + \frac{i}{2\rho}kbLl_z = 0\,,
\end{aligned} \tag{3.49}$$

where $\omega_{tk} = s_t k$, $s_t^2 = \mu/\rho$.

The dispersion equation of the set of equations (3.49) in the approximation $\omega_E \gg \omega_{31}$, $\omega_H$ and $r_1 \approx r_2 \ll 1$ can be written as

$$\begin{aligned}
&(1-\eta)i\omega^5 - r_1\omega_E(2-\eta)\omega^4 - i\Big\{(1-\eta)\big[\omega_{1k}^2\\
&\quad + (1-\eta)\omega_H^2 + \omega_{tk}^2\big] + r_1^2\omega_E^2\Big\}\omega^3\\
&\quad + r_1\omega_E\big[\omega_{1k}^2 + \omega_{tk}^2(2-\eta)\big]\omega^2\\
&\quad + i\omega_{tk}^2\Big\{(1-\eta)\big[\omega_{1k}^2(1-\xi_{tk}) + (1-\eta)\omega_H^2\big]\\
&\quad + r_1^2\omega_E^2\Big\}\omega - r_1\omega_{tk}^2\omega_{1k}^2\omega_E(1-\xi_{tk}) = 0\,,
\end{aligned} \tag{3.50}$$

where

$$\omega_{1k}^2 = \omega_{sk}^2 + \omega_E\omega_{me}\,,\quad \omega_{sk}^2 = \omega_{31}\omega_E\,,$$
$$\omega_{me} = \frac{gb^2M_0^3}{\mu}\,,\quad \xi_{tk} = \frac{\omega_E\omega_{me}}{\omega_{1k}^2}\,. \tag{3.50a}$$

First, let us consider the spectrum of coupled magnetoelastic waves in the antiferromagnet at $k = 0$. In this case, the dispersion equation is divided into two equations. A solution to the first of these are two zero frequencies

$$\omega_{4,5} = 0\,, \tag{3.51}$$

and the other three frequencies ($\omega_{1,2,3}$) are determined from the cubic equation

$$\begin{aligned}
&(1-\eta)i\omega^3 - r_1\omega_E(2-\eta)\omega^2 - i\Big\{(1-\eta)\big[\omega_{10}^2\\
&\quad + (1-\eta)\omega_H^2\big] + r_1^2\omega_E^2\Big\}\omega + r_1\omega_E\omega_{10}^2 = 0\,.
\end{aligned} \tag{3.52}$$

This equation coincides with equation (3.38) in which $\omega_{32}$ is replaced by $\omega_{10}^2/\omega_E$. With allowance for the magnetoelastic interaction at the point of the $3 \to 1$ RPT ($\omega_{31}(0) = 0$), the frequency $\omega_{10}$ does not vanish ($\omega_{10}^2(0) = \omega_E\omega_{me}$ is the magnetoelastic gap in the spectrum of quasispin waves). Therefore, both at the RPT point and near it and even far from it, the approximate solutions to the dispersion equation (3.52) will be expressed by formulas (3.40)–(3.42) in which, again, $\omega_{32}$ is replaced by $\omega_{10}^2/\omega_E$.

Thus, at the point of the RPT where $\omega_{31}(0) = 0$ at $k = 0$, as well as at large attenuation in the magnetic subsystem and in small fields (or low temperatures, $\eta \to 1$), the spectrum of coupled magnetoelastic vibrations consists of three activational branches $\omega_{1,2,3}$ (3.40) and two activationless branches $\omega_{4,5}$ (3.51). All three activational branches are relaxational. The $\omega_1$ mode, which in the absence of a magnetoelastic coupling was soft, with the allowance for the magnetoelastic interaction becomes activational, with an activation that is determined by this interaction.

In the case when at the RPT point the relaxation frequency in the magnetic subsystem is small in comparison with the magnetoelastic gap ($\omega_{10} \gg r_1\omega_E$) and the magnetic field is small or the RPT occurs at low temperatures, the frequency $\omega_1$ (3.41a) remains, as before, relaxational with an activation that is determined by the magnetoelastic coupling. The other two frequencies $\omega_{2,3}$ (3.41b) describe weakly damped precessional vibrations, i.e., quasispin waves (only positive frequencies are physically meaningful). It follows from (3.41b) that if the RPT occurs at low temperatures and in relatively low magnetic fields, then the dependence of the activation of the quasispin waves on the magnetic field is weak; it shows up only in the second order in the expansion of the frequency $\omega_{2,3}$ in powers of the small parameter $1-\eta$. The activation of the quasispin waves upon changes in the magnetic field remains in this case virtually unaltered and is determined by the magnetoelastic interaction.

And, finally, if the RPT occurs at high temperatures and in high magnetic fields, then the activational branches are expressed by formulas (3.42). The first of these, as before, remains relaxational, while the others describe quasispin vibrations. According to (3.42), the activation of quasispin branches in this case can completely be determined by the magnetic field and the longitudinal susceptibility (if this contribution dominates over the magnetoelastic one).

At $k \neq 0$ in the long-wavelength approximation ($\omega_{tk}^2 \ll \omega_E\omega_{me}$) the spectrum of coupled magnetoelastic waves also consists of five branches. Three branches $\omega_{1,2,3}$ as before are activational, but now their dispersion law depends on the wave vector **k**. The dispersion laws for these branches in the zeroth approximation in the small parameter $\omega_{tk}^2/(\omega_E\omega_{me})$ are expressed by formulas analogous to (3.40)–(3.42) at $k \neq 0$. In the first approximation, additions will appear in formulas (3.40)–(3.42), which are proportional to this small parameter [7]. The dispersion laws for the last two branches of coupled vibrations in the long-wavelength approximation and at $(1-\eta)\omega_{tk}\Omega_{1k}(\Omega_{1k}^2 + \omega_E\omega_{me})^{1/2}/\omega_{1k}^2 \ll r_1\omega_E$ are expressed

by the formulas

$$\omega_{4,5}=\frac{1}{2}\left(\pm\left\{4\omega_{tk}^2(1-\xi_{tk})-\frac{\omega_{tk}^4\left[(1-\eta)\Omega_{1k}^2+r_1^2\omega_E^2\right]^2}{r_1^2\omega_E^2\omega_{1k}^4}\right\}^{1/2}-\mathrm{i}\frac{\omega_{tk}^2\left[(1-\eta)\Omega_{1k}^2+r_1^2\omega_E^2\right]}{r_1\omega_E\omega_{1k}^2}\right), \tag{3.53}$$

where $\Omega_{1k}^2=\omega_{sk}^2+(1-\eta)\omega_H^2$. This means that at $r_1\omega_E\omega_{1k}^2(1-\xi_{tk})^{1/2}/[(1-\eta)\Omega_{1k}^2+r_1^2\omega_E^2]\gg\omega_{tk}$ these branches are weakly damped quasielastic branches with a quadratic law of dispersion

$$\omega_{4,5}=\pm\omega_{tk}\left(\frac{g\alpha Lk^2}{\omega_E\omega_{me}}\right)^{1/2}-\mathrm{i}\,\frac{\omega_{tk}^2\left[(1-\eta)\Omega_{1k}^2+r_1^2\omega_E^2\right]}{2r_1\omega_E\omega_{1k}^2}\,. \tag{3.54}$$

In the opposite case, the $\omega_{4,5}$ branches become purely relaxational with a quadratic dependence on $k$:

$$\omega_4=-\mathrm{i}\,\frac{\omega_{tk}^2\left[(1-\eta)\Omega_{1k}^2+r_1^2\omega_E^2\right]}{r_1\omega_E\omega_{1k}^2}\,,$$
$$\omega_5=-\mathrm{i}r_1\frac{\omega_E\omega_{1k}^2(1-\xi_{tk})}{(1-\eta)\Omega_{1k}^2+r_1^2\omega_E^2}\,. \tag{3.55}$$

The first of these branches is quasielastic and the second is quasirelaxational.

At $(1-\eta)\omega_{tk}\Omega_{1k}(\Omega_{1k}^2+\omega_E\omega_{me})^{1/2}/\omega_{1k}^2\gg r_1\omega_E$, the $\omega_{4,5}$ branches describe weakly damped quasielastic branches of vibrations with a linear dispersion law at the RPT point:

$$\omega_{4,5}=\pm\frac{\omega_{tk}\Omega_{1k}}{\left[\omega_{1k}^2+(1-\eta)\omega_H^2\right]^{1/2}}-\frac{1}{2}\,\mathrm{i}r_1\omega_E\omega_{1k}^2\frac{\xi_{tk}(1-\eta)\omega_H^2-(1-\xi_{tk})\omega_{tk}^2}{(1-\eta)\Omega_{1k}^2\left[\omega_{1k}^2+(1-\eta)\omega_H^2\right]}\,. \tag{3.56}$$

In the range of large $k$ ($\omega_{tk}^2\gg\omega_E\omega_{me}$), the spectrum of coupled vibrations again will consist of weakly damped quasispin (precessional) and quasielastic and quasirelaxational branches. The dispersion law for the quasielastic vibrations in this case will only slightly deviate from linearity.

Note that the condition $r_1\omega_E\omega_{1k}^2(1-\xi_{tk})^{1/2}/[(1-\eta)\Omega_{1k}^2+r_1^2\omega_E^2]\ll\omega_{tk}$ imposed on the magnitude of the wave vector $k$ goes into the inequality imposed on the parameters of the antiferromagnet. Indeed, using the above-introduced designations for the frequencies that enter into this inequality, we obtain $\omega_{31}(0)=0$ at the RPT point and a new condition $(g\alpha L\omega_{me})^{1/2}\ll\tilde{r}_1 s_t$, where $\tilde{r}_1=r_1\{1+(1-\eta)^2\times[\omega_H/(r_1\omega_E)]^2\}$, instead of the above-written condition, at $k\to 0$. This new condition is actually imposed on the attenuation parameter $\tilde{r}_1$. At typical values of the antiferromagnet parameters, e.g., $g\approx 1.8\times 10^7$ Oe$^{-1}$ s$^{-1}$, $\alpha\approx 10^{-12}$ cm$^2$, $L\approx 10^2$ G, $bL^2\approx 10^7$ erg cm$^{-3}$, and $s_t\approx 3\times 10^5$ cm s$^{-1}$, we obtain that the activationless branches will be purely relaxational for the damping parameter $\tilde{r}_1\gg 10^{-4}$. As in the case of ferromagnets, in the RPT region this condition can be fulfilled here with a high probability. As a result of the fulfillment of this condition and, thereby, of the transformation of the quasielastic branch into a purely relaxational one, a 100% decrease in the velocity of the transverse quasielastic waves at the RPT points may take place, which was not observed in experiments and in antiferromagnets.

With allowance for the Dzyaloshinskiĭ interaction in the equilibrium state of the antiferromagnet in a field $\mathbf{H}\|\mathbf{x}$, again three magnetic phases will exist: (1) $M_x$, $M_z$, $L_x$, $L_z$; (2) $M_x$, $L_y$, $L_z$; and (3) $M_x$, $L_z$. The first two phases are canted. The condition $\mathbf{ML}=0$ is fulfilled only for phases 2 and 3. An analysis of the equations of motion (3.33) shows that the spectrum of coupled vibrations in phase 3 will be determined by formulas analogous to (3.39)–(3.43) and (3.53) but with new expressions for the characteristic frequencies entering into these formulas. The behavior of the branches of coupled vibrations of the antiferromagnet near the second-order $3\to 1$ and $3\to 2$ RPTs in this phase remains the same as in the absence of the Dzyaloshinskiĭ interaction. The spectrum of vibrations in the canted phases 1 and 2 is expressed by more complex formulas than (3.40)–(3.42). However, in these phases too, the behavior of the spectrum near the second-order $1\to 3$ and $2\to 3$ RPTs and near the first-order $1\to 2$ RPT will be analogous to that for phases 1 and 2 of an antiferromagnet without allowance for the Dzyaloshinskiĭ interaction.

Thus, the investigation of the vibrational spectrum of an antiferromagnet on discarding the condition of the constancy and the equality of the absolute values of the sublattice magnetizations in statics and dynamics, performed in this section, makes it possible to arrive at the following conclusions.

The abandonment of the condition $\mathbf{ML}=0$ in statics leads to the appearance in the antiferromagnet located in a magnetic field of a phase in which $\mathbf{M}\|\mathbf{L}$ and, consequently, $\mathbf{ML}\neq 0$.

The abandonment of the conditions $\mathbf{ML}=0$ and $\mathbf{M}^2+\mathbf{L}^2=\text{const}$ in the dynamics of the antiferromagnet also leads to the situation when, apart from a precessional motions of the $\mathbf{M}$ and $\mathbf{L}$ vectors, their transverse and longitudinal relaxational motions become possible. In this case, in the absence of a magnetoelastic interaction, the soft mode near the RPT is the relaxational mode corresponding to the transverse relaxation of the antiferromagnetism vector. With allowance for the magnetoelastic coupling, the soft relaxational mode becomes activational near the RPT, with the activation determined by the magnetoelastic interaction. In this case, the soft mode is the quasielastic vibrational mode with a quadratic dispersion law at the RPT point. At a sufficiently large value of the attenuation parameter of the antiferromagnet, the quasielastic branch can become purely relaxational.

## 4. Discussion of results

### 4.1 Ferromagnet. Main features of the vibrational spectrum

As the above theoretical results show, in calculations of the spectrum of vibrations of a ferromagnet, as well as of an antiferromagnet, allowance for the relaxation is necessary. The effect of relaxational vibrations on the precessional vibrations especially increases near the points of phase transitions. Thus, in neglect of the magnetoelastic interaction, the spectrum of vibrations of transverse components of magnetization in a ferromagnet far from an RPT represents weakly damped spin waves (3.14), whereas near the RPT the precessional character of motion of these components changes to become purely relaxational (3.15); the soft mode in this case is the relaxational transverse mode (at the

transition point at $k = 0$ its frequency becomes zero). The longitudinal frequencies in a ferromagnet are always relaxational.

With allowance for the magnetoelastic interaction, in the ground state of the ferromagnet selected in Section 3.1, the vibrations of the transverse components of the magnetization interact with the transverse elastic vibrations and the longitudinal vibrations of the magnetization interact with the longitudinal elastic waves.

The spectrum of transverse magnetoelastic waves consists of six branches (only positive frequencies are physically meaningful). The $\omega_{1,2}$ branch is activational, with a gap magnitude that is determined according to (3.17) by the magnetoelastic coupling and magnetization relaxation. The other branches are activationless. One of the quasielastic branches of vibrations ($\omega_{3,4}$) near the RPT has a linear dispersion law (3.17). The allowance for the magnetization relaxation leads to the attenuation of this elastic branch. The second activationless branch of coupled vibrations [$\omega_{5,6}$ (3.18), (3.19)] may be both quasielastic and quasimagnetic. In both cases the dispersion law for this branch is quadratic in $k$. At $\omega_{2k}\omega_{2sk} \gg r_1^2\omega_t^2$, the $\omega_{5,6}$ branch is quasielastic. At $\omega_{2k}\omega_{2sk} \ll r_1^2\omega_t^2$, the $\omega_{5,6}$ branches describe purely relaxational vibrations — quasispin and quasielastic, respectively. It is these two modes that become softened on approaching the RPT point.

Thus, near the RPT all types of transverse motion of both magnetization and lattice can become relaxational. Note that at the RPT point itself, the soft mode is relaxational (the transition itself occurs through a relaxational soft mode).

With allowance for the magnetoelastic interaction, the spectrum of coupled vibrations of a ferromagnet always contains a weakly damped activational quasispin mode with an activation that is determined by the extent of the magnetoelastic coupling. The mode that becomes soft at the RPT point is the quasielastic branch, which may become purely relaxational.

The spectrum of longitudinal magnetoelastic vibrations of a ferromagnet consists of three branches (3.20) – (3.22).

Far from the Curie point, in the case where the minimum phase velocity of relaxational modes $v_{\min}$ is less than the velocity of the longitudinal sound $s_l$, there exists a range of wave numbers (3.21) where all vibrations are nonpropagating.

If the phase transition at the Curie point is of the first order (this is possible if the exchange constant $\widetilde{B}$ is negative), then at $v_{\min} \gg s_l$ and $k \to 0$ the dispersion law of quasielastic waves is cubic in $k$ (3.25) and the velocity of these waves tends to zero as $k \to 0$ (3.26). This behavior of longitudinal quasisound is observed at a certain relationship between the elasticity and magnetoelasticity constants of the ferromagnet (3.24).

An anomalous decrease in the velocity of the longitudinal sound is also possible (at $\widetilde{B} > 0$) near a second-order phase transition (3.29), but its velocity in this case cannot reach the theoretical limit equal to zero, in contrast to the first-order phase transition at $\widetilde{B} < 0$.

One of the relaxational branches (3.20), corresponding to the relaxation of magnetization, has an activation at the Curie point that is determined by the magnetoelastic interaction. This suggests that the time of the longitudinal relaxation of magnetization at the Curie point remains finite rather than tends to infinity, in contrast to the case where the magnetoelastic coupling is absent.

### 4.2 Antiferromagnet. Main features of the spectrum near phase transitions

The review of experimental and theoretical works on the dynamics of magnets in the region of magnetic phase transitions that was given in this paper and in Ref. [1] shows that the gap at the points of phase transitions in the spectrum of precessional spin vibrations is formed at the expense of a whole number of contributions, such as magnetoelastic, relaxational and dipolar contributions, as well as contributions from other magnetic subsystems if the magnet contains magnetic ions of other atoms. The role of all contributions, except for relaxational, was considered in detail in Ref. [1]. Therefore, here we will discuss the role of the longitudinal susceptibility and relaxation in the dynamics of magnets.

First, we consider how the spectrum of magnetic vibrations changes with the allowance for only the longitudinal susceptibility and relaxational contribution, i.e., we neglect the magnetoelastic and dipole contributions and the effects of other magnetic subsystems. This will permit us to clarify which of the magnetic vibrational branches is softened at the point of phase transition.

1. Phase $\mathbf{M}||\mathbf{L}||\mathbf{x}$. Near the point of the first-order reorientation phase transition of type $1 \to 2$ ($\omega_{23}(0) = 0$), the spectrum of spin vibrations consists, according to (3.36), of four relaxational branches $\omega_{1,2,3,4}$ and one precessional branch $\omega_{5,6}$ (only positive frequencies are physically meaningful). The soft mode for this transition is the relaxational branch $\omega_3$ that corresponds to the transverse vibrations of the ferromagnetism and antiferromagnetism vectors. At the transition point itself it vanishes. The precessional branch $\omega_{5,6}$ is activational. At the transition point, its activation is determined by the anisotropy, magnetic field, and longitudinal susceptibility (3.36c). A more exact calculation using the complete dispersion equation [see Appendix, Eqn (A.1)] leads to the appearance of a relaxational contribution in the activation of this branch at the point of the $1 \to 2$ transition:

$$\operatorname{Re}\omega_{5,6}^2 = \omega_{\mathrm{E}}\omega_{13} + \omega_H^2(1+\eta)^2 + r_1 r_2 \omega_{\mathrm{E}}\omega_{13}\,. \qquad (4.1)$$

Note that the anisotropy contribution to the activation of this branch is caused by the interaction of the vibrations of the transverse components of the ferromagnetism and antiferromagnetism vectors and by the choice of the model of the antiferromagnet as a biaxial magnet. In the case of a uniaxial antiferromagnet ($\beta_1 = \beta_3$), this contribution in (4.1) will be absent and the gap in the precessional branch will be determined by the magnetic field, longitudinal susceptibility, and relaxational contribution [second and third terms in (4.1)]. Note that even in the case of a uniaxial crystal and spontaneous RPT (i.e., at $H = 0$) the gap in the spectrum of the precessional branch is not equal to zero. In this case, it is determined by the purely relaxational contribution [third term in (4.1)].

In the region of the phase transition $1 \to 3$ ($\omega_{13}(0) = 0$), the vibrational spectrum behaves in a similar way and is described by the same formulas that were considered above, with the replacement of $\omega_{23}$ by $\omega_{13}$.

An analysis of the linearized Landau – Lifshitz equations (3.34) and of the complete dispersion equation (A.1) shows that in the region of the second-order phase transition $1 \to 4$ the spectrum of magnetic vibrations consists of two relaxational branches

$$\omega_1 = -\mathrm{i}r_1\omega_{\mathrm{E}}\,, \quad \omega_2 = -\mathrm{i}r_2(\omega_B - \tilde{\omega}_B)\,, \qquad (4.2a)$$

and four precessional branches

$$\omega_{3,4}=\frac{1}{2}\left\{\pm\left[\frac{4\omega_H^2\omega_{13}\omega_{23}}{\omega_E^2}-r_2^2(\omega_{13}+\omega_{23})^2\right]^{1/2}-ir_2(\omega_{13}+\omega_{23})\right\},$$

$$\omega_{5,6}=\pm\omega_H-ir_1\omega_E\,. \qquad (4.2b)$$

Directly at the phase transition point ($\omega_B=0$, $\eta=0$, since $L=0$), softening of the relaxational branch $\omega_2$, which corresponds to longitudinal vibrations of the antiferromagnetism vector, occurs. Note that near the Néel point the $\omega_{3,4,5,6}$ branches can also become relaxational, since in this case the transition occurs in small magnetic fields.

2. Phase $\mathbf{M}||\mathbf{x}$, $\mathbf{L}||\mathbf{y}$. Near the first-order phase transition $2\to1$ ($\omega_{32}(0)=0$), the spectrum of magnetic vibrations in the case of small magnetic fields consists of four relaxational branches $\omega_{1,2,3,4}$ and two precessional branches $\omega_{5,6}$ [formulas (3.40) and (3.43)]. Far from the phase transition and in large magnetic fields, the vibrational spectrum consists of two relaxational branches ($\omega_1$, $\omega_4$) and two precessional branches ($\omega_{2,3}$, $\omega_{5,6}$) [formulas (3.41)–(3.43)]. It follows from the linearized set of equations (3.37) that the vibrations of the transverse components of the ferromagnetism and antiferromagnetism vectors are separated. Therefore, at the point of the RPT at large magnetic fields the activation of the precessional branch $\omega_{2,3}$ (3.39) is determined only by the magnetic field and is not masked by the anisotropy contribution from the frequencies of the $\omega_{12}$ branch, as took place in the previous phase. Since the phase transitions $1\to2$ and $2\to1$ are first-order phase transitions, the activations of the precessional branch $\omega_{2,3}$ do not coincide on the phase 1 and 2 sides, i.e., a jump of the activation of this precessional branch occurs at the transition point. The activation of the second precessional branch $\omega_{5,6}$ near the transition at hand is always mainly determined by anisotropy. The soft mode in the region of the $2\to1$ RPT is the relaxational mode $\omega_1$.

In the vicinity of the RPT $2\to3$ ($\omega_{12}(0)=0$), the spectrum of magnetic vibrations at $r_1\omega_E\gg(\omega_{12}\omega_E)^{1/2}$ also consists of four relaxational branches ($\omega_1$, $\omega_{4,5,6}$) and two precessional branches ($\omega_{2,3}$). In the opposite case, at $r_1\omega_E\ll(\omega_{12}\omega_E)^{1/2}$, there are two relaxational branches ($\omega_1$, $\omega_4$) and four precessional branches ($\omega_{2,3}$, $\omega_{5,6}$). The soft mode in the region of this transition is the relaxational mode $\omega_4$. Note that in its nature the $2\to3$ RPT is the spontaneous reorientation transition, since according to (3.32) this transition is accompanied by the replacement of the sign of the difference of the anisotropy constants $\beta_1-\beta_2$. From this and from (3.43) it follows that the activation of the $\omega_{5,6}$ branch is always determined only by anisotropy.

From the linearized set of Landau–Lifshitz equations (3.37) and the complete dispersion equations (A.2) and (A.3), it follows that in the region of the second-order phase transition $2\to4$ the spectrum of magnetic vibrations consists of four relaxational branches

$$\omega_1=-ir_1\omega_E\,,\quad \omega_2=-ir_2\omega_{12}\,,\quad \omega_3=-ir_2\omega_{32}\,,$$

$$\omega_4=-i\omega'_B\frac{\omega_H^2}{r_1\omega_E^2} \qquad (4.3a)$$

and two precessional branches

$$\omega_{5,6}=\pm\omega_H-ir_1\omega_E\,. \qquad (4.3б)$$

At the phase transition point ($\omega'_B=0$), softening of the relaxational branch $\omega_4$ that corresponds to longitudinal vibrations of the antiferromagnetism vector occurs. Near the Néel point, as in the region of the $1\to4$ transition, all branches can become relaxational.

3. Phase $\mathbf{M}||\mathbf{x}$, $\mathbf{L}||\mathbf{z}$. All features of the spectrum of magnetic vibrations follow from the results obtained for the previous phase with the replacement of the index 1 by 2 at the characteristic frequencies and constants.

With allowance for the magnetoelastic interaction in the region of the $2\to1$ RPT, in the case of large attenuation in the magnetic subsystem $r_1\omega_E\gg(\omega_{me}\omega_E)^{1/2}$ (or small value of the parameter of magnetoelastic coupling), the spectrum of the interacting magnetic and elastic vibrations consists of three quasimagnetic relaxational branches (3.52) and two quasielastic branches (3.53). However, the magnetoelastic interaction leads to the appearance of a magnetoelastic gap in the dispersion law of soft relaxational modes of vibrations [the frequency $\omega_1$ at $\omega_{32}=\omega_{me}$ (3.40)]. The soft modes in this case are the magnetoelastic modes with a quadratic dispersion law at the transition point (3.54), (3.55). These modes in the case of large attenuation in the magnetic subsystem can also become purely relaxational.

In the opposite case, at $r_1\omega_E\ll(\omega_{me}\omega_E)^{1/2}$, the spectrum of coupled vibrations consists of one relaxational branch with a gap determined by the magnetoelastic interaction, two precessional quasispin branches [$\omega_1$ and $\omega_{2,3}$ at $\omega_{32}=\omega_{me}$ (3.41) and (3.42)], and two quasielastic branches. The latter are, as before, softening at the RPT point.

Similar behavior is exhibited by the spectrum of coupled magnetoelastic vibration in the RPT region in other phases at hand.

With the allowance for the interaction of magnetoelastic vibrations with electromagnetic waves, a contribution caused by this interaction can additively enter into the activational branches of vibrations. As was shown in Ref. [1], in this case the frequency of the magnetoelastic gap $\omega_{me}$ in the expressions for the frequencies of quasimagnetic vibrations should be replaced by $\omega_{me}+\omega_{dip}$, where the latter term is just that term that describes the interaction between the magnetoelastic and electromagnetic waves.

If the antiferromagnet contains one more subsystem of magnetic ions (e.g., a rare-earth subsystem in orthoferrites), then the activation of the quasimagnetic branches also can contain an additive contribution from this subsystem (see Ref. [1]).

### 4.3 Antiferromagnet. Comparison of theory and experiment

Let us compare theoretical results on the magnitude of the activation in the spectra of quasimagnetic vibrations with the results of the above experiments.

**1.** $\Gamma_2-\Gamma_{24}$ and $\Gamma_4-\Gamma_{24}$ phase transitions in the orthoferrites $YbFeO_3$ and $TmFeO_3$ and the $\Gamma_2-\Gamma_{24}$ phase transition in $ErFeO_3$. To estimate the gaps in the spectrum of quasispin waves, we will use formulas (3.41b) and (3.42). As follows from the experimental results (see Fig. 2, 5, and 6), the magnitude of the gap in the spectrum of quasispin branches of vibrations at the points of these transitions is independent of the magnetic field up to fields of 10 kOe. According to the experimental data of Refs [25, 37], the magnitude of $\eta$ in the region of these transitions is approximately 0.9. Using the experimental value of the gap in the spectrum of quasispin vibrations $2\pi\nu=(\omega_{32}\omega_E)^{1/2}\approx126$ GHz (the smallest value from all the results in the figures considered) and the value 1.8 GHz kOe$^{-1}$ for the gyromagnetic ratio $g$, we obtain the

following value for the contribution from the magnetic field to the gap of quasispin waves at the maximum value of the magnetic field $H = 10$ kOe: $2\pi\Delta\nu_H \cong 0.6$ GHz according to (3.41b) and $2\pi\Delta\nu_H \cong 55.7$ GHz according to (3.42b). The last value is at least twice as large as the experimental error. This suggests that, near these transitions, the condition $(\omega_{32}\omega_E)^{1/2} \gg r_1\omega_E \gg (1-\eta)^{1/2}\tilde{\omega}_{32}$ should be fulfilled in phase 2 and the gap width should be described by formula (3.41b). In this case, the activation is virtually independent of the magnitude of the magnetic field. In reality, under the experimental conditions, a situation which is intermediate between those described by formulas (3.41b) and (3.42b) can arise, since, according to estimates [1], the exchange frequency is $\omega_E \approx 2.5 \times 10^{14}$ s$^{-1}$, and the parameter of relaxation is $r_1 \sim 10^{-4}$. In this case, the quantities $r_1\omega_E$ and $(1-\eta)^{1/2}\tilde{\omega}_{32}$ are of the same order of magnitude, and it is this circumstance that leads to the intermediate result. An estimate of the relaxation parameter $r_1$ in Ref. [1] is very rough; therefore, it is difficult to expect better agreement between the experiment and the theory. Nevertheless, the existence in the theory of an interval of parameters [formula (3.41b)] in which at low temperatures a weak dependence on the magnetic field is revealed suggests good qualitative agreement between the theory and experiment.

**2.** $\Gamma_2-\Gamma_{24}$ and $\Gamma_4-\Gamma_{24}$ phase transitions in $Fe_3BO_6$. According to experimental data (see Section 2.2.2), the magnitude of $\eta$ in $Fe_3BO_6$ in the region of the phase transitions at hand is 0.7. Assuming that in $Fe_3BO_6$ the magnitude of the gap in the spectrum of quasispin waves in a zero magnetic field is $2\pi\nu \cong 94$ GHz (see Fig. 9) and taking the same values of the exchange frequency and relaxation parameter as those used for the orthoferrites of ytterbium, thulium and erbium, we obtain that for this antiferromagnet conditions (iii) and formulas (3.42) should be valid in phase 2. Thus, a strong dependence of the gap magnitude on the magnetic field should be observed for $Fe_3BO_6$, which indeed was observed in experiments (see Fig. 9). The estimation of the gap increment from formula (3.42) at $g = 1.8$ GHz kOe$^{-1}$ in a field of 10 kOe yields a frequency $\nu \approx 10$ GHz. This result agrees well with the experimental value $\nu \approx 7$ GHz.

In calculations performed in Refs [30, 34] and in the works cited therein, the effect of the magnetoelastic and dipolar interaction on the spectrum of spin vibrations was ignored, although it is known [1, 2, 6, 7] that the influence of these interactions in the region of phase transitions on the spectrum of spin waves can even become decisive. This statement is valid for both first- and second-order phase transitions. The spectra of quasispin vibrations in REOFs and in the region of spontaneous first-order phase transitions were calculated in Ref. [2]. It is natural to compare the results obtained in [2] for resonance frequencies with the experimental results of Refs. [31, 32]. In order that such a comparison of theoretical and experimental results in the case of phase transitions induced by a magnetic field could be possible, we should combine the expressions for the resonance frequencies obtained in Ref. [2] for spontaneous phase transitions with those obtained in Refs. [30, 34] for induced transitions. Here, we only give a formula for the ferromagnetic $\sigma$ mode. In the $\Gamma_2$ phase, the activation for this mode is

$$\nu_{10}^2 = \left(\frac{g}{2\pi}\right)^2 \left[\frac{H_E K_1}{M_0} + H_E(H_{me5} + H_{dip1}) + H(H + H_{D1})\right], \tag{4.4}$$

and in the $\Gamma_4$ phase, it will be as follows:

$$\nu_{10}^2 = \left(\frac{g}{2\pi}\right)^2 \left[-\frac{H_E(K_1 + 2K_2)}{M_0} + H_E(H_{me5} + H_{dip2}) + H(H + H_{D2})\right]. \tag{4.5}$$

Here, $H_E$, $H_{me5}$, $H_D$, and $H_{dip}$ are the fields of the uniform exchange, magnetostriction, Dzyaloshinskiĭ interaction, and dipole interaction, respectively; and $K_{1,2}$ are the effective second- and fourth-order anisotropy constants of REOFs [2, 30]. Formulas (4.4) and (4.5) correspond to the cases where no longitudinal vibrations exist ($\eta = 0$), since the exact expressions for the frequencies of vibrations of the spin subsystem of antiferromagnets with allowance for the Dzyaloshinskiĭ interaction and longitudinal susceptibility are absent in the literature. As below we will mainly be interested in the behavior of the frequency of the quasiferromagnetic mode at $H = 0$ and in the region of weak fields and since, according to formulas (3.42), the parameter $\eta$ enters into the expression for the frequencies of spin vibrations mainly in combination with the magnetic field, the neglect of the longitudinal susceptibility in weak fields seems to be justified.

The point of the first-order spontaneous $\Gamma_2-\Gamma_4$ RPT is determined by the condition $K_1 + K_2 = 0$ (a first-order phase transition is only possible at $K_2 < 0$). From this, it follows that, at $H = 0$ and in neglect of the magnetoelastic and dipolar interactions ($H_{me5} = 0$ and $H_{dip} = 0$) at the point of the phase transition, the activations in the spectrum of spin waves on both the $\Gamma_2$ and $\Gamma_4$ phase sides are the same and are determined as

$$\nu_{10}^2 = \left(\frac{g}{2\pi}\right)^2 \left(-\frac{H_E K_2}{M_0}\right). \tag{4.6}$$

Thus, in this case no frequency jump arises at the point of the phase transition. Just this result was obtained in [30, 34]. In reality, as follows from the exact formulas (4.4) and (4.5), this jump does exist and is determined in the zero magnetic field by the dipole contribution:

$$\Delta\nu = \frac{g}{2\pi}\left[H_E(H_{dip2} - H_{dip1})\right]^{1/2}. \tag{4.7}$$

Now, we estimate the magnitude of the jump at the point of the spontaneous phase transition. To this end, we will use the following values of the exchange and dipole fields: $H_E \approx 5 \times 10^6$ Oe and $H_{dip2} - H_{dip1} \approx 1$ Oe [2, 30, 34]. Then, we obtain a numerical value of the frequency jump at the point of the spontaneous RPT equal to $\Delta\nu \approx 7$ GHz. This value agrees well with the experimental value $\Delta\nu \approx 5.7$ GHz (see Fig. 8). Thus, the allowance for the dipole interaction permits us to satisfactorily describe the experimentally observed frequency jump at the point of the spontaneous RPT. Allowing for the longitudinal vibrations, the expressions for the frequencies of quasispin waves (4.4) and (4.5) will also contain a gap of relaxational origin, similar to that given by formula (3.42). In principle, given the anisotropic character of this gap, it also can yield a contribution to the frequency jump upon the spontaneous RPT. Along with the dipole contribution, a relaxation contribution to the gap in formula (3.42), caused by the interaction of precessional and relaxational vibrations, may lead to discrepancies between the values of the gap at the RPT points for gaps obtained from formula (3.42) at $H = 0$ and the extrapolation of the spectrum to $H = 0$ from the region of greater values of the magnetic field (see Fig. 9).

Note that the modified formulas (4.4) and (4.5) also permit us to explain the nonzero value of the frequency derivative with respect to field at $H \to 0$. As follows from these formulas, this fact was caused by the allowance for the Dzyaloshinskiĭ interaction (terms linear in field in (4.4) and (4.5)).

**3.** $\Gamma_{124} - \Gamma_{24}$ phase transition in $ErFeO_3$. In its nature, this transition is an antiferromagnet – ferromagnet transition in the subsystem of rare-earth erbium ions and simultaneously a reorientation phase transition in the subsystem of iron ions. If we could separately describe the phase transition in the RE subsystem, then the spectrum of magnetic vibrations in the region of this transition would be described by formulas (4.2a) and (4.2b) and the gap in the activational branches of vibrations at the point of the transition would grow proportionally to the magnitude of the magnetic field. However, because of the presence of the iron subsystem, the parameter $\eta$ at the point of this transition is not zero and, consequently, the magnitude of the gap should also depend on the ratio between the longitudinal and transverse magnetic susceptibilities. Since the $\chi_{||}/\chi_{\perp}$ ratio and, consequently, the parameter $\eta$ in the region of this RPT is much greater than unity, the gap magnitude and its dependence on the magnetic field will be described by a formula analogous to (3.42b) or (4.1). According to these formulas, the magnitude of the activation in the spectrum of the quasispin branch is proportional to the parameter $\eta$. This fact agrees well with the experimental dependence of the gap magnitude in the spectrum of magnetic vibrations at the point of the considered phase transition (see Figs 11 and 12b). It follows from a comparison of these figures that the dependence of the gap magnitude on the temperature completely duplicates the temperature dependence of the $\chi_{||}/\chi_{\perp}$ ratio. Note that here we can only speak of a qualitative agreement between the theory and experiment, since the theory was developed for the case of a single magnetic subsystem.

### 4.4 Comparative analysis of various contributions to the spectrum of quasispin waves

It follows from the expressions for the gap magnitude at the RPT point [see, e.g., (3.41), (3.42)] that it is formed by the precessional contribution [first terms in (3.41b), (3.42b)], external magnetic field, and longitudinal susceptibility [second and third terms in (3.41b) and second term in (3.42b)], and by the relaxational contribution [third term in (3.42b)]. Since the corresponding contributions to the gap magnitude are additive, we may set a goal to experimentally separate them. This section will mainly be devoted to this problem. We will not consider any results of new measurements in it; the conclusions will be deduced from a comparative analysis of the whole body of experimental data given above and those obtained previously.

It has already been reliably established that the dynamics, caused mainly by the interaction of various vibrational subsystems of a magnet with precessional vibrations of the spin subsystem [first terms in (3.41b) and (3.42b)], can only be observed at moderately low temperatures and in weak (or zero) magnetic fields. In the corresponding magnets, the spontaneous RPTs should occur at relatively low temperatures. The theory and experimental data that satisfy these conditions were presented in review [1].

The separation of the field and temperature contributions to the dynamics caused by the second term in (3.42b) can be realized as follows. In order to separate the field contribution, the experiments should be performed at low temperatures (where $\chi_{||}$ is relatively small) but in a strong magnetic field. For example, to carry out corresponding measurements in REOFs, fields as high as 70 – 100 kOe are required. To separate the contribution which is mainly caused by the longitudinal susceptibility $\chi_{||}$, the measurements, on the contrary, should be conducted in a minimum magnetic field but at a sufficiently high temperature. Below, we give a comparative analysis of experiments performed in weak magnetic fields, but over a wide range of reorientation temperatures that satisfy the last condition. The role of the longitudinal susceptibility in the formation of energy gaps may be established on the basis of a series of experiments carried out over a wide range of values of the parameter $\tau_{SR}$. In this case, the contribution of the longitudinal vibrations of magnetization to the dynamics of REOFs in the region of spontaneous reorientation is actually separated. The above-described experiments permit one to trace the evolution of this contribution over the range of $\tau_{SR}$ from 0.01 to 1.

It follows from (3.42b) that the gap increases only if both related gradients (in both the field and temperature) are positive simultaneously. However, as can be seen from, e.g., Fig. 1, the simultaneous increase in $\chi_{||}$ and $H$ is only characteristic of the $\Gamma_{24} - \Gamma_2$ transition. In the $\Gamma_{24} - \Gamma_4$ transition, an increase in field is associated with a decrease in $\chi_{||}$. This circumstance does not imply, of course, that the increase in $H$ is necessarily compensated by a corresponding decrease in $\chi_{||}$ and that the theoretically predicted [4] effect (an increase of the gap with increasing applied field) will be suppressed. In the general case, the longitudinal susceptibility and the field may affect the magnitude of the gap with different efficiencies. But below, for definiteness, we will take into account a model situation, where the growth of the field upon the transition is associated with the growth of the longitudinal susceptibility as well, i.e., a situation characteristic of the $\Gamma_{24} - \Gamma_2$ transition in a field $\mathbf{H}||\mathbf{a}$. Correspondingly, we will only be interested in the magnitude of the energy gap $\nu_{02}$ in the vicinity of the temperature $T = T_2$. It is just on the example of such a transition in $YFeO_3$ that the thermodynamic theory of Ref. [4] has been developed and tested for the first time. In $YFeO_3$, no spontaneous reorientation occurs; therefore, only a $\Gamma_{24} - \Gamma_2$ transition can occur there in the presence of a magnetic field. The $H - T$ phase diagram of $YFeO_3$ in a field $\mathbf{H}||\mathbf{a}$ is such [62] that this transition in the temperature region accessible for experiments can only be induced in fields of 70 – 80 kOe. It is clear that it is impossible to do without field when considering the formation of the gap in the case of $YFeO_3$. However, this proves to be possible if reorientation of a similar type can occur spontaneously. Then, the entire magnitude of the gap can be ascribed to the precessional contribution. This could be checked using $DyFeO_3$, which was employed to test the thermodynamic theory in Ref. [5]. In this REOF, a spontaneous $\Gamma_1 - \Gamma_4$ Morin transition occurs at $T = 40$ K. Near this temperature, the $\Gamma_{24} - \Gamma_2$ transition can be induced by a relatively small field $\mathbf{H}||\mathbf{a}$. Such an experiment has not, unfortunately, been performed. But already at temperatures $T > 100$ K, as follows from [5], this transition can be induced only by a sufficiently strong field of at least 60 kOe. At such values of the field and temperature, the contribution of longitudinal vibrations and magnetic field to the magnitude of the energy gap is already sufficiently large. Although the thermodynamic theory of Ref. [4] was developed for transitions induced by an external field, it can be concluded from general

considerations that the longitudinal vibrations of magnetization will also contribute to the dynamics of REOFs in the reorientation region upon induced transitions close in nature to spontaneous transitions if the latter are realized at sufficiently high temperatures. Let us substantiate this assumption proceeding from the results of experiments on compounds with various values of the parameter $\tau_{SR}$.

Since the thermodynamic theory of Ref. [4] ignores the above-considered mechanisms of gap formation (at the expense of the interaction of various vibrational subsystems), it follows that as $H \to 0$ the gap also tends to zero. Since this is not the case in reality (significant gaps were observed in all REOFs even at $H = 0$), it is logical to search for the manifestation of effects of longitudinal vibrations in the form of an increment in the initial gap on 'switching-on' of the field. Therefore, the general methodical technique that was used in the experiments described above consisted in the following. First, the energy gap was measured upon a corresponding spontaneous transition and then the temperature (field) dependence of this gap was restored in a relatively small field (less than 10–12 kOe) that was rigorously oriented along the crystal axis. The sought effect was estimated by the magnitude of the derivatives $\partial\nu_0/\partial T$ and $\partial\nu_0/\partial H$. The latter of these should always be positive (according to [4, 5]); but for the $\Gamma_{24}-\Gamma_2$ transition the derivative $\partial\nu_0/\partial T$ also is always positive. If the temperature (field) dependence of the gap is such that $\partial\nu_{02}/\partial T$, $\partial\nu_{02}/\partial H \neq 0$ as $T \to T_2$, $H \to 0$, then we can estimate which contribution come from the longitudinal vibrations to the dynamics of REOFs in the region of the field-induced transition close to the spontaneous transition. Since the transition field can be sufficiently small in this case, it is clear that at a certain value the prevailing contribution to the effect will be determined only by the longitudinal susceptibility. It is natural that the 'fieldless' situation has not been considered in [4, 5], and the results that were obtained upon the testing of this model using $YFeO_3$ and $DyFeO_3$ [5] look rather like the 'effect of a strong field.' Therefore, it is unlikely that a detailed comparison of the actually observed dynamics of REOFs upon spontaneous RPTs with this theory is correct. Here, we only use its principal conclusion (and experimental test): the fact that longitudinal vibrations of magnetization contribute to the dynamics of REOFs in the reorientation region is confirmed by the increase in the magnitude of the gap with increasing field. As was shown experimentally [32, 34], this contribution can grow not only with increasing, but also with decreasing temperature. As was already noted, we will restrict ourselves to the first case. Let us analyze all the experiments in the sequence corresponding to the increase in the parameter $\tau_{SR}$. For convenience, the main results and the data on the REOFs and $Fe_3BO_6$ obtained in experiments are listed in the table.

It can be seen from this table that in the orthoferrites with relatively low temperatures of spontaneous reorientation transition $\Gamma_{24}-\Gamma_2$ ($\tau_{SR} < 0.15$), the gradient $\partial\nu_{02}/\partial H$ vanishes. Moreover, in the orthoferrites of ytterbium, thulium and erbium, this gradient vanishes not only at $H = 0$, but even in fields of up to 6–10 kOe. This is seen from the field dependences of the energy gaps shown in Fig. 14.

The general result of measurements consists in that in $YbFeO_3$, $TmFeO_3$, and $ErFeO_3$ the gap $\nu_{02}$ inherent in the spontaneous $\Gamma_{24}-\Gamma_2$ transition does not change upon the 'switching-on' of a field and upon the corresponding increase in the reorientation temperature. This means that in these orthoferrites the energy gaps at the points of the above spontaneous transition are mainly formed by the precessional mechanisms. They can be explained in terms of the spin-wave approximation [1]. At $\tau_{SR} < 0.15$, the contribution of the longitudinal vibrations of magnetization and magnetic field to the gap is hardly noticeable against this background and has not shown up itself in the limits of the experimental accuracy in experiments.

For fullness of the picture, we should mention measurements performed on $NdFeO_3$, which is closest to the above 'low-temperature' REOFs in the magnitude of $\tau_{SR}$. It follows from magnetoresistance measurements performed on this compound [63] that the width of the region of the canted phase and the magnitude of the energy gap in this orthoferrite are very sensitive to the quality of the starting materials used for the preparation of its samples. Therefore, the experiments required for the purposes of this work would have too large an error. But the corresponding measurements on $NdFeO_3$ have not been carried out mainly for the reason that it was clear in advance that they could not give qualitatively new results in comparison with those already known from experiments performed on $ErFeO_3$. Indeed, in $NdFeO_3$ $\tau_{SR} \approx 0.17$, i.e., in this parameter the neodymium and erbium orthoferrites are very close to one another. Therefore, it was hopeless to expect that we could find an increase in the gap in $NdFeO_3$ with increasing field and temperature.

**Table.** Experimental results for rare-earth orthoferrites and $Fe_3BO_6$. For $ErFeO_3$(2), $T_{SR}$, $T_N$, and $T_2$ should be replaced by $T_{N2}$, and $\nu_{02}$ should be replaced by $\nu_{0N2}$. Asterisks mark expected values.

| Compound | $YbFeO_3$ | $TmFeO_3$ | $ErFeO_3$ (1) | $NdFeO_3$ | $SmFeO_3$ | $Fe_3BO_6$ | $ErFeO_3$ (2) |
|---|---|---|---|---|---|---|---|
| Transition / Parameters | $\Gamma_{24}-\Gamma_2$ | $\Gamma_{24}-\Gamma_2$ | $\Gamma_{24}-\Gamma_2$ | $\Gamma_{24}-\Gamma_2$ | $\Gamma_{24}-\Gamma_2$ | $\Gamma_{24}-\Gamma_2$ | $\Gamma_{124}-\Gamma_{24}$ |
| $T_{SR} = (T_1 + T_2)/2$, K | 7.4 | 88 | 95 | 123 | 463 | 415 | 3.9 |
| Energy gap upon spontaneous transition at point $T = T_2$, GHz | 37.5 | 20 | 26.2 | 56 | 35 | 17.5 | 26.1 |
| $\tau_{SR} = T_{SR}/T_N$ | 0.01 | 0.14 | 0.15 | 0.17 | 0.7 | 0.8 | 1 |
| $\partial\nu_{02}/\partial T$ at $T \to T_2$, GHz K$^{-1}$ | 0 | 0 | 0 | 0* | 0.3* | 0.5 | 60 |
| $\partial\nu_{02}/\partial H$ at $H \to 0$, GHz kOe$^{-1}$ | 0 | 0 | 0 | 0* | | 0.7 | 4 |

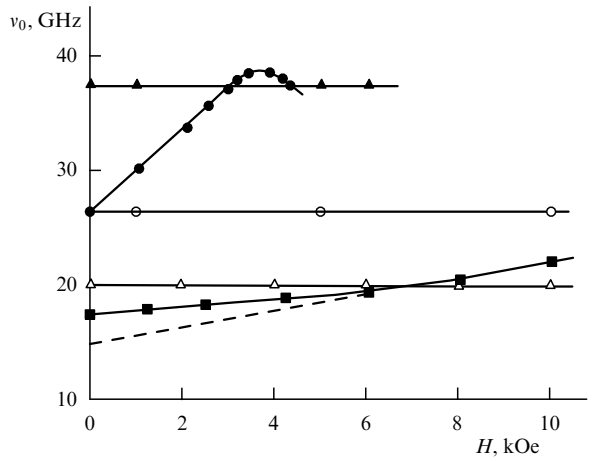


**Figure 14.** Field dependences of the energy gaps for various magnets: at the line of the $\Gamma_{24}-\Gamma_2$ transition induced by the field $\mathbf{H}\|\mathbf{a}$ in $TmFeO_3$ (△), $ErFeO_3$ (○), $YbFeO_3$ (▲), and $Fe_3BO_6$ (■); and at the line of the metamagnetic $\Gamma_{124}-\Gamma_{24}$ transition induced by the field $\mathbf{H}\|\mathbf{c}$ in the erbium subsystem of $ErFeO_3$ (●). Dashed line corresponds to the linear extrapolation of the field dependence of the gap in $Fe_3BO_6$ from the region of fields $H > 8$ kOe.

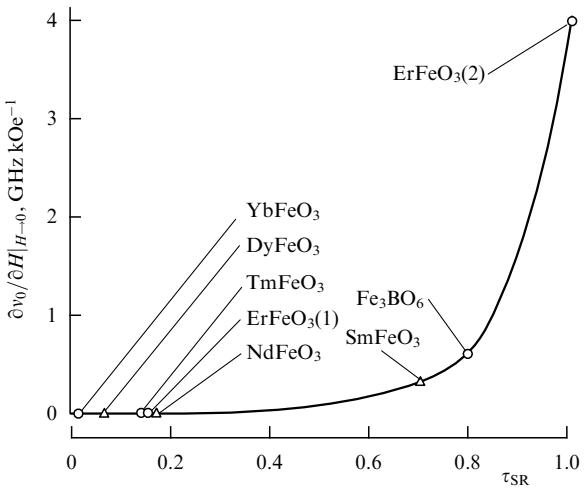


**Figure 15.** Values of $\partial\nu_0/\partial H$ at the points of spontaneous transitions in various compounds at the corresponding dimensionless temperatures $\tau_{SR} = (T_1 + T_2)/(2T_N)$: (○) measured values; (△) expected values. $ErFeO_3(1)$ corresponds to the $\Gamma_{24}-\Gamma_2$ transition in the iron subsystem of $ErFeO_3$; $ErFeO_3(2)$ stands for the $\Gamma_{124}-\Gamma_{24}$ transition in the erbium subsystem of $ErFeO_3$.

Of much more interest is $SmFeO_3$ with its record (among the REOFs) value of $\tau_{SR}$ of about 0.7. However, for the reasons that were indicated in Section 2.2, the traditional magnetoresonance measurements on this compound have not given information required for an analysis. Only measurements on $Fe_3BO_6$ and $ErFeO_3$ in the region of the ordering of erbium ions yield the clearly pronounced sought effects. In these compounds, the gradients of the energy gap with respect to the field and temperature significantly exceed the measurement error even near the spontaneous RPTs.

Note the unusually large increase in the gradients of the gap with respect to the field and temperature at the point of the spontaneous metamagnetic transition in $ErFeO_3$ as compared to $Fe_3BO_6$. Indeed, with increasing $\tau_{SR}$ from 0.8 at $Fe_3BO_6$ to 1.0 at $ErFeO_3(2)$ (see table), the gradient of the gap with respect to the temperature increased by a factor of 120 and with respect to the field, by a factor of about 6. However, it cannot be stated that the existence of such great gradients of the gap near $T = T_{N2}$ is evidence for an adequate contribution of longitudinal vibrations into its 'starting' value $\nu_{0N2}$. These gradients are most likely to arise only in the field and are caused by the specificity of this metamagnetic transition shown in Section 2.3.2, i.e., by the changes in the structure of the initial phases. As for the contribution of longitudinal vibrations to the magnitude of the gap at the point of the spontaneous RPT, it should correspond to the value of $\tilde{\chi}_{\|}/\tilde{\chi}_{\perp} = 1$ at the point $T_{SR} = T_{N2}$, according to the logic of the theory of Refs [4, 5]. Measurements of the high-frequency susceptibility (Fig. 12b) yield a value $\tilde{\chi}_{\|}/\tilde{\chi}_{\perp} = 3$ at this point.

Figure 15 displays an aggregate two-dimensional diagram that characterizes the evolution of $\partial\nu_0/\partial H$ as $H \to 0$ on changing the parameter $\tau_{SR}$, which in its meaning is a dimensionless temperature. It is evident that this diagram can be supplemented with a third coordinate, which characterizes the dependence of $\partial\nu_0/\partial H$ on field. However, to do this, high-field measurements of the gap should be performed on the REOFs under study, using the method that was realized in Refs [4, 5] for $YFeO_3$ and $DyFeO_3$.

The smooth line that runs through the 'experimental' points in Fig. 15 gives an idea of the magnitudes of $\partial\nu_0/\partial H$ at $H \to 0$ that may be expected for some other REOFs proceeding from the known values of $\tau_{SR}$ (e.g., for $DyFeO_3$, $NdFeO_3$, $SmFeO_3$). In $DyFeO_3$ and $NdFeO_3$, the situation is most likely to be the same as in the orthoferrites of Yb, Tm, and Er, i.e., $\partial\nu_{02}/\partial H = 0$. As for the samarium orthoferrite, here the contribution of the longitudinal vibrations to the dynamics of the magnet in the spontaneous reorientation region should already be sufficiently noticeable, e.g., $\partial\nu_{02}/\partial H \approx 0.3$ GHz kOe$^{-1}$. This is understandable, since the $\Gamma_{24}-\Gamma_2$ transition here occurs at a relatively large value of $\chi_{\|}/\chi_{\perp}$. From the temperature dependence of $\chi_{\|}/\chi_{\perp}$ obtained in Ref. [5] and from the magnitude $\tau_{SR} = 0.8$ in $SnFeO_3$, it follows that here the susceptibility ratio is equal to 0.7. Unfortunately, among the REOFs, there are no compounds suitable for filling the range between $NdFeO_3$ and $SmFeO_3$ in the diagram of Fig. 15. In principle, this could be made if there existed suitable isomorphic compounds of other groups. The most evident and most accessible way of obtaining a continuous set of magnets for this purpose is mutual substitution of rare-earth ions in the REOF with the same nature of the soft mode but with substantially different temperatures of spontaneous reorientation (e.g., $Sm^{3+}$ for $Tm^{3+}$). Even without resorting to additional experiments, we may state with a certain degree of surety that, at the modern level of the measurement accuracy and quality of starting materials, the contribution of longitudinal vibrations to the dynamics of REOFs in the spontaneous reorientation region should be sought at $\tau_{SR} > 0.5$. On the other hand, the corresponding effects should show up themselves in all the 'low-temperature' orthoferrites that were considered here, in which the transitions are induced by a sufficiently high magnetic field. Such transitions have already been revealed in $DyFeO_3$ [5], but they may also be expected with a large degree of certainty for the orthoferrites of Yb, Tm, Er, and Nd. Proceeding from an $H-T$ phase diagram of a corresponding compound, we may even estimate the magnitude of the required magnetic field. Thus, for example, for the $\Gamma_{24}-\Gamma_2$ transition in $ErFeO_3$, this field should be at least 60 – 70 kOe (see the $H-T$ phase diagram given in Ref. [38]). It is only for such a field one can expect that $\tau_{IR} = T_{IR}/T_N$ will

be equal to 0.5 ($T_{IR}$ is the temperature of the induced reorientation transition). And, finally, as follows from the table and Figs 14 and 15, it is by no means necessary that the greater value of the energy gap upon the spontaneous transition corresponded to a greater contribution to the dynamics of reorientation from longitudinal vibrations. No such correlation could be found for this in the results presented. This once more confirms that the 'starting' value of the gap and its increment in a magnetic field are caused by different mechanisms. They give additive contributions to the dynamics. The competition of these contributions in a certain transition region of $T$ and $H$ may lead to a situation where one of the contributions becomes intangible against the background of the other, which, on the contrary, becomes prevalent. We have already noted in Section 2.1.1 that evidence for such competition was observed previously in experiments [5] on $YFeO_3$ and $DyFeO_3$ at $T < 100$ K. The experimental values of the $\chi_{||}/\chi_{\perp}$ and gaps here become virtually independent of $T$, whereas a calculation based on the thermodynamic model of Ref. [4] predicts their further decrease with decreasing temperature in the range $T < 100$ K. In reality, at these temperatures the decisive factors for the formation of the gap apparently become spin-wave mechanisms [1], while the contribution of longitudinal vibrations is insensible on this background. This agrees with the experimental results of this work obtained on ytterbium, thulium, and erbium orthoferrites, in which the gap is also independent of the temperature in the region of $T < 100$ K.

## 5. Conclusion

The review of the experimental and theoretical work on the dynamics of magnets near magnetic phase transitions given in this paper and in Ref. [1] shows that the gap at the points of phase transitions in the spectrum of precessional spin vibrations is formed by many factors. These are magnetoelastic and dipole interactions, the interactions between the subsystems of various magnetic ions, the interaction with relaxational vibrations, and the effect of the longitudinal susceptibility, especially in the case of phase transitions induced by a magnetic field. The contributions caused by each of the above factors enter additively into the expressions for the frequencies of precessional quasispin vibrations. They manifest themselves differently at different values of the external parameters, e.g., temperature and magnetic field. At low temperatures and in weak magnetic fields, the magnetoelastic and dipole contributions are prevalent, as well as the contribution from the interaction between the subsystems of various magnetic ions. At high temperatures or in strong magnetic fields, the effect of the magnetic field and longitudinal susceptibility become decisive. All these features are observed in experiments that have been reviewed in this paper. The theory presented in this paper, which takes into account all these interactions, permits one qualitatively and, in some cases, even quantitatively to explain all the experimentally observed peculiarities in the behavior of the gap in the spectra of quasispin branches both near the spontaneous and field-induced reorientation phase transitions.

Unfortunately, most experiments were performed on rare-earth orthoferrites, in which there is an ordered subsystem of iron ions and a paramagnetic (or also an ordered) subsystem of rare-earth ions, whereas the theory that takes into account the relaxation and the longitudinal susceptibility was developed only for the case of magnets with a single ordered magnetic subsystem. However, allowing for the fact that the different contributions enter additively to the activation of quasispin branches, the theory considered above, along with the theory of Ref. [1], permit one to qualitatively explain experimental results in the case of the orthoferrites as well.

The problem of finding the spectrum of vibrations in rare-earth orthoferrites with allowance for all factors that can determine the activation of quasispin branches is very laborious (especially, at low temperatures, where the subsystem of rare-earth ions can also become ordered). We hope that our review will stimulate new works on the experimental and theoretical study of coupled vibrations in complex magnets such as rare-earth orthoferrites.

## 6. Appendix

The complete dispersion equation for the vibrations of transverse components of the vectors of ferromagnetism and antiferromagnetism in the phase with $\mathbf{M}||\mathbf{L}||\mathbf{x}$ of a two-sublattice antiferromagnet has the form

$$
\begin{aligned}
&\omega^4 + \mathrm{i}\omega^3\left[2r_1\omega_E + r_2\left(\omega_{13}+\omega_{23}+2\eta^2\frac{\omega_H^2}{\omega_E}\right)\right]\\
&-\omega^2\left\{r_1^2\omega_E^2 + r_2^2\left[\omega_{13}\omega_{23}+\eta^2\frac{\omega_H^2(\omega_{13}+\omega_{23})}{\omega_E}+\eta^4\frac{\omega_H^4}{\omega_E^2}\right]\right.\\
&+2r_1r_2\omega_E\left(\omega_{13}+\omega_{23}+\eta^2\frac{\omega_H^2}{\omega_E}\right)\\
&+\omega_E(\omega_{13}+\omega_{23})\left[1+\frac{\omega_H^2\eta(1-\eta)}{\omega_E^2}\right]^2\\
&+\omega_H^2\left[1+\eta+\frac{\omega_H^2\eta^2(1-\eta)}{\omega_E^2}\right]^2\\
&\left.+\frac{(1-\eta)^2\omega_H^2\omega_{13}\omega_{23}}{\omega_E^2}\right\}\\
&-\mathrm{i}\omega\left(r_1\left\{\omega_E^2(\omega_{13}+\omega_{23})\left[1+\frac{\omega_H^2\eta^2(1-\eta)}{\omega_E^2}\right]^2\right.\right.\\
&\left.+\frac{2(1-\eta)^2\omega_H^2\omega_{13}\omega_{23}}{\omega_E}\right\}+r_2\left[2\omega_E\omega_{13}\omega_{23}\right.\\
&\left.+\omega_H^2(\omega_{13}+\omega_{23})\right]+r_1^2r_2\omega_E^2(\omega_{13}+\omega_{23})\\
&\left.+r_1r_2^2\left[2\omega_E\omega_{13}\omega_{23}+\eta^2\omega_H^2(\omega_{13}+\omega_{23})\right]\right)\\
&+\omega_{13}\omega_{23}\left\{r_1^2r_2^2\omega_E^2+2r_1r_2\omega_E^2+(1-\eta)^2\omega_H^2(r_1^2+r_2^2)\right.\\
&\left.+\frac{\left[\omega_E^2-(1-\eta)^2\omega_H^2\right]^2}{\omega_E^2}\right\}=0\,. \qquad \text{(A.1)}
\end{aligned}
$$

The complete dispersion equations that describe the vibrations of the magnetic subsystem in the phase with $\mathbf{M}||\mathbf{x}$, $\mathbf{L}||\mathbf{y}$ in an antiferromagnet look as follows:

$$
\begin{aligned}
&\mathrm{i}(1-\eta)\omega^3-\omega^2\omega_E\left[r_1(2-\eta)+r_2(1-\eta)\frac{\omega_{32}}{\omega_E}+r_2\eta^2\frac{\omega_H^2}{\omega_E^2}\right]\\
&\quad-\mathrm{i}\omega\left\{r_1r_2\left[(2-\eta)\omega_{32}\omega_E+\eta^2\omega_H^2\right]+r_1^2\omega_E^2+\right.\\
&\quad+(1-\eta)\left[\omega_E\omega_{32}+\omega_H^2(1-\eta)\right]\Big\}+\\
&\quad+\left[r_1+r_2r_1^2+r_2\frac{\omega_H^2}{\omega_E^2}\right]\omega_{32}\omega_E^2=0\,, \qquad \text{(A.2)}
\end{aligned}
$$

$$
\begin{aligned}
&\mathrm{i}\omega^3 - \omega^2\left[r_1\omega_{\mathrm{E}} + r_2(\omega_B + \omega_{12})\right] \\
&\quad - \mathrm{i}\omega\left[r_1 r_2\omega_{\mathrm{E}}(\omega_{12} + \omega'_B) + r_2^2\omega_{12}\omega_B + \omega_{12}\omega'_{\mathrm{E}}\right] \\
&\quad + \omega_{12}\omega_{\mathrm{E}}\omega'_B\left[r_2 + r_1 r_2^2 + r_1\frac{\omega_H^2}{\omega_{\mathrm{E}}^2}\right] = 0\,. \qquad \text{(A.3)}
\end{aligned}
$$

## References


1. Buchel'nikov V D, Dan'shin N K, Tsymbal L T, Shavrov V G *Usp. Fiz. Nauk* **166** 585 (1996) [*Phys. Usp.* **39** 547 (1996)]
2. Dikshteĭn I E, Tarasenko V V, Shavrov V G *Fiz. Tverd. Tela* (Leningrad) **19** 1107 (1977) [*Sov. Phys. Solid State* **19** 644 (1977)]
3. Gufan Yu M *Zh. Eksp. Teor. Fiz.* **60** 1537 (1971) [*Sov. Phys. JETP* **33** 804 (1971)]
4. Balbashov A M et al. *Zh. Eksp. Teor. Fiz.* **93** 302 (1987) [*Sov. Phys. JETP* **66** 174 (1987)]
5. Balbashov A M et al. *Zh. Eksp. Teor. Fiz.* **94** 305 (1988) [*Sov. Phys. JETP* **67** 821 (1988)]
6. Buchel'nikov V D, Shavrov V G *Pis'ma Zh. Eksp. Teor. Fiz.* **60** 534 (1994) [*JETP Lett.* **60** 548 (1994)]
7. Buchel'nikov V D, Shavrov V G *Zh. Eksp. Teor. Fiz.* **106** 1756 (1994) [*JETP* **79** 951 (1994)]
8. Dzyaloshinskiĭ I E, Kukharenko B G *Zh. Eksp. Teor. Fiz.* **70** 2360 (1976) [*Sov. Phys. JETP* **43** 1232 (1976)]
9. Gufan Yu M, Prokhorov A S, Rudashevskiĭ E G *Dokl. Akad. Nauk SSSR* **238** 57 (1978) [*Sov. Phys. Dokl.* **23** 39 (1978)]
10. Gufan Yu M, Prokhorov A S, Rudashevskiĭ E G, Preprint of Physical Inst. Acad. Sci. SSSR No. 60 (Moscow: Fiz. Inst. Akad. Nauk SSSR, 1979)
11. Mukhin A A, Prokhorov A S *Fiz. Tverd. Tela* (Leningrad) **34** 3323 (1992) [*Sov. Phys. Solid State* **34** 1778 (1992)]
12. Bar'yakhtar V G *Zh. Eksp. Teor. Fiz.* **94** 196 (1988) [*Sov. Phys. JETP* **67** 757 (1988)]
13. Belov K P *Orientatsionnye Perekhody v Redkozemel'nykh Magnetikakh* (Reorientation Transitions in Rare-Earth Magnetic Materials) (Moscow: Nauka, 1977)
14. Shane J R *Phys. Rev. Lett.* **20** 728 (1968)
15. Buchel'nikov V D, Bychkov I V, Shavrov V G *Zh. Eksp. Teor. Fiz.* **101** 1869 (1992) [*Sov. Phys. JETP* **74** 999 (1992)]
16. Buchel'nikov V D, Bychkov I V, Shavrov V G *Fiz. Nizk. Temp.* **18** 1342 (1992) [*Sov. J. Low Temp. Phys.* **18** 935 (1992)]
17. Turov E A, Shavrov V G *Usp Fiz. Nauk* **14**0 429 (1983) [*Sov. Phys. Usp.* **26** 593 (1983)]
18. Dan'shin N K, Kramarchuk G G, Sdvizhkov M A *Pis'ma Zh. Eksp. Teor. Fiz.* **44** 85 (1986) [*JETP Lett.* **44** 107 (1986)]
19. Vitebskiĭ I M et al. *Zh. Eksp. Teor. Fiz.* **90** 1118 (1986) [*Sov. Phys. JETP* **63** 652 (1986)]
20. Dan'shin N K, Kramarchuk G G, Sdvizhkov M A, in *Tr. 18-i Vsesoyuz. Konf. "Fizika Magnitnykh Yavleniĭ"* (Proceedings of the Eighteenth All-Union Conference on the Physics of Magnetic Phenomena) (Kalinin, 1988) p. 710
21. Dan'shin N K et al. *Fiz. Tverd. Tela* (Leningrad) **31** (5) 198 (1989) [*Sov. Phys. Solid State* **31** 832 (1989)]
22. Mukhin A A, Prokhorov A S *Tr. Inst. Obshch. Fiz. Akad. Nauk SSSR* **25** 162 (1990)
23. Volkov A A et al. *Pis'ma Zh. Eksp. Teor. Fiz.* **39** 140 (1984) [*JETP Lett.* **39** 166 (1984)]
24. Balbashov A M et al. *Zh. Eksp. Teor. Fiz.* **88** 974 (1985) [*Sov. Phys. JETP* **61** 573 (1985)]
25. Dan'shin N K, Kramarchuk G G *Fiz. Nizk. Temp.* **19** 888 (1993) [*Low Temp. Phys.* **19** 632 (1992)]
26. Dan'shin N K, Kramarchuk G G *Fiz. Tverd. Tela* (S.-Peterburg) **35** 3586 (1993) [*Phys. Solid State* **35** 1282 (1993)]
27. Dan'shin N K, Kramarchuk G G, Nepochatykh Yu I *Zh. Eksp. Teor. Fiz.* **105** 660 (1994) [*JETP* **78** 354 (994)]
28. Barilo S N et al. *Zh. Eksp. Teor. Fiz.* **96** 1921 (1990) [*JETP* **70** 1083 (1990)]
29. Voigt C *Phys. Lett. A* **53** 223 (1975)
30. Arutyunyan V É, Kocharyan K N, Martirosyan R M *Zh. Eksp. Teor. Fiz.* **96** 1381 (1989) [*Sov. Phys. JETP* **69** 783 (1989)]
31. Arutyunyan V É et al. *Fiz. Tverd. Tela* (Leningrad) **34** 2251 (1992) [*Sov. Phys. Solid State* **34** 1203 (1992)]
32. Dan'shin N K, Nepochatykh Yu I, Shkar' V F *Zh. Eksp. Teor. Fiz.* **109** 639 (1996) [*JETP* **82** 341 (1996)]
33. Tsymbal L T et al. *Zh. Eksp. Teor. Fiz.* **105** 948 (1994) [*JETP* **78** 508 (1994)]
34. Arutyunyan V E et al. *Zh. Eksp. Teor. Fiz.* **98** 712 (1990) [*Sov. Phys. JETP* **71** 398 (1990)]
35. Dan'shin N K et al. *Fiz. Tverd. Tela* (Leningrad) **28** 2609 (1986) [*Sov. Phys. Solid State* **28** 1461 (1986)]
36. Dan'shin N K, Kovtun N M, Sdvizhkov M A *Fiz. Tverd. Tela* (Leningrad) **27** 3635 (1985) [*Sov. Phys. Solid State* **27** 2189 (1985)]
37. Dan'shin N K *Fiz. Nizk. Temp.* **20** 353 (1994) [*Low Temp. Phys.* **20** 281 (1994)]
38. Belov K P et al *Phys. Status Solidi A* **36** 415 (1976)
39. Vitebskiĭ N M et al. *Fiz. Tverd. Tela* (Leningrad) **30** 1271 (1988) [*Sov. Phys. Solid State* **30** 738 (1988)]
40. Gufan Yu M, Sadkov A N *Fiz. Tverd. Tela* (Leningrad) **28** 2991 (1986) [*Sov. Phys. Solid State* **28** 1682 (1986)]
41. Dan'shin N K, Tsymbal L T *Zh. Eksp. Teor. Fiz.* **106** 1765 (1994) [*JETP* **79** 956 (1994)]
42. Balbashov A M et al. *Fiz. Tverd. Tela* (Leningrad) **31** (7) 279 (1989) [*Sov. Phys. Solid State* **31** 1259 (1989)]
43. Vitebskiĭ N M et al. *Zh. Eksp. Teor. Fiz.* **98** 334 (1990) [*Sov. Phys. JETP* **71** 187 (1990)]
44. Tsymbal L T, Izotov A I *Zh. Eksp. Teor. Fiz.* **102** 963 (1992) [*Sov. Phys. JETP* **75** 525 (1992)]
45. Gorodetsky G, Shaft S, Wanklyn B M *Phys. Rev. B* **14** 2051 (1976)
46. Vitebskiĭ N M et al. *Fiz. Tverd. Tela* (Leningrad) **29** 2738 (1987) [*Sov. Phys. Solid State* **29** 1575 (1987)]
47. Akhiezer A I, Bar'yakhtar V G, Peletminskiĭ S V *Spinovye Volny* (Spin Waves) (Moscow: Nauka, 1967) [Translated into English (Amsterdam: North-Holland, 1968)]
48. Buchel'nikov V D, Shavrov V G *J. Magn. Magn. Mater.* **140 – 144** 1587 (1995)
49. Lifshitz E M, Pitaevskiĭ L P *Statisticheskaya Fizika*, chast' 2, (Statistical Physics, part 2) (Moscow: Nauka, 1978) [Translated under the title: Landau L D, Lifshitz E M *Statistical Physics* Vols. 2, 3rd edition (Oxford: Pergamon, 1980)]
50. Landau E M, Lifshitz E M *Teoriya Uprugosti* (Theory of Elasticity) (Moscow: Nauka, 1987) [Translated into English (Oxford: Pergamon, 1986)]
51. Buchel'nikov V D, Shavrov V G *Fiz. Met. Metalloved.* **68** 421 (1989)
52. Ozhogin V I, Preobrazhenskiĭ V L *Usp. Fiz. Nauk* **155** 593 (1988) [*Sov. Phys. Usp.* **31** 713 (1988)]
53. Gorodetsky G, Luthi B *Phys. Rev. B* **2** 3688 (1970)
54. Dan'shin N K et al. *Zh. Eksp. Teor. Fiz.* **93** 2151 (1987) [*Sov. Phys. JETP* **66** 1227 (1987)]
55. LeCraw R C, Comstock R L, in *Physical Acoustics: Principles and Methods* Vol. III, Part B: *Lattice Dynamics* (Ed. W P Mason) (New York: Academic, 1965)
56. Buchel'nikov V D, Shavrov V G *Fiz. Tverd. Tela* (S.-Peterburg) **37** 1402 (1995) [*Phys. Solid State* **37** 760 (1995)]
57. Gufan Yu M *Termodinamicheskaya Teoriya Fazovykh Perekhodov* (Thermodynamic Theory of Phase Transitions) (Rostov: Rostov. Gos. Univ., 1982)
58. Belov K P *Magnitostriktsionnye Yavleniya i Ikh Tekhnicheskie Prilozheniya* (Magnetostrictive Phenomena and Their Engineering Application) (Moscow: Nauka, 1987)
59. Izyumov Yu A, Syromyatnikov V N *Fazovye Perekhody i Simmetriya Kristallov* (Phase Transitions and Crystal Symmetry) (Moscow: Nauka, 1984) [Translated into English (Dordrecht: Kluwer Acad. Publ., 1990)]
60. Patashinskiĭ A Z, Pokrovskiĭ V L *Fluktuatsionnaya Teoriya Fazovykh Perekhodov* (Fluctuational Theory of Phase Transitions) (Moscow: Nauka, 1982) [Translated into English (Oxford: Pergamon, 1979)]
61. Landau L D, Lifshitz E M *Elektrodinamika Sploshnykh Sred* (Electrodynamics of Continuous Media) (Moscow: Nauka, 1982) [Translated into Russian (Oxford: Pergamon, 1960)]
62. Egoyan A É, Mukhin A A *Fiz. Tverd. Tela* (S.-Peterburg) **36** 1715 (1994) [*Phys. Solid State* **36** 938 (1994)]
63. Barilo S N et al. *Fiz. Tverd. Tela* (Leningrad) **33** 62 (1991) [*Sov. Phys. Solid State* **33** 354 (1991)]